Occluding Junctions in Tissue Morphogenesis: Roles for Septate Junction Proteins in *Drosophila melanogaster* Egg Morphogenesis

BY

Haifa Abdulrahman Alhadyian

Submitted to the graduate degree program in Molecular Biosciences and the Graduate Faculty of the University of Kansas in partial fulfillment of the requirements for the degree of Doctor of Philosophy

_____
Chairperson – Dr. Robert Unckless

_____
Dr. Brian Ackley

_____
Dr. Stuart Macdonald

_____
Dr. Kristi Neufeld

_____
Dr. Robert Ward

_____
Dr. Justin Blumenstiel

Date defended: March 16, 2021

The dissertation committee for Haifa Abdulrahman Alhadyian
Certifies that this is the approved version of the following dissertation:

Occluding Junctions in Tissue Morphogenesis: Roles for Septate Junction Proteins in *Drosophila melanogaster* Egg Morphogenesis

_____
Chairperson – Dr. Robert Unckless

Date Approved: March 16, 2021

Abstract

Tissue morphogenesis underlies many developmental processes in multicellular organisms and is essential for the basic organization of tissues and organs. Several cellular processes contribute to morphogenesis, including cell shape changes, cellular rearrangements, and cell movement. These morphological processes are regulated via protein trafficking and secretion, the cell cytoskeleton, and propagation of mechanical forces within cells and across tissues. In *Drosophila*, components of the invertebrate occluding junction, known as the septate junction (SJ), are required for several morphogenetic events during the embryonic and larval stages. Recent studies revealed a non-occluding functional requirement for SJ proteins in tissue morphogenesis during embryogenesis. However, whether a similar requirement is present in the adult tissue of the fly remains unknown. To explore this question, we used the *Drosophila* egg chamber as a model system. In Chapter II, we examined the expression pattern of four SJ proteins (Macroglobulin complement-related (Mcr), Contactin, Neuraxin IV, and Coracle) in the egg chambers throughout oogenesis. The examined SJ proteins localize along the lateral membrane of the follicle cells (FCs) of early-stage egg chambers but become enriched at the apical-lateral membrane in late-stage egg chambers, where they form the SJ. In addition, we determined that the re-localization event of SJ proteins in the follicular epithelium requires Rab5-mediated endocytosis and Rab11-mediated recycling. Next, we examined the role of SJ proteins in egg morphogenesis. We find that SJ proteins are required for morphogenetic events during oogenesis, including border cell migration, egg elongation, and the formation of the dorsal appendages. To further examine the cellular mechanism by which SJ proteins are required for egg morphogenesis, we focused our analysis on the role of Mcr in egg elongation. In Chapter III, we show that Mcr is required for egg elongation late in oogenesis. This requirement is mediated

via maintaining a monolayered epithelium and cell-extracellular matrix adhesion. We also show that Mcr is required for eggshell layers formation, including the wax and chorion layers. The findings in this study set the foundation for the SJ field to study the role of SJ proteins in morphogenesis in post-embryonic epithelia and indicate a conserved role for SJ proteins in morphogenesis.

Keywords: Morphogenesis, septate junctions, oogenesis, egg elongation, eggshell

Acknowledgements

To my family, you have been such an instrumental part of my success throughout my life. I thank you for your constant support and belief in my abilities. My mother, Nora Alkatheri, thank you for your unconditional support during my graduate training. To my dad, Abdulrahman Alhadyian, you instilled in me to always aim higher in everything I do, and I thank you for that. My sisters, Heba, Hadeel, Haya, Hotoon, and my brother Hammad, thank you for being by my side and encouraging me throughout my graduate career.

To my mentor, Dr. Robert Ward, thank you for giving me the opportunity to explore science under your mentorship. You have given me the freedom to develop this project on my own, which has given me great confidence in my abilities as a young scientist. Thank you for your patience, motivation, and enthusiasm about my project and science in general, which reminds me of why I am in this business. I also would like to thank you for allowing me to participate in outreach programs during my time in your lab.

My thesis committee members, Dr. Robert Unckless, Dr. Brian Ackley, Dr. Stuart MacDonald, Dr. Kristi Neufeld, Dr. Justin Bluemenstiel, and former committee member, Dr. Matthew Buechner, thank you for serving on my committee and your continued support and encouragement during my graduate career in the Department of Molecular Biosciences.

Dr. Brian Ackley and the members of the Ackley lab, I cannot thank you enough for your generosity in the use of your confocal microscope, for always being available to answer my questions and troubleshoot confocal-related issues. I appreciate your time and accommodation.

Former and current members of the Ward lab, I am lucky that I got to work alongside amazing and supportive scientists. Thank you for your friendship, support, and stimulating discussions about science, and your feedback on my dissertation. The undergraduate students I worked with, Lindsay Ussher and Dania Shoaib, working with you taught me how to be a good mentor and a better educator, and I am thankful for that. Dr. Sonia Hall, I appreciate the time you took to train me when I first joined the lab and for your continuous support during my graduate training.

Many of the experiments in this study would not have been possible without the generosity of the fly community. Dr. Sally Horne-Badovinac and the members of the Horne-Badovinac lab, I would like to extend my appreciation to you for the insightful discussions about my project and for sharing fly stocks and reagents. Dr. Jocelyn McDonald and the members of the McDonald lab, thank you for accommodating me in your lab and training me on the live imaging experiment. Dr. Julie Merkle and Dr. Stefan Luschnig, thank you for sharing fly stocks with us.

Finally, I would like to thank Dr. Eduardo Rosa-Molinar and Dr. Noraida Martinez-Rivera for conducting the electron microscopy experiments. Heather Decker, and the members of the Microscopy and Analytical Imaging Facility, thank you for training me to use the microscopes in your facility, and for always being available to answer my questions.

Table of Contents

List of figures

List of tables

Chapter I: Introduction

Morphogenesis is a developmental process that involves precise and coordinated cell shape changes, cellular rearrangement, and cell movement (Zallen and Goldstein 2017). Examples of morphogenetic events during embryogenesis include tissue convergence/extension and gastrulation (Shindo 2018; Solnica-Krezel and Sepich 2012). *Drosophila melanogaster* has served as a key model in investigating the genetic control of cellular processes contributing to morphogenesis.

Our lab became interested in studying morphogenesis as a result of a modifier genetic screen for genes that enhance the malformed leg phenotype during imaginal disc morphogenesis during metamorphosis (Ward, Evans, and Thummel 2003). One of these identified genes, Macroglobulin complement-related, has been further characterized as a core component of the pleated septate junction (hereafter referred to as SJ) (Hall et al. 2014; Bätz, Förster, and Luschnig 2014).

The SJ is the invertebrate occluding junction and is located at the apical-lateral membrane of ectodermally-derived epithelia (Izumi and Furuse 2014). The function of the SJ is to prevent transepithelial diffusion, which is critical for epithelial formation (Izumi and Furuse 2014). Over the last two decades, more than 20 SJ proteins have been identified (Table 1. 1) (Izumi and Furuse 2014; Rice et al. 2021). Initially, SJ proteins localize along the lateral membrane of epithelial cells before becoming enriched at the apical-lateral membrane via endocytosis and recycling (Tiklová et al. 2010; Hall and Ward, 2016). A few studies indicate that SJ core proteins are required for embryonic and larval imaginal discs morphogenesis (Lamb et al. 1998; Venema, Zeev-Ben-Mordehai, and Auld 2004; Moyer and Jacobs 2008; Banerjee et al. 2008; Hall et al. 2014). Moreover, mutations in many SJ genes result in embryonic lethality due to compromised blood-brain barrier and/or developmental defects (e.g., Baumgartner et al.

1996). Interestingly, although the main function of the SJ is to seal the paracellular flow within an epithelium (Izumi and Furuse 2014), the requirement of SJ proteins in morphogenesis during embryogenesis seems to be independent of their role in forming an occluding junction (Hall and Ward 2016). Further, due to their requirement in animal development and survival, our understanding of SJ biogenesis is limited to studies conducted in the embryonic epithelia.

My dissertation is set to examine SJ biogenesis and the role of SJ proteins in morphogenesis using the adult *Drosophila melanogaster* egg chamber as a model system. The *Drosophila* egg chamber is a useful model system to investigate the role of SJ proteins in morphogenesis for the following reasons. First, several SJ proteins are expressed in the ovary (Wei, Hortsch, and Goode 2004; Schneider et al. 2006; Maimon, Popliker, and Gilboa 2014; Hall et al. 2014; Ben-Zvi and Volk 2019), although the subcellular localization of these proteins has not been determined. Second, ultrastructural studies indicate the formation of ladder-like septa in the follicular epithelium by stage 10B/11 of oogenesis and a functional junction at stage 11 (14 developmental stages in total) (Mahowald 1972; Müller 2000; Isasti-Sanchez, Munz-Zeise, and Luschnig 2020). Finally, egg chambers undergo a number of morphogenetic events that span oogenesis (Horne-Badovinac and Bilder 2005), which allows for exploring the non-occluding functions for SJ proteins in morphogenesis.

The following section provides an overview of the SJ, the molecular components of the junction, and our current understanding of the requirement of SJ proteins in tissue morphogenesis. Next, I provide an overview of *Drosophila* oogenesis and egg chamber morphogenesis with a brief review on egg elongation, which is the primary morphogenetic process discussed in this work. Finally, I share how this work advances our knowledge in the field of SJ and tissue morphogenesis in general.

1.1. SJ proteins and their requirement in tissue morphogenesis

Components and biogenesis of SJs

The invertebrate pleated SJ is the equivalent of the tight junction (TJ) in vertebrates (Izumi and Furuse 2014). Both provide permeability barriers to regulate the passage of solutes between epithelial cells (Izumi and Furuse 2014; Jonusaite, Donini, and Kelly 2016; Noirot-timothée et al. 1978) **(**Figure 1. 1). The SJ resides basal to the adherens junction in polarized epithelia and shows a ladder-like appearance between adjacent cell membranes (Green and Bergquist 1982). Even though the SJs and TJs serve the same biological function, they are distinct at the ultrastructural and molecular level (Izumi and Furuse 2014; Jonusaite, Donini, and Kelly 2016).

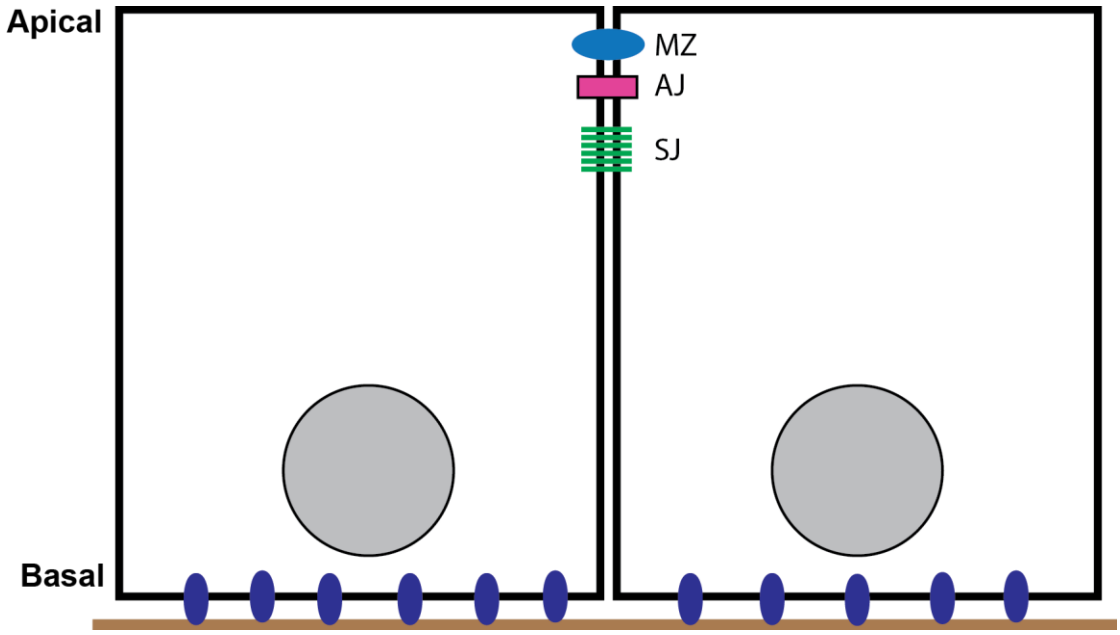

Figure 1. 1 Lateral cell-cell junctions of an invertebrate epithelium.
A mature epithelium has defined apical-basal polarity, where the apical surface faces the lumen. Cell-cell junctions localize along the lateral membrane. These junctions include marginal zone (MZ, blue oval), adherens junction (AJ, magenta rectangle), and septate junction (SJ, green lines). The basal surface of the epithelium is linked to the extracellular matrix (ECM) (brown line) via ECM receptors (oval dark blue).

In *Drosophila melanogaster*, ultrastructural studies show that SJ forms ladder-like septa that reside at the apical-lateral membrane of ectoderm-derived epithelium, including the embryonic hindgut, the trachea, the salivary glands, and the epidermis (Tepass et al. 2001). The SJ consists of more than 20 proteins that are required for either the formation or organization of the junction (Table 1. 1) (Izumi and Furuse 2014; Rice et al. 2021). Before their enrichment at the apical-lateral membrane, SJ proteins are found along the lateral membrane of the embryonic hindgut (Tiklová et al. 2010). SJ proteins apical-lateral re-localization is a multistep process and requires proteins involved in endocytosis and recycling pathways (Tiklová et al. 2010). Moreover, the localization of SJ proteins at the apical-lateral membrane is mutually interdependent, as the loss of function of one SJ gene is sufficient to disrupt the organization of the junctional complexes (Ward, Lamb, and Fehon 1998; Behr, Riedel, and Schuh 2003; Paul et al. 2003; Wu et al. 2007; Bachmann et al. 2008; Hall et al. 2014; Bätz, Förster, and Luschnig 2014; Königsmann et al. 2020). Whether SJ biogenesis and their interdependent relationship are similar in non-embryonic epithelia is unknown.

Protein name	Reference
Core	
α subunits of Na^+/K^+ ATPase	Genova and Fehon 2003
β subunits of Na^+/K^+ ATPase (Nervana 2)	Paul et al. 2003
Contactin	Faivre-Sarrailh et al. 2004
Coracle	Fehon, Dawson, and Artavanis-Tsakonas 1994; Lamb et al. 1998
Crimpled	Nilton et al. 2010
Kune-Kune	Nelson, Furuse, and Beitel 2010
Lachesin	Llimargas et al. 2004
Macroglobulin complement-related	Bätz, Förster, and Luschnig 2014; Hall et al. 2014
Megatrachea	Behr, Riedel, and Schuh 2003
Melanotransferrin (Transferrin2)	Tiklová et al. 2010
Neurexin IV	Baumgartner et al. 1996
Neuroglian	Genova and Fehon 2003
Pasiflora 1 and Pasiflora 2	Deligiannaki et al. 2015
Sinuous	Wu et al., 2004
Varicose	Mayor and Jacob, 2008
Würmchen 1	Königsmann et al. 2020
Resident	
Discs Large	Woods and Bryant 1991
Fasciclin III	Snow, Bieber, and Goodman 1989
Lethal (2) Giant Larvea	Bilder 2004
Scribble	Bilder and Perrimon 2000
Accessory	
Boudin	Hijazi et al. 2009
Clathrin heavy chain	Tiklová et al. 2010
Coiled	Hijazi et al. 2011; Nilton et al. 2010
Crooked	Nilton et al. 2010
Rab 5	Tiklová et al. 2010
Rab 11	Tiklová et al. 2010
Shibire	Tiklová et al. 2010
Wunen/ Wunen 2	Ile et al. 2012

Table 1. 1 Components of the SJs.
Modified from Rice et al. 2021.

SJ proteins are required for morphogenetic developmental events

A thorough analysis of nine SJ genes revealed an essential role for these genes in morphogenetic processes during embryogenesis, including dorsal closure and head involution (Fehon, Dawson, and Artavanis-Tsakonas 1994; Hall & Ward, 2016). In addition, the trachea of *Macroglobulin*

completed-related (Mcr), *Lachesin (Lac)*, *ATPase* α, *Nervana 2 (Nrv2) (*known as *ATPase* β*)*, *sinuous (sinu)*, *kune-kune (kune)*, and *Varicose (Vari)* mutant embryos are highly convoluted when compared to the trachea of control animals (Paul et al. 2003; Wu et al. 2004; Llimargas et al. 2004; Wang et al. 2006; Nelson, Furuse, and Beitel 2010; Hall et al. 2014). These data suggest that core SJ proteins are essential for morphogenetic events to occur normally during embryogenesis.

Because SJ mutants are embryonic lethal, few studies shed light on the role of SJ proteins in morphogenesis at post-embryonic stages (Lamb et al. 1998; Venema, Zeev-Ben-Mordehai, and Auld 2004; Bachmann et al., 2008; Banerjee et al. 2008; Hall and Ward 2016). These studies were completed by analyzing adult escapers of SJ homozygous mutant animals, the use of tissue-specific RNA interference (RNAi)-mediated knockdown or clonal analysis. For example, adult escapers expressing a hypomorphic allele of *coracle (cora)* display morphogenetic defects, including in the formation of the eye and cuticle and defects in the rotation of the male genital apparatus (Lamb et al. 1998). Furthermore, expressing RNAi against *Vari* in the wing imaginal disc results in wing development and expansion defects (Bachmann et al., 2008). Moreover, adult flies expressing *Vari-RNAi* in the eye imaginal discs have downsized and malformed eyes (Bachmann et al., 2008). *Neurexin IV* (*Nrx-IV*) was shown to be required for ommatidia development of the third instar larvae imaginal discs and adult eye (Banerjee et al. 2008). Lastly, the parallel alignment of adult wing hairs is lost in *cora* mutant animals, suggesting a role for *cora* in planar cell polarity (Venema, Zeev-Ben-Mordehai, and Auld 2004). Together, these studies indicate a requirement for SJ proteins in embryonic and larval imaginal disc morphogenesis. However, the cellular mechanism by which SJ proteins are involved in morphogenesis remains elusive.

A possible role for SJ proteins in morphogenesis independent of the occluding function

Given that mutations in SJ genes result in compromised epithelium barriers (e.g., Hall et al. 2014; Behr, Riedel, and Schuh 2003), it is assumed that the morphogenetic defects observed in SJ mutant animals are due to disruption of the occluding function. However, recent studies point to an additional role for SJ proteins in development that is independent of the occluding function (Laprise et al. 2009; Wells et al. 2013; Hall et al. 2014; Hall and Ward 2016; Lim et al. 2019). As mentioned above, SJ mutant embryos display defects in dorsal closure and head involution (Hall and Ward, 2016). Interestingly, the dorsal closure (completed at stages 13–14) and head involution (completed at stage 15) defects in SJ mutant embryos occur prior to SJ maturation (at stage 16/17) (Hall & Ward, 2016). Therefore, the role SJ proteins play in these morphogenetic processes is likely independent of the occluding function.

In support of this assertion, several studies indicate a requirement for SJ proteins in apical-basal polarity, cell-cell adhesion, and protein secretion between stages 11–15 of embryogenesis (prior to SJ maturation at stage 16/17). In the epidermis of stage 11/12 embryos, *cora*, *Nrx-IV*, and *ATPase* α form a complex with *yurt* to maintain apical-basal polarity by interacting negatively with the apical determinant, Crumbs (Laprise et al. 2009). Moreover, (Fasciclin) Fas3 asymmetric localization in hindgut cells promotes hindgut curvature by mediating intercellular adhesions between stages 12-14 of embryogenesis (Wells et al. 2013). Further, SJ proteins control the length of the embryonic trachea by regulating cell shape and the secretion of apical extracellular matrix proteins, which occurs beginning at stage 13 of embryogenesis (Hayashi and Kondo 2018; Bätz, Förster, and Luschnig 2014; Hall et al. 2014; Luschnig et al. 2006; Wang et al. 2006; Behr, Riedel, and Schuh 2003). Another example of the

independent-junctional requirement of SJ proteins in morphogenesis is their role in the embryonic dorsal vessel (heart) formation (Yi et al. 2008). Although the embryonic cardiac tissue does not contain an SJ, *Nrx-IV*, *sinu*, *cora*, *Nrv2*, *Lac*, and *Contactin* (*Cont*) are expressed in this tissue and localize at the plasma membrane (Yi et al. 2008). Mutations in any of these genes result in cardiac lumen collapse, lower heart rate, and lack of cell–cell adhesion (Yi et al. 2008).

1.2. *Drosophila melanogaster* egg chamber as a model system to study the role of SJ proteins in morphogenesis

Drosophila oogenesis

Drosophila females possess a pair of ovaries joined by a common oviduct. Each ovary contains approximately 16–20 ovarioles of progressively developing egg chambers or follicles (**Figure 1. 2**A) (Spradling 1993). At the tip of one ovariole is the germarium region, which contains two populations of stem cells: the germline and somatic stem cells (Xie and Spradling 2000). After an egg is formed in the germarium, it leaves as 16 germline cysts – 15 nurse cells and an oocyte – that are surrounded by a layer of follicle cells (FCs) (**Figure 1. 2** B) (Horne-Badovinac & Bilder, 2005). Throughout 14 developmental stages, each egg chamber increases approximately 8-fold in volume and elongates approximately 2.5-fold along the anterior–posterior axis, forming an ellipsoid shaped egg. The FCs drive the majority of the morphogenetic events during oogenesis (Duhart, Parsons, and Raftery 2017). Therefore, maintaining an intact epithelium that is capable of undergoing cell shape changes, cellular rearrangements, and cell movements is essential for egg morphogenesis.

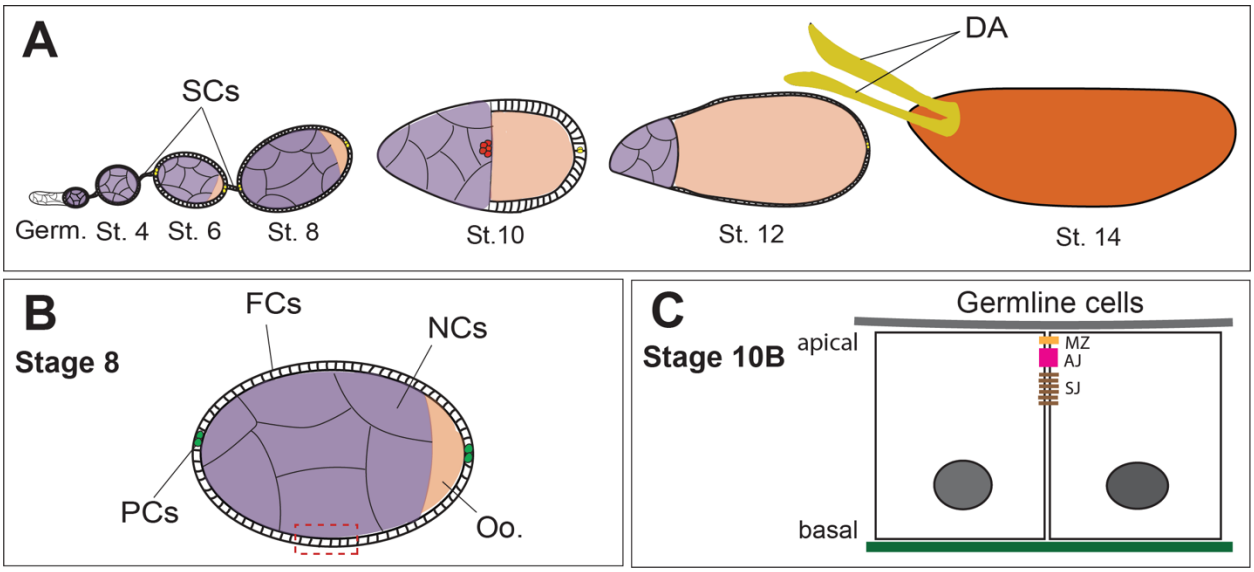

Figure 1. 2 Schematic diagram of *Drosophila* oogenesis.
(A) Female *Drosophila* have 16–20 ovarioles, which are strings of egg chambers. An egg is formed in the germarium (Germ.), where germline and somatic stem cells reside. After an egg is formed, it leaves the germarium region and progresses through 14 developmental stages through which the egg increases in length along the anterior-posterior axis. (B) Each egg consists of 16 germline cells – 15 nurse cells (NCs) and one oocyte (Oo.) – which are encapsulated by a monolayer of follicle cells (FCs). At the anterior and posterior tip of the egg chamber is a specialized pair of FCs known as the polar cells (PCs). (C) The FCs have defined apical-basal polarity, where the apical surface faces the germline cells, and the basal surface maintains an attachment to the extracellular matrix. Moreover, FCs form specialized junctions along the lateral membrane. At the most apical membrane is the marginal zone (MZ, orange), basal to the MZ is the adherens junction (AJ, magenta). At stage 10B of oogenesis, the septate junction (SJ) forms ladder-like septa just basal to the AJ. Anterior is to the left and posterior to the right. This figure is adapted from Alhadyian, Shoaib, and Ward 2021, *G3* Journal (see chapter II for details).

Characteristics of the *Drosophila* egg epithelium

The FCs of the *Drosophila* egg chamber are similar to epithelial cells in higher animals (**Figure 1. 2** C). The apical surface of the FCs contacts the oocyte, whereas the basal surface attaches to the extracellular matrix underlying it. FCs have defined apical-basal polarity with lateral junctional complexes (Müller 2000; Horne-Badovinac and Bilder 2005). In the most apical domain of the cell is the sub-apical zone known as the marginal zone. Basal to the marginal zone is the adherens junction, which provides cell–cell adhesion. Basal to the adherens junction is the SJ, which acts as a physical barrier between cells. Ultrastructural analysis and dye exclusion

experiments indicate that SJ formation and maturation occur at stage 10B and 11 egg chambers, respectively (Mahowald 1972; Müller 2000; Isasti-Sanchez, Munz-Zeise, and Luschnig 2021). The basal surface of the FCs adheres to the extracellular matrix via cell–extracellular matrix (ECM) adhesion receptors, including the α and β subunits of integrins (Isabella and Horne-Badovinac 2015a).

SJ proteins are expressed in the ovary

A few SJ proteins were shown to be expressed in the ovary as early as in the germarium region. For example, Mcr is expressed in the anterior region of the germarium (Hall et al. 2014), whereas Cora is used as a marker for escort cells, which are differentiated FCs that encapsulate individual germline cysts within the germarium (Maimon, Popliker, and Gilboa, 2014). In the FCs of early-stage egg chambers, Cora and Fas3 are expressed along the lateral membrane, but become slightly enriched at the apical-lateral membrane from stage 7 egg chambers (Ng et al. 2016). Finally, a study by Schneider et al. shows that Cont, Nrx-IV, and Nrg are expressed in the FCs (Schneider et al. 2006). These studies indicate that at least five SJ proteins are expressed in the FCs, yet their sub-cellular localization throughout oogenesis has not been determined. Moreover, although SJ proteins localize at the FC membrane, which is the driving force of egg morphogenetic events, our understanding of SJ proteins contribution to egg morphogenesis remains unknown.

Morphogenesis of the *Drosophila* egg chamber

Epithelial tissues undergo dynamic morphogenetic processes to obtain specific morphologies, and the epithelium of the *Drosophila* egg chamber is no exception. The first morphogenetic

process occurs in the germarium region, where the FC precursors undergo centripetal movements to encase the germline cyst (Horne-Badovinac and Bilder 2005). By stage 9 of oogenesis, 6–10 anterior FCs delaminate from the surrounding epithelium and migrate between the nurse cells until they reach the oocyte – a process known as *border cell migration* (Montell 2003). Border cell migration is required to form the micropyle, a hole through which sperm enters the egg (Horne-Badovinac, 2020). By stage 10B, two populations of dorsal FCs undergo cell shape changes and rearrangements while migrating to form the dorsal appendages, which act as respiratory organs for the developing embryo (Osterfield, Berg, and Shvartsman 2017). Throughout the 14 developmental stages of oogenesis, a spherical egg becomes an ellipsoid that is 2.2–2.5 times longer than its width, a process known as *egg elongation* (compare stage 3 to stage 14 egg chambers in **Figure 1. 2**) (Horne-Badovinac and Bilder 2005; Horne-Badovinac 2014). Since the FCs are the main driving force for egg morphogenesis, maintaining an intact epithelium throughout oogenesis is essential for the morphogenetic processes to occur normally. In the following subsection, I provide a brief overview of the known mechanisms that contribute to egg elongation, which is the primary morphogenetic event discussed in this study.

Drosophila egg elongation as a model system to study the role of SJ proteins in morphogenesis

Four cellular events contribute to egg elongation and occur in three phases (**Figure 1. 3** A). In phase I, pulsatile contractions at the apical domain of the FCs promote egg elongation from stages 3–6 (Alégot et al. 2018). The second process is at stages 7–8 and involves FC migration. FC migration reinforces the formation of planar-polarized basal actin filaments and ECM protein fibrils, which is the third cellular process required for egg elongation (Cetera and Horne-

Badovinac 2015; Crest et al. 2017; Viktorinová et al. 2009). Phase II happens over stages 9–10B and is mediated via basal actomyosin contractions (Qin et al. 2017; He et al. 2010; Koride et al. 2014; Popkova et al. 2020). In the last phase (stages 11–14), the fourth and final cellular process requires the formation and re-orientation of basal actin stress fibers and the maintenance of planar-polarized ECM proteins fibrils (Cerqueira Campos et al. 2020; Haigo and Bilder 2011). The majority of the genes required for egg elongation encode members of the cell cytoskeleton and ECM, and their associated proteins (Table 1. 2). Therefore, it is generally accepted that disruption to the actin cytoskeleton and/or ECM is the primary cause of egg elongation defects. Whether SJ proteins contribute to egg elongation is unknown.

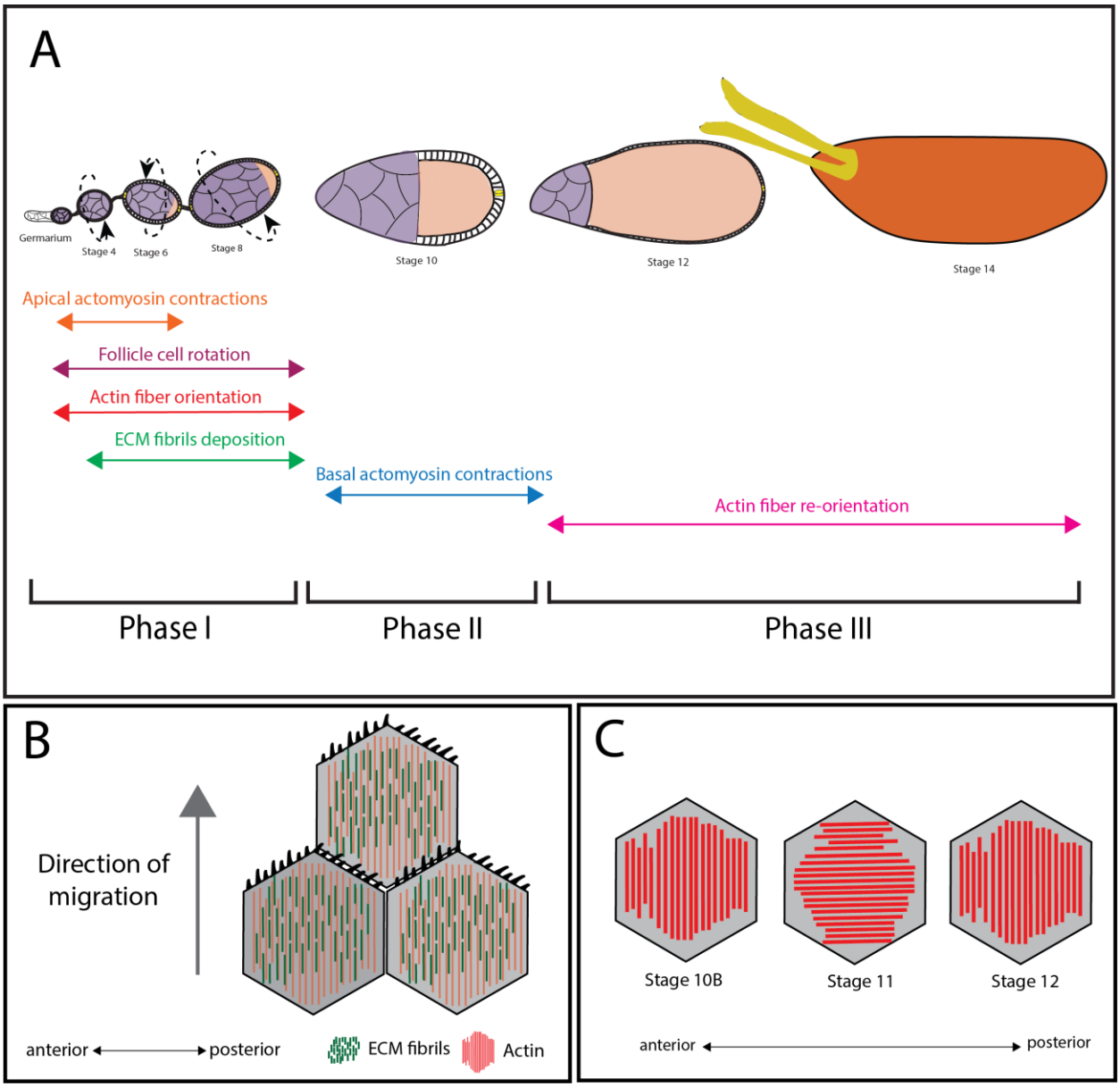

Figure 1. 3 Elongation of the *Drosophila* egg chamber.
(A) Diagram of an ovariole, which is a line of progressively developing egg chambers. Each egg chamber buds off from the germarium region as a sphere-shaped egg and undergoes 14 developmental stages resulting in an elongated egg. In phase I (stages 1–8), four cellular processes contribute to egg elongation. From stages 3–6, apical actomyosin contractions, mediated via a gradient of JAK-STAT signaling pathway. From stages 4-6, follicle cells (FCs) migration orients basal actin stress fibers perpendicular to the anterior-posterior axis. As the FCs migrate, they secrete extracellular matrix (ECM) fibrils. Together, basal actin stress fibers and ECM fibrils form the molecular corset, which constrains egg growth in the dorsal-ventral axis. In Phase II (stages 9–10), basal actin stress fibers undergo periodic contractions, contributing to egg elongation. The last phase of egg elongation is Phase III (stages 10B-14), where the egg shape is maintained via the formally formed planar-polarized molecular corset. (B) Diagram of the basal surface of migratory FCs showing the planar-polarized orientation of actin stress fibers (red lines) and ECM fibrils (green lines), which align perpendicular to the anterior-posterior axis. (C)

Diagram of a basal view of stage 10B, 11, and 12 FCs showing the re-orientation event of basal actin stress fibers late in oogenesis. Anterior is to the left and posterior is to the right.

	Gene name	Protein function	Reference
1	Fat2	Atypical cadherin	(Gutzeit et al., 1991; Viktorinová et al., 2009)
2	M6	Proteolipid protein	(Zappia et al., 2011)
3	Abi	A component of the WAVE actin nucleator complex	(Cetera et al., 2014; Squarr et al., 2016)
4	WAVE	Primary regulator of the Arp2/3 complex	(Squarr et al., 2016)
5	Furry	Activator of the nuclear DBF-2-related kinase signaling	(Horne-Badovinac et al., 2012)
6	Tricornered	Activator of the nuclear DBF-2-related kinase signaling	(Horne-Badovinac et al., 2012)
7	Sra-1	Component of the WAVE actin nucleator complex	(Squarr et al., 2016)
8	Misshapen	Ste20-like kinase	(Lewellyn et al., 2013)
9	Pak	p21-activated kinase	(Vlachos & Harden, 2011)
10	Rho1	Small GTPase	(Vlachos & Harden, 2011)
11	Semaphorin	A member of the Semaphorins family	(Stedden et al., 2019)
12	Plexin A	Transmembrane receptor for Semaphorin ligands	(Stedden et al., 2019)
13	CLASP	Microtubules stabilizing complex	(Chen et al., 2017)
14	Spastin	Microtubules severing complex	(Chen et al., 2017)
15	Collagen IV	BM component	(Haigo S. L. & Bilder, 2011; Isabella & Horne-Badovinac, 2015b)
16	Trol (Perlecan)	BM component	(Isabella & Horne-Badovinac, 2015b)
17	Rab10 GTPase	Exocytosis Rab	(Lerner et al., 2013)
18	SPARC	Collagen binding protein	(Isabella & Horne-Badovinac, 2015b)
19	Plod	Endoplasmic Reticulum-resident enzyme	(Lerner et al., 2013)
20	beta-integrin	ECM receptor	(Bateman et al., 2001)
21	Alpha-integrin (if)	ECM receptor	(Bateman et al., 2001)
22	Alpha-integrin (mew)	ECM receptor	(Bateman et al., 2001)
23	Leukocyte-antigen-related-like (Lar)	ECM receptor	(Bateman et al., 2001)
24	Dystroglycan	ECM receptor	(Cerqueira Campos et al., 2020)
25	Dystrophin	Cytoplasmic protein links actin to the ECM receptor Dystroglycan	(Cerqueira Campos et al., 2020)
26	Talin	Adaptor protein of integrin	(He et al., 2010; Qin et al., 2017)
27	Tensin	Adaptor protein of integrin	(Cha et al., 2017)
28	Paxillin	Adaptor protein of integrin	(He et al., 2010)
29	Yorki	Transcriptional co-activator of Hippo	(Fletcher et al., 2018)
30	Dynamin	Clarthin	(Peters & Berg, 2016)
31	Short egg	Unknown	(Wieschaus et al., 1981)
32	Tiny	Unknown	(Falk & King, 1964)

Transmembrane proteins
Actin associated proteins
Secreted signals and their associated proteins
Microtubules associated proteins
ECM and its associated proteins
Other
Unknown

Table 1. 2 Summary of genes that are required for egg elongation.
A literature review of the genes required for egg elongation revealed that the majority of these genes are componenets of the actin cytoskeleton, Extracellular matrix (ECM), and their associated proteins.

Phase I (stages 1–8): The establishment phase of egg elongation

At stage 6 of oogenesis, the anterior–posterior axis increases in length (e.g., Haigo and Bilder 2011). At the same time, basal actin filaments and ECM proteins begin to align perpendicular to the anterior–posterior axis (Haigo and Bilder, 2011; Cetera and Horne-Badovinac, 2014; Isabella and Horne-Badovinac, 2016). The first gene identified to disrupt the planar polarization of actin filaments and the ECM protein laminin was *fat2*, which encodes an atypical cadherin (Gutzeit, Eberhardt, and Gratwohl 1991; Viktorinová et al. 2009). *fat2* mutant eggs are shorter and wider than wild-type eggs (Gutzeit, Eberhardt, and Gratwohl 1991). Since the FCs of *fat2* mutant eggs lack planar-polarized actin and laminin and fail to elongate, Gutzeit has introduced the idea that planar-polarized actin filaments and ECM proteins form a *molecular corset* (**Figure 1. 3** B). The function of the corset is to constrain egg growth along the dorsal–ventral axis, channeling egg elongation across the anterior–posterior axis (Gutzeit, Eberhardt, and Gratwohl 1991). Since then, the identification of genes involved in the formation of planar-polarized molecular corset has been pursued. The results of these studies identified genes associated with the ECM or actin cytoskeleton, supporting Gutzeit's molecular corset model (Frydman and Spradling 2001; Bateman et al. 2001; Conder et al. 2007; Delon and Brown 2009; Vlachos and Harden 2011). However, it was unclear how actin and ECM proteins establish their planar polarization and through which mechanism the molecular corset influences egg elongation.

With the advancement of live imaging techniques, a fascinating cellular process in the FCs has been discovered (Haigo and Bilder 2011). Surprisingly, FCs are mobile during the

establishment phase of egg elongation. FCs extend actin-rich filopodia and lamellipodial protrusions and migrate against a static ECM (Cetera & Horne-Badovinac 2015; Haigo and Bilder 2011). Since the discovery of FC movement, several studies have focused specifically on FC migration and its relationship to the formation of a planar-polarized molecular corset (Haigo S. L. and Bilder 2011; Lewellyn, Cetera, and Horne-Badovinac 2013; Lerner et al. 2013; Cetera et al. 2014; Isabella and Horne-Badovinac 2016). As the FCs move against a static ECM, they secrete ECM protein fibrils via Rab10-mediated exocytosis, which results in the formation of the planar-polarized fibrils observed by Gutzeit (Lerner et al. 2013; Isabella and Horne-Badovinac 2015b; 2016). Moreover, a recent study by Alégot et al. demonstrated that egg elongation is more complex than originally thought. The authors show that apical contractions at each pole of the egg promote egg elongation from stages 3–6 and this event does not require FC migration and planar polarization of the molecular corset (Alégot et al. 2018).

Phase II (stages 9–10B): Actomyosin contraction counteracts the pressure from a growing cyst

Between stages 8–10, the egg gradually increases in volume due to yolk uptake from the FCs and hemolymph (Spradling 1993). A combination of live imaging analysis, quantitative modeling, and chemical and genetic manipulation experiments revealed a role for basal actomyosin contractions in egg elongation. These studies show the accumulation of a basal actomyosin network consisting of the non-muscle myosin II and polarized actin stress fibers (He et al. 2010; Qin et al. 2017; Popkova et al. 2020). Actin stress fibers are attached to the ECM via integrins (ECM receptors), talin (adopter protein essential for integrin adhesions), and paxillin (a linker of integrin to F-actin) (Koride et al. 2014; Qin et al. 2017; Popkova et al. 2020). Since actin stress

fibers are linked to the ECM as they contract, the mechanical force generated from these contractions feeds into the ECM, constricting egg growth to the poles, thus, promoting egg elongation (He et al. 2010).

Phase III (stages 11–14): Maintenance of an elongated-shaped egg

Throughout stages 6-10B, basal actin stress fibers are aligned perpendicular to the anterior-posterior axis (**Figure 1. 3** C). However, by stage 11, actin stress fibers change their orientation by 90º relative to their original direction (Delon & Brown, 2009). This process requires the disassembly of pre-existing actin fibers and the formation of new fibers perpendicular to the anterior–posterior axis (Delon & Brown, 2009) (**Figure 1. 3** C). Actin stress fibers rely on the planar-polarized ECM fibrils to determine their orientation (Cerqueira Campos et al. 2020). As stress fibers re-orient, focal adhesion complexes become enriched at the basal side of the FC (Delon & Brown, 2009). Eggs mutant for ECM receptors genes are round, reflecting the importance of maintaining cell-ECM adhesions in egg elongation (Bateman et al., 2001; Cha et al., 2017; Delon & Brown, 2009; He et al., 2010). Consistent with this idea, treating wild-type stage 12 eggs with collagenase results in collapsed round eggs (Haigo and Bilder 2011). Thus, actin stress fibers, ECM components, and the coupling between them ensure the maintenance of the egg shape late in oogenesis.

1.3. **Dissertation Overview**

The goal of my dissertation is to examine SJ biogenesis and the role of SJ proteins in morphogenesis using the *Drosophila* egg chamber as a model system. The second chapter demonstrates that SJ biogenesis is similar in the follicular epithelium as it is in the embryonic epithelia. It also shows that SJ proteins are required for the major morphogenetic events during oogenesis, including egg elongation, border cell migration, and the formation of the dorsal appendages. The third chapter investigates the mechanism by which Mcr is required for egg elongation. We find that Mcr requirement in egg elongation is late in oogenesis and is likely to be SJ-dependent. Late in oogenesis, RNAi-mediated knockdown of Mcr results in abnormal follicular epithelium morphology, disruption to actin stress fiber organization, and defective eggshell formation. Moreover, Mcr-depleted egg chambers have a compromised eggshell with defects in the formation of the wax and chorion layers.

Overall, this work contributes new data to the field of SJ and *Drosophila* oogenesis. We find interesting similarities in SJ biogenesis between the primary embryonic epithelia and secondary follicular epithelium. Because SJ proteins are similarly required for morphogenesis of the egg chamber, we think that this requirement is dependent on the formation of a SJ. Finally, the follicular epithelium could serve as a parallel system for further studies on the cellular and molecular mechanisms by which SJ proteins are required for tissue morphogenesis.

Chapter II: Septate junction proteins are required for egg elongation and border cell migration during oogenesis in *Drosophila*

The data and text in Chapter II has been accepted at *G3 Genes: Genomes: Genetics* journal (March 2021) with minor revisions to the text and figures' legends. At the time of submitting this dissertation, the manuscript has not been published. Below are the authors who contributed to this chapter.

Alhadyian, H., Shoaib, D. and Ward R. "Septate junction proteins are required for egg elongation and border cell migration during oogenesis in *Drosophila.*"

2.1 Abstract

Protein components of the invertebrate occluding junction - known as the septate junction (SJ) - are required for morphogenetic developmental events during embryogenesis in *Drosophila melanogaster*. In order to determine whether SJ proteins are similarly required for morphogenesis during other developmental stages, we investigated the localization and requirement of four representative SJ proteins during oogenesis: Contactin, Macroglobulin complement-related, Neurexin IV, and Coracle. A number of morphogenetic processes occur during oogenesis, including egg elongation, formation of dorsal appendages, and border cell migration. We found that all four SJ proteins are expressed in egg chambers throughout oogenesis, with the highest and most sustained levels in the follicular epithelium (FE). In the FE, SJ proteins localize along the lateral membrane during early and mid-oogenesis, but become enriched in an apical-lateral domain (the presumptive SJ) by stage 10b. SJ protein relocalization requires the expression of other SJ proteins, as well as rab5 and rab11 in a manner similar to SJ biogenesis in the embryo. Knocking down the expression of these SJ proteins in follicle cells throughout oogenesis results in egg elongation defects and abnormal dorsal appendages. Similarly, reducing the expression of SJ genes in the border cell cluster results in border cell migration defects. Together, these results demonstrate an essential requirement for SJ genes in morphogenesis during oogenesis, and suggest that SJ proteins may have conserved functions in epithelial morphogenesis across developmental stages.

2.2 Introduction

The septate junction (hereafter referred to as SJ) provides an essential paracellular barrier to epithelial tissues in invertebrate animals (Noirot-timothée et al. 1978). As such, the SJ is functionally equivalent to the tight junction in vertebrate tissues, although the molecular components and ultrastructure of these junctions differ (reviewed in Izumi and Furuse 2014).

Studies in *Drosophila* have identified more than 20 proteins that are required for the organization or maintenance of the SJ (Fehon et al. 1994; Baumgartner et al. 1996; Behr et al. 2003; Paul et al. 2003; Genova and Fehon 2003; Faivre-Sarrailh et al. 2004; Wu et al. 2004; Wu et al. 2007; Tiklová et al. 2010; Nelson et al. 2010; Ile et al. 2012; Bätz et al. 2014; Hall et al. 2014). Given that some of these genes have clear developmental functions (e.g. *coracle*'s name derives from its dorsal open embryonic phenotype; (Fehon et al. 1994), we previously undertook an examination of the developmental requirements for a set of core SJ genes (Hall and Ward 2016). We found that all of the genes we analyzed (9 in all) are required for morphogenetic developmental events during embryogenesis including head involution, dorsal closure and salivary gland organogenesis. Interestingly, these embryonic developmental events occur prior to the formation of an intact SJ, suggesting that these proteins have a function independent of their role in creating the occluding junction (Hall and Ward 2016). Since strong loss of function mutations in every SJ gene are embryonic lethal (due to these morphogenetic defects and/or a failure in establishing a blood-brain barrier in glial cells; Baumgartner et al. 1996), only a few studies have examined the role of SJ proteins in morphogenesis at a later stages of development. These studies have revealed roles for SJ proteins in planar polarization of the wing imaginal disc, for epithelial rotations in the eye and genital imaginal discs, and ommatidia integrity (Lamb et al. 1998; Venema et al. 2004; Moyer and Jacobs 2008; Banerjee et al. 2008).

To further explore the role of SJ proteins in morphogenesis beyond the embryonic stage, we set out to examine the expression and function of a subset of SJ genes in the *Drosophila* egg chamber during oogenesis. Each of the two *Drosophila* ovaries is comprised of approximately 16-20 ovarioles, which are organized into strings of progressively developing egg chambers (**Figure 2. 1** A). Each egg chamber forms in a structure called the germarium, where the germline and somatic stem cells reside. Once the egg chamber is formed, it leaves the germarium as 16-cell germline cyst consisting of 15 nurse cells and an oocyte surrounded by a layer of somatic follicle cells (FCs) (**Figure 2. 1**B). An egg chamber undergoes 14 developmental stages ending in a mature egg that is ready for fertilization (reviewed in Horne-Badovinac and Bilder 2005). Interfollicular cells called stalk cells connect egg chambers to each other. During oogenesis, the FE undergoes several morphogenetic events including border cell migration, dorsal appendage formation and egg elongation (reviewed in Horne-Badovinac and Bilder 2005; reviewed in Duhart et al. 2017).

Previous studies have revealed that a few core components of the SJ are expressed in the ovary, including Macroglobulin complement-related (Mcr), Neurexin IV (Nrx-IV), Contactin (Cont), Neuroglian (Nrg), and Coracle (Cora) (Wei et al. 2004; Schneider et al. 2006; Maimon et al. 2014; Hall et al. 2014; Ben-Zvi and Volk 2019), although the developmental expression pattern and subcellular localizations of these proteins have not been thoroughly investigated. Furthermore, ultrastructural analysis has revealed the presence of mature SJs in the FE by stage 10/10B of oogenesis (**Figure 2. 1** C), while incipient SJ structures have been observed in egg chambers as early as stage 6 (Mahowald 1972; Müller 2000). The biogenesis of SJs in embryonic epithelia is a multistep process in which SJ proteins are initially localized along the lateral membrane, but become restricted to an apical-lateral region (the SJ) in a process that required

endocytosis and recycling of SJ proteins (Tiklová et al. 2010). How SJ maturation occurs in the FE is unknown.

Here, we analyzed the expression and subcellular localization of the core SJ proteins Mcr, Cont, Nrx-IV, and Cora throughout oogenesis. We find that all of these SJ proteins are expressed in the FE throughout oogenesis. Interestingly, Mcr, Cont, Nrx-IV, and Cora become enriched at the most apical-lateral region of the membrane in stage 10B/11 egg chambers, coincident with the formation of the SJ as revealed by electron microscopy (Mahowald 1972; Müller 2000) . Similar to the biogenesis of SJs in the embryo, the localization of SJ proteins to the presumptive SJ requires the function of other SJ genes, as well as *Rab5* and *Rab11*. Functional studies using RNA interference (RNAi) of SJ genes in FCs results in defects in egg elongation, dorsal appendage morphogenesis and border cell migration. Together, these results reveal a strong similarity in the biogenesis of SJ between embryonic and follicular epithelia, demonstrate that at least some components of the SJs are required for morphogenesis in the ovary, and suggest that these requirements may be independent of SJ proteins role in forming an occluding junction.

2.3 Results

Septate junction proteins are expressed in follicle cells throughout oogenesis

While a few SJ *proteins* have previously been reported to be expressed in the *Drosophila* ovary (Wei et al. 2004; Schneider et al. 2006; Hall et al. 2014; Maimon et al. 2014; Felix et al. 2015; Ben-Zvi and Volk 2019), a thorough analysis of their tissue distribution and subcellular localization throughout oogenesis is lacking. We therefore examined the spatial and temporal expression of four SJ proteins: Mcr, Cont, Nrx-IV and Cora (Fehon et al. 1994; Baumgartner et al. 1996; Faivre-Sarrailh et al. 2004; Bätz et al. 2014; Hall et al. 2014). These four proteins are core components of the junction for which well-characterized antibodies are available.

At early stages of oogenesis (stages 2–8), Mcr, Cont, and Nrx-IV all localize in puncta at the lateral membrane of FCs and nurse cells, and show a punctate distribution in these cells (**Figure 2. 1** D-G). Mcr, Cont, and Nrx-IV are also more strongly expressed in polar cells (PCs) than the surrounding FCs (asterisks in **Figure 2. 1** D-F). Cora is more uniformly localized along the lateral membrane of the FCs, including the PCs (**Figure 2. 1** G and data not shown). These SJ proteins are additionally expressed in stalk cells (arrowheads in **Figure 2. 1**D and E and data not shown). Beginning at stage 10B, Mcr, Nrx-IV, Cont and Cora are gradually enriched at the apical-lateral membrane of the FCs just basal to the AJ. This localization is complete by stage 11 and persists to the end of oogenesis (arrows in **Figure 2. 2** B, D, F, and H). The timing of this apical-lateral enrichment of Mcr, Cont, Nrx-IV and Cora coincides with the maturation of the SJ in the FCs based upon ultrastructural analysis (Mahowald 1972; Müller 2000), and so we will refer to this region as the presumptive SJ. Finally, all of these SJ proteins continue to be expressed in the FCs until stage 14 of oogenesis (**Figure 2. 1** C, E, G and I).

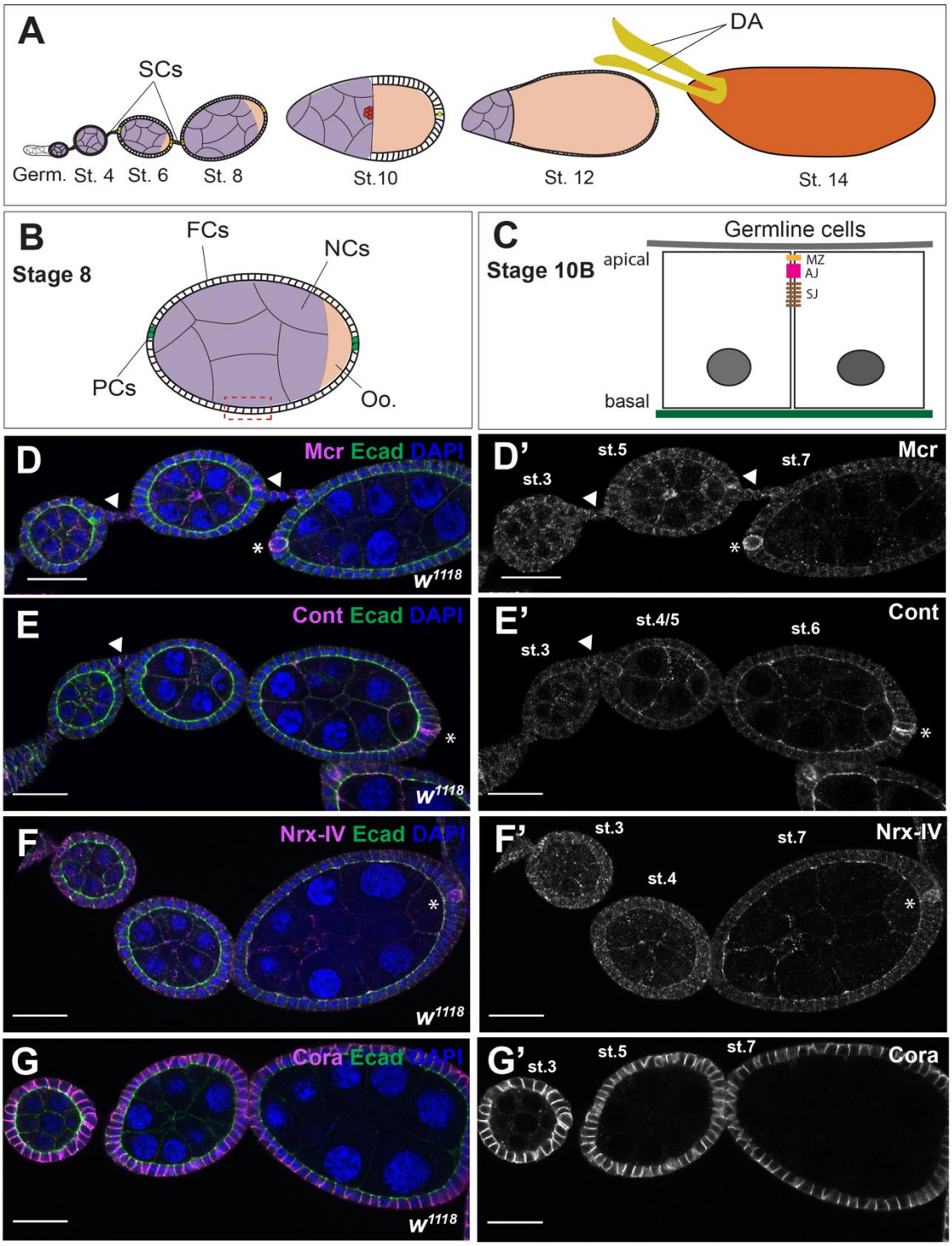

Figure 2. 1 Mcr, Cont, Nrx-IV, and Cora expression during early stages of oogenesis. (A) Diagram of a female *Drosophila* ovariole. Egg chambers are formed in the most anterior region of the ovariole called the germarium (Germ). Each egg chamber undergoes 14 developmental stages while connected to each other through stalk cells (SCs) to form a mature stage 14 egg. (B) Diagram of a stage 8 egg chamber. The egg chamber consists of 15 nurse cells (NCs) and one oocyte (Oo.), which are surrounded by a monolayer of follicle cells (FCs). At the anterior and posterior ends of an egg chamber resides a pair of differentiated FCs called polar

cells (PCs). (C) Diagram of a lateral view of a portion of a stage 10B egg chamber. FCs face the germline and have defined apical-basal polarity with the apical surface facing the germline and a lateral junctional complex consisting of a marginal zone (MZ), an adherens junction (AJ), and a septate junction (SJ). (D-G) Confocal optical sections of wild-type early stages egg chambers stained with antibodies against Mcr (D), Cont (E), Nrx-IV (F), and Cora (G) (Magenta and in individual channel in D'-G'), and co-stained with antibodies against Ecad (green) and labeled with DAPI (blue). All four SJ proteins are expressed throughout the egg chamber along FC membranes, including SCs (arrowheads in D and E, and data not shown for Nrx-IV and Cora) and in the NCs. Mcr, Cont, and Nrx-IV (D-F) are found along the membrane and in puncta, whereas Cora is found predominantly at the membrane (G). In addition, Mcr, Cont, and Nrx-IV are highly expressed in the PCs (asterisks in D-F), whereas Cora is expressed in these cells with same level of expression relative to the FCs. Note that the focal plane of these images shows strong staining in PCs in only one side of the egg chamber, but Mcr, Cont and Nrx-IV are equally expressed in both anterior and posterior PCs. Anterior is to the left in each ovariole. Scale bar= 25μm.

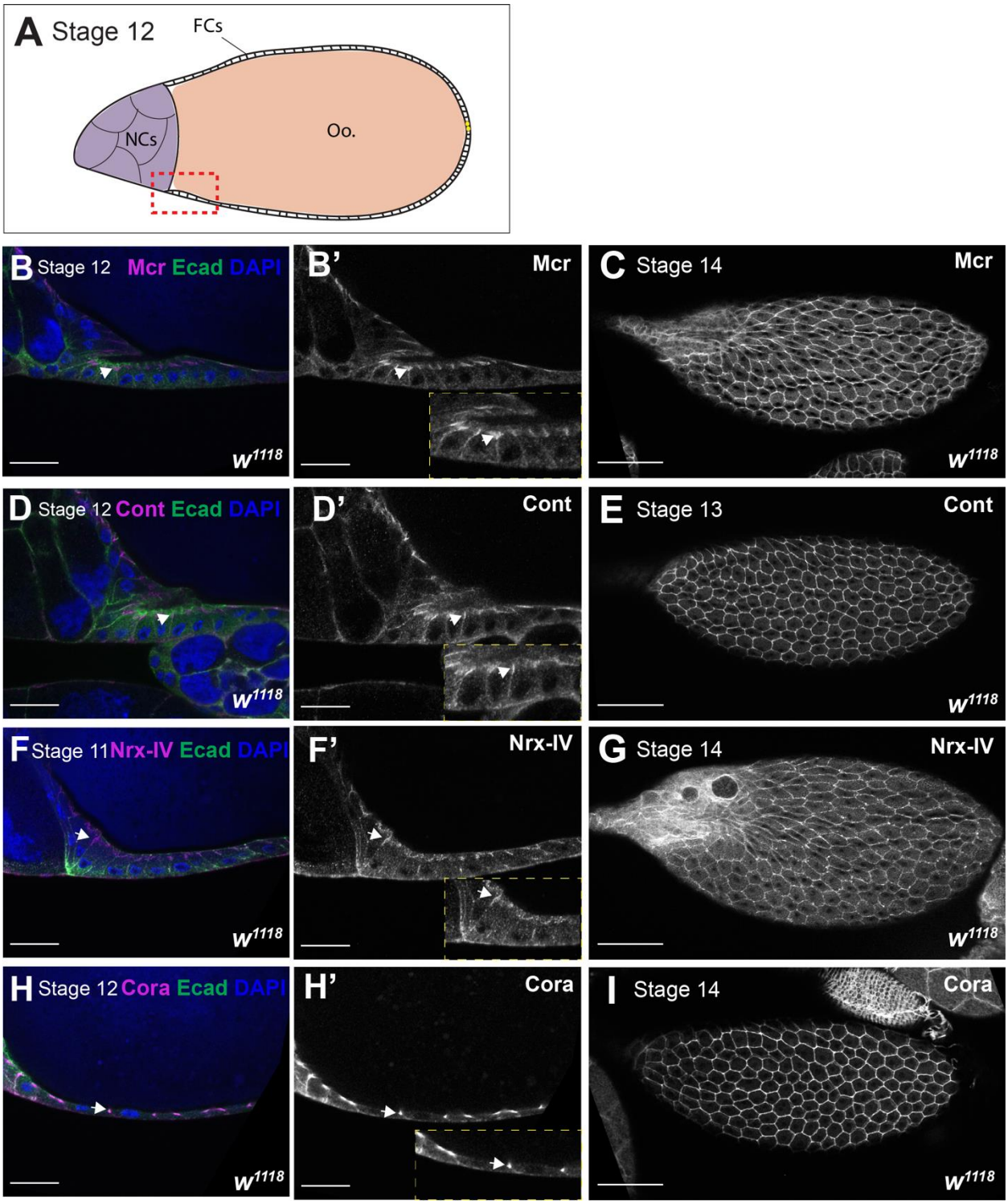

Figure 2. 2 Mcr, Cont, Nrx-IV, and Cora localization at later stages of oogenesis.
(A) Diagram of a stage 12 egg chamber. (B–I) Confocal optical sections of wild-type stage 11 – 12 egg chambers (B, D, F, and H) or stage 14/13 egg chamber (C, E, G, and I) stained with antibodies against Mcr (B and C), Cont (D and E), Nrx-IV (F and G), or Cora (H and I) (magenta and in individual channel in B', D', F', and H') and co-stained with antibodies against Ecad (green) and labeled with DAPI (blue). The location of these sections overlaps the boundary

between the oocyte (Oo.) and nurse cells (NCs) and is depicted as the red box in the diagram shown in (A). Note that Mcr, Cont, Nrx-IV, and Cora become enriched at the apical-lateral region of FCs membrane (arrows in B, D, F, and H). Insets show higher magnification of the indicated areas. The expression of all of these proteins persists in stage 14/13 egg chambers (C, E, G, and I). Anterior is to the left. Scale bar = 25µm in B, D, F, and H and 100µm in C, E, G, and I.

SJ proteins are required for egg elongation and dorsal appendage morphogenesis

Given our findings that these four SJ proteins are expressed in the FE throughout oogenesis, and our previous studies indicating a role for SJ proteins in morphogenesis, we wondered whether SJ proteins might be required for morphogenetic processes in the FE. The FE plays a critical role in shaping the egg chamber and producing the dorsal appendage, while a subset of FE cells participates in border cell migration to form the micropyle (Montell 2003; Horne-Badovinac 2020). Because SJ mutant animals die during embryogenesis, we used the *GAL4-UAS-RNAi* system to knock-down the expression of SJ proteins in the FCs (Brand and Perrimon 1993). To knock down expression of SJ proteins throughout the majority of oogenesis, we used *GR1-GAL4*, which is expressed in the FCs from stage 4 to 14 of oogenesis (Gupta and Schüpbach 2003; Wittes and Schüpbach 2018). In all, we tested Bloomington Transgenic RNAi Project (TRiP) lines made against six different SJ genes (*Cont*, *cora*, *Mcr*, *Lac*, *Nrx-IV*, and *sinu*). To examine overall egg chamber shape, we dissected stage 14 egg chambers from females expressing *SJ-RNAi* under the control of *GR1-GAL4*, imaged them on a compound microscope, and determined the aspect ratio of the egg chambers using measurements of egg chamber length and width using ImageJ/Fiji. Control stage 14 egg chambers (*GR1-GAL4>UAS-GFP*) had a mean aspect ratio of 2.3 (Figure 2. 3A and J). In contrast, the aspect ratio of stage 14 egg chambers from all *GR1-GAL4>SJ-RNAi* is significantly lower than control egg chambers (aspect ratios from 1.7 to 2.1; *t*-test *P* value <0.0001; Figure 2. 3B-G and J). All *SJ-RNAi* egg chambers

are significantly shorter than control (*t*-test *P* value <0.0001; Figure 2. 3H), and all but *Mcr-RNAi (BDSC) and Cont-RNAi* are also wider than control egg chamber (*t*-test *P* value <0.0001; Figure 2. 3I). To address the specificity of these results we also tested VDRC RNAi lines directed against Mcr, Cora, and Nrx-IV, and found similar effects on egg shape (Figure 2. 3). We also examined SJ protein expression in late-stage egg chambers for *Mcr*, *cora*, and *Nrx-IV-RNAi* to demonstrate that the RNAi was efficiently knocking down protein expression in this tissue (Figure S2. 1).

Further examination of stage 14 SJ mutant egg chambers revealed defects in dorsal appendage morphogenesis. Dorsal appendages are tubular respiratory structures that form from two populations of the dorsal FE known as floor and roof cells (Duhart et al. 2017). The primary phenotypes we observed in the *SJ-RNAi*-expressing egg chambers were missing dorsal appendages, or appendages that appeared to be short or broken (Figure 2. 3 and S2. 2**).** In addition, nearly all of the *SJ-RNAi*-expressing dorsal appendages that were present appeared to have a thinner stalk than found in control egg chambers (**Figure S2. 2**). In quantifying these phenotypes, both BDSC and VDRC RNAi lines against Mcr (BDSC: 52%, VDRC:18%) and Cora (BDSC: 15% and VDRC: 21%) produced egg chambers with defective dorsal appendages (Figure 2. 3M). However, the *Nrx-IV-RNAi* BDSC line did not produce abnormal dorsal appendages, whereas 33% of VDRC *Nrx-IV-RNAi* line results in defective dorsal appendages. Moreover, 19% of *Cont-RNAi-* and 13% of *Lac-RNAi*-expressing egg chambers have either missing or broken dorsal appendages. We did not observe these phenotypes in *sinu-RNAi*-expressing egg chambers (Figure 2. 3M).

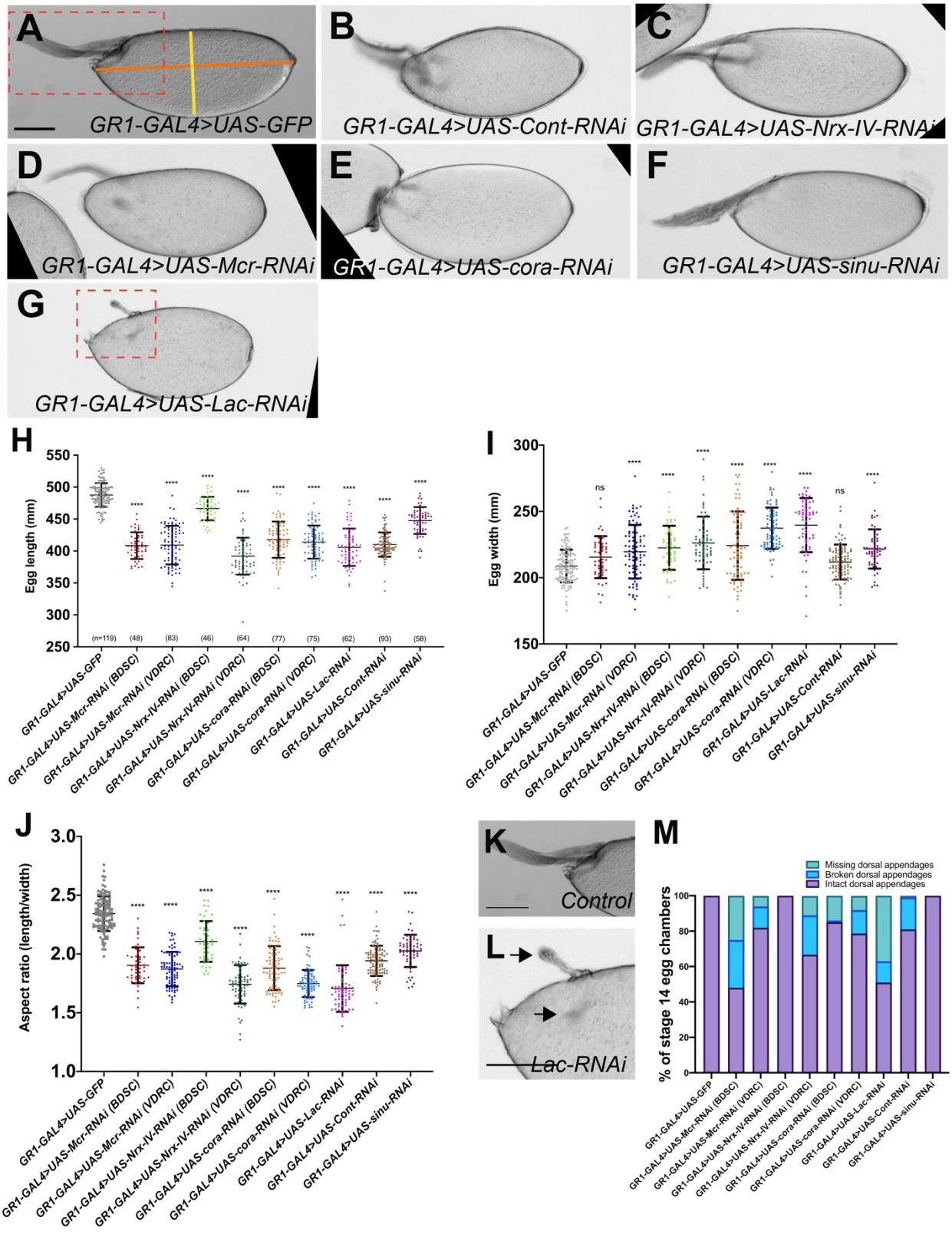

Figure 2. 3 *SJ* genes are required for egg elongation.

(A-G) Brightfield photomicrographs of stage 14 egg chambers. (A) *GR1-GAL4>UAS-GFP*, (B) *GR1-GAL4>UAS-Cont-RNAi*, (C) *GR1-GAL4>UAS-Nrx-IV-RNAi*, (D) *GR1-GAL4>UAS-Mcr-RNAi*, (E) *GR1-GAL4>UAS-cora-RNAi*, (F) *GR1-GAL4>UAS-sinu-RNAi*, and (G) *GR1-GAL4>UAS-Lac-RNAi*. Images in this figure represent average phenotypes observed in each genotype. (H and I) Quantification of length and width of stage 14 egg chambers from control and *SJ-RNAi* egg chambers. (J) Quantification of the aspect ratio of length (orange line in A) to width (yellow line in A) from control and *SJ-RNAi* stage 14 egg chambers. Note that the aspect ratio of all *SJ-RNAi* expressing egg chambers are statistically significant from the control egg chambers (unpaired *t*-test; P<0.0001). (K and L) Zoomed images of *GR1-GAL4>UAS-GFP* (K) and *GR1-GAL4>UAS-Lac-RNAi* (L) stage 14 egg chambers (from A and G) showing the dorsal appendages. The dorsal appendages in the *Lac-RNAi* egg chamber are either deformed or absent (arrows) compared to control dorsal appendages. (M) Quantification of dorsal appendage defects from control and *SJ-RNAi* stage 14 egg chambers. *n*, total number of egg chambers measured per genotype. Data represents individual values with mean ± s.d. *P* value <0.0001. Anterior is to the left. Scale bar = 100µm.

SJ proteins are expressed in polar and border cells and are required for effective border cell migration

The observation that Mcr, Cont, and Nrx-IV are strongly expressed in PCs and in all FCs (**Figure 2. 1**D-F), motivated us to investigate their expression during the process of border cell migration. Border cell migration occurs during stages 9-10 of oogenesis (**Figure 2. 4**A). During stage 9, signaling from the anterior PCs recruits a group of 4-8 adjacent FCs to form a cluster and delaminate apically into the egg chamber. The border cell cluster is organized with a pair of PCs in the center surrounded by border cells. This cluster of cells migrates between the nurse cells until they reach the anterior side of the oocyte (**Figure 2. 4**A). This process takes approximately 4-6 hours and is complete in wild-type egg chambers by stage 10 of oogenesis (Prasad and Montell 2007).. Previous studies show that Cora and Nrg are expressed in the PCs during their migration (Wei et al. 2004; Felix et al. 2015). To determine if other SJ proteins are also expressed during border cell migration, we stained stage 9-10 wild-type egg chambers with antibodies against Mcr, Cont, Nrx-IV and Cora. To mark the PCs, we co-stained the egg chambers with Fasciclin 3 (Fas3; Snow et al. 1989; Khammari et al. 2011). Mcr, Cont, Nrx-IV

and Cora are all expressed in border cell clusters throughout their migration (**Figure 2. 4**B-D and **Figure S2. 3**-5). Interestingly, the expression of these SJ proteins in PCs appears highest at the interfaces between PC and BCs (**Figure 2. 4**B-D and **Figure S2. 3**-5). SJ protein expression is also asymmetric in the border cell cluster, with higher expression along border cells closest to the oocyte, raising the possibility that these proteins may respond to or direct leading-edge polarity in the migrating border cell cluster (red arrows in **Figure 2. 4**B-D).

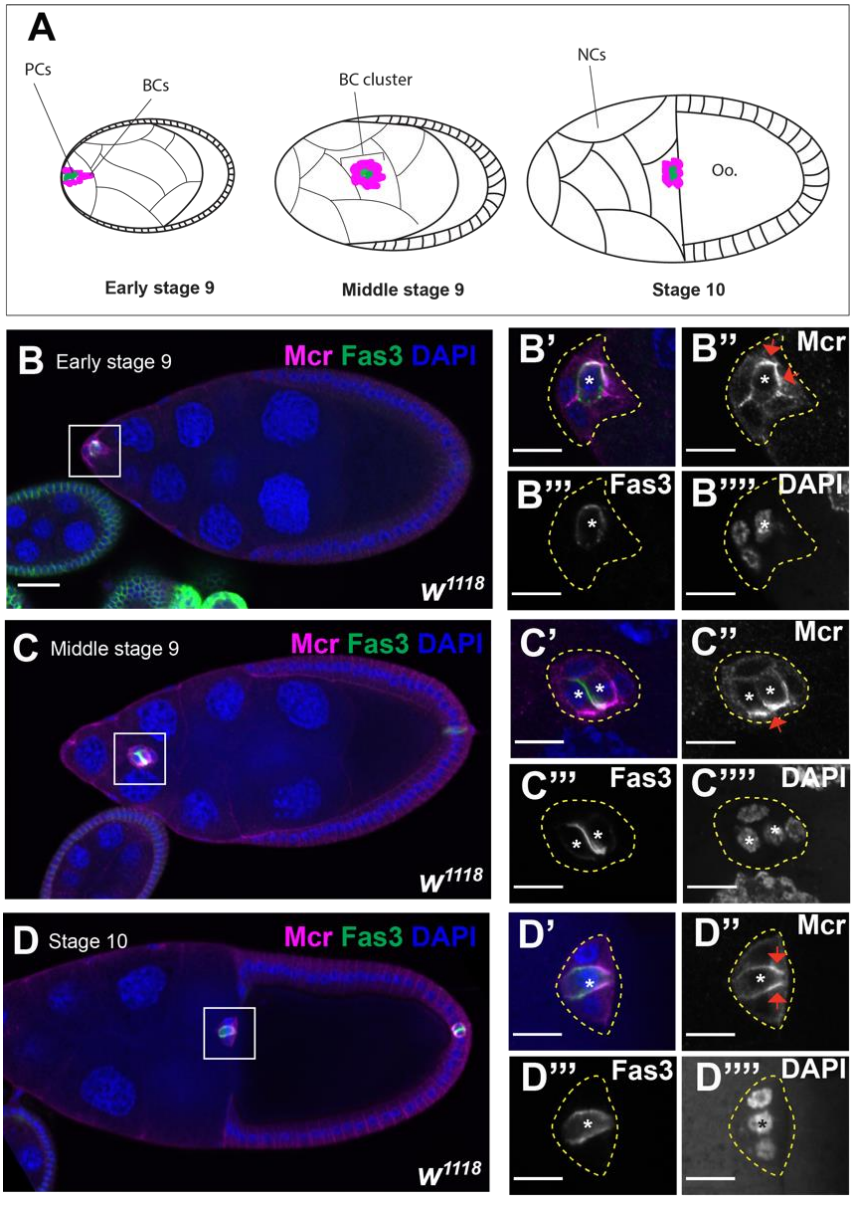

Figure 2. 4 Mcr expression during border cell migration.

(A) Diagram of border cell migration. At early stage 9 of oogenesis, a group of 4-6 follicle cells are specified by the polar cells (PCs) (green) to become border cells (BCs) (magenta). The BC/PC cluster delaminates apically and migrates between the nurse cells (NCs) until it reaches the oocyte (Oo.) by stage 10 of oogenesis. (B-D) Confocal optical images of wild-type stage 9-10 egg chambers stained with antibodies against Mcr (magenta, and in ” panels), Fas3 (green, and in ”’ panels), and labeled with DAPI (blue, and in ”” panels). PCs are indicated with asterisks. Mcr is expressed in the PCs and BCs with higher expression at the interface between the PCs and BCs. Note that Mcr appears to be most enriched along the boundary with BCs at the leading edge of the border cell cluster (red arrows in B”-D”). Anterior is to the left. Scale bar = 25µm in (B-D) and 10µm in (B’-B’’’’ - D’-D’’’’).

Given that Mcr, Cont, Nrx-IV and Cora are expressed in border cell clusters throughout border cell migration, we wondered if they are also required for some aspect of this process. To address this issue, we used *Slbo-GAL4* (Ogienko et al. 2018) to express RNAi against individual SJ genes specifically in border cells and analyzed the border cell clusters at stage 10 in these ovaries. We noticed a range of defective migration phenotypes in these egg chambers and classified them into three non-exclusive groups: failed, incomplete and dissociated clusters. Complete migration (**Figure 2. 5**A-C) is characterized by having the entire border cell cluster physically touching or just adjacent the oocyte by the end of stage 10 (**Figure 2. 5**C). A failed cluster is characterized by a border cell cluster that has not delaminated from the FE by stage 10 (**Figure 2. 5**D). An incomplete migration phenotype is characterized as an intact cluster that has not reached the oocyte by the end of stage 10 (**Figure 2. 5**E, where the two dashed lines indicate the range of distances at which border cell clusters were categorized as incomplete). Finally, a dissociated cluster phenotype is characterized by a cluster that has broken into a linear string of border cells or that has one or more border cells that remain between nurse cells and are not connected to the larger border cell cluster (**Figure 2. 5**F and H). In control stage 10 egg chambers (*Slbo-GAL4; UAS-mCD8-GFP/UAS-mCherry-RNAi*), 86% (n=81) of border cell clusters completed their migration, with the remainder showing incomplete migration (**Figure 2.**

5I). In contrast, stage 10 egg chambers expressing RNAi against *cora*, *Nrx-IV,* or *Cont* in the border cells resulted in 58% (n=67), 50% (n=74), and 40% (n=85) of border cell clusters completing migration, respectively (**Figure 2. 5**I). The remaining *cora-RNAi-* and *Nrx-IV-RNAi-*border cell clusters showed a combination of incomplete migration or failed to delaminate (**Figure 2. 5**I). *Cont-RNAi*-border cell clusters also showed 35% of incomplete border cell migration, but additionally had 17% of the clusters disassociating during their migration (**Figure 2. 5** E, F, H and I). *Mcr-RNAi*-border cell clusters were indistinguishable from controls with 86% (n=94) completing their migration and the remainder showing only 13% incomplete migration (**Figure 2. 5**I).

To extend these studies, we examined border cell migration in egg chambers expressing RNAi against SJ genes using the *C306-GAL4* driver. *C306-GAL4* is expressed in the border cells throughout the process of border cell migration (Murphy and Montell 1996) and in PCs just at stage 10 (H.A., unpublished observation). In control egg chambers (*C306-GAL4/UAS-Dcr; GAL80^{ts}*/+), 78% (n=91) of BC clusters completed their migration and 19% displayed incomplete migration (**Figure 2. 5**J). Stage 10 egg chambers expressing *C306>Mcr-RNAi* displayed 66% (n=98) complete border cell migration with 30% showing incomplete migration, 5% showing dissociated clusters and 3% showing failed border cell migration (**Figure 2. 5**J). Similarly, egg chambers expressing *C306>Nrx-IV-RNAi* displayed 66% (n=59) complete border cell migration with 30% showing incomplete migration and 3% failing to delaminate (**Figure 2. 5**J). Finally, 78% (n=70) of stage 10 *C306>cora-RNAi*-expressing border cells displayed complete border cell migration, whereas 20% showed incomplete migration and 3% failed to delaminate (**Figure 2.**

5J).

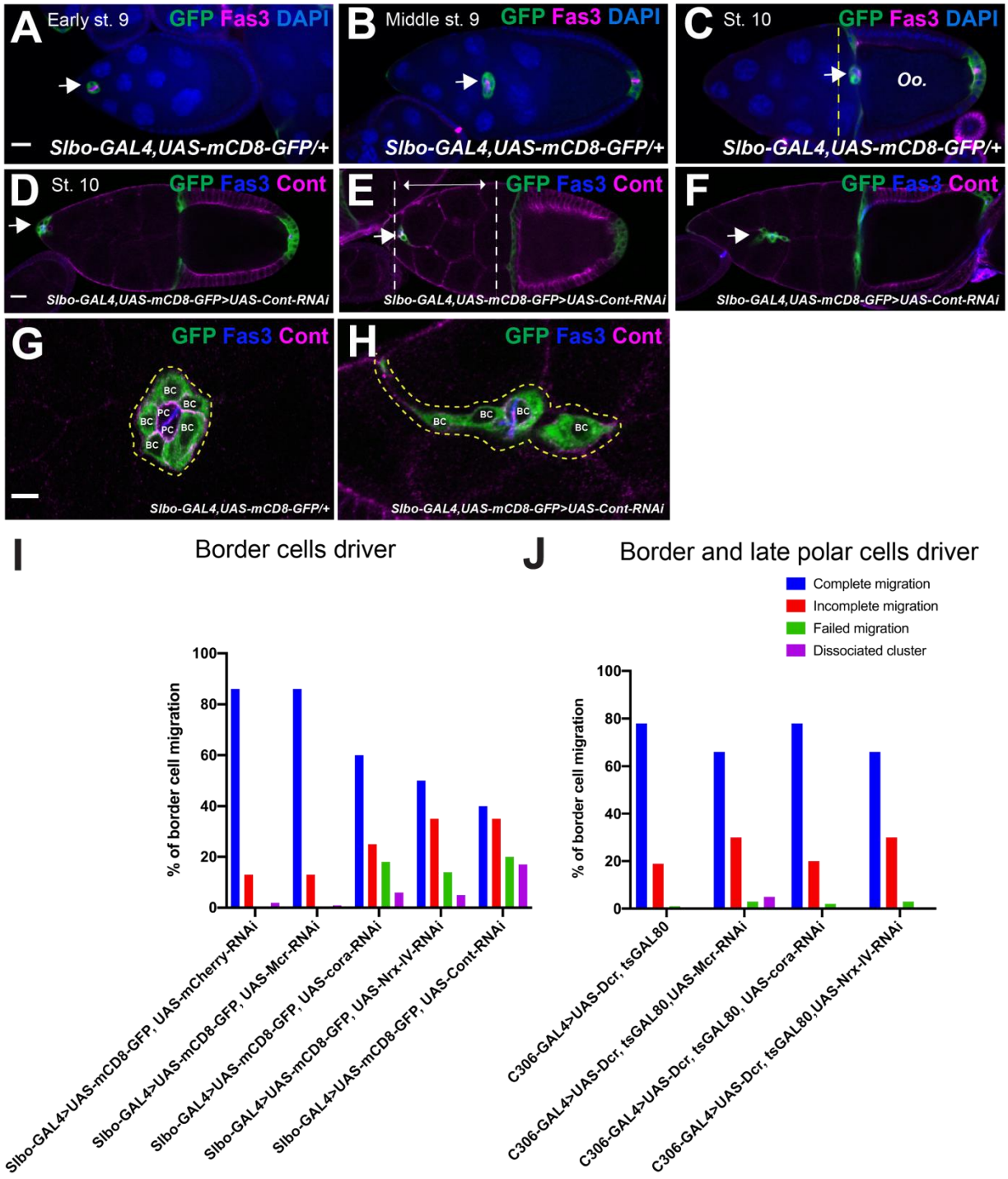

Figure 2. 5 Mcr, Cont, Nrx-IV, and Cora are required for effective border cell migration. (A-C) Border cell migration in control egg chambers. Egg chambers are immunostained with anti-Fas3 (magenta) to mark the polar cells, GFP (green) to mark border cells, and labeled with DAPI (blue). Arrows indicates border cell clusters. Note that in control egg chambers the border cell cluster reaches the oocyte (Oo.) at stage 10 (C). (D-F) Stage 10 egg chambers expressing

Cont-RNAi in border cells immunostained with anti-Cont (magenta) and anti-Fas3 (blue) showing examples of BC cluster migration defects: failed (arrow in D), incomplete (arrow in E), and disassociated border cell migration (arrow in F). Higher magnification of control (G) and *Cont-RNAi*-expressing (H) border cell clusters showing the dissociation of a border cell cluster observed in *SJ-RNAi* clusters. (I and J) Quantification of border cell cluster phenotypes at stage 10 egg chambers in control and *SJ-RNAi* driven by either *Slbo-GAL4* (I) or *C306-GAL4* (J). Anterior is to the left. Scale bar = 25μm.

SJ biogenesis in the FE

The redistribution of SJ proteins in the FCs of later stage egg chambers resembles the dynamic relocalization of SJ proteins during the biogenesis of the junction during embryogenesis (Tiklová et al. 2010). In embryonic epithelia, SJ protein enrichment at the apical-lateral domain (presumptive SJ) requires endocytosis and recycling of SJ proteins to the membrane, and is interdependent on the presence of all core SJ proteins (Ward et al. 1998; Hall et al. 2014). Coincident with the strong localization of SJ proteins to the presumptive SJ at stage 16 of embryogenesis, ladder-like electron-dense intermembrane septae are visible by electron microscopy that become progressively organized by stage 17 (Schulte et al. 2003; Hildebrandt et al. 2015). We therefore sought to determine if SJ biogenesis in the follicular epithelium requires endocytosis and recycling.

To test for the interdependence of SJ proteins for localization, we examined Cora and Mcr expression in wild-type, *Mcr-RNAi*, and *Nrx-IV-RNAi* stage 12 FCs. In wild-type stage 12 egg chambers, Cora is strongly co-localized with Mcr at the apical-lateral domain of the FCs (completely penetrant in 95 cells from 31 egg chambers) (**Figure 2. 6**A). In contrast, Cora and Mcr are mislocalized along the lateral domain in stage 12 *Nrx-IV-RNAi* FCs (Figure 2.6 B), much like they are in stage 2-8 wild-type FCs (**Figure 2. 1**D). Specifically, 6 out of 20 *Nrx-IV-RNAi* FCs cells from 19 egg chambers showed complete mislocalization, whereas 13 of these 20 cells showed largely lateral localization with some degree of apical enrichment. Similarly, in

stage 12 *Mcr-RNAi* FCs, Cora was mislocalized along the lateral membrane in 39 out of 47 cells examined from 19 egg chambers, with the remaining 8 cells showing some enrichment of Cora at the apical lateral domain (**Figure 2. 6**C). Notably, cells that showed apical enrichment of Cora also retained small foci of Mcr expression that overlaps with the enriched Cora (**Figure 2. 6**D), suggesting the perdurance of Mcr in these cells may have allowed for normal SJ organization. Together, these experiments indicate that SJ biogenesis in the FE of late-stage egg chambers requires the expression of at least some core SJ proteins.

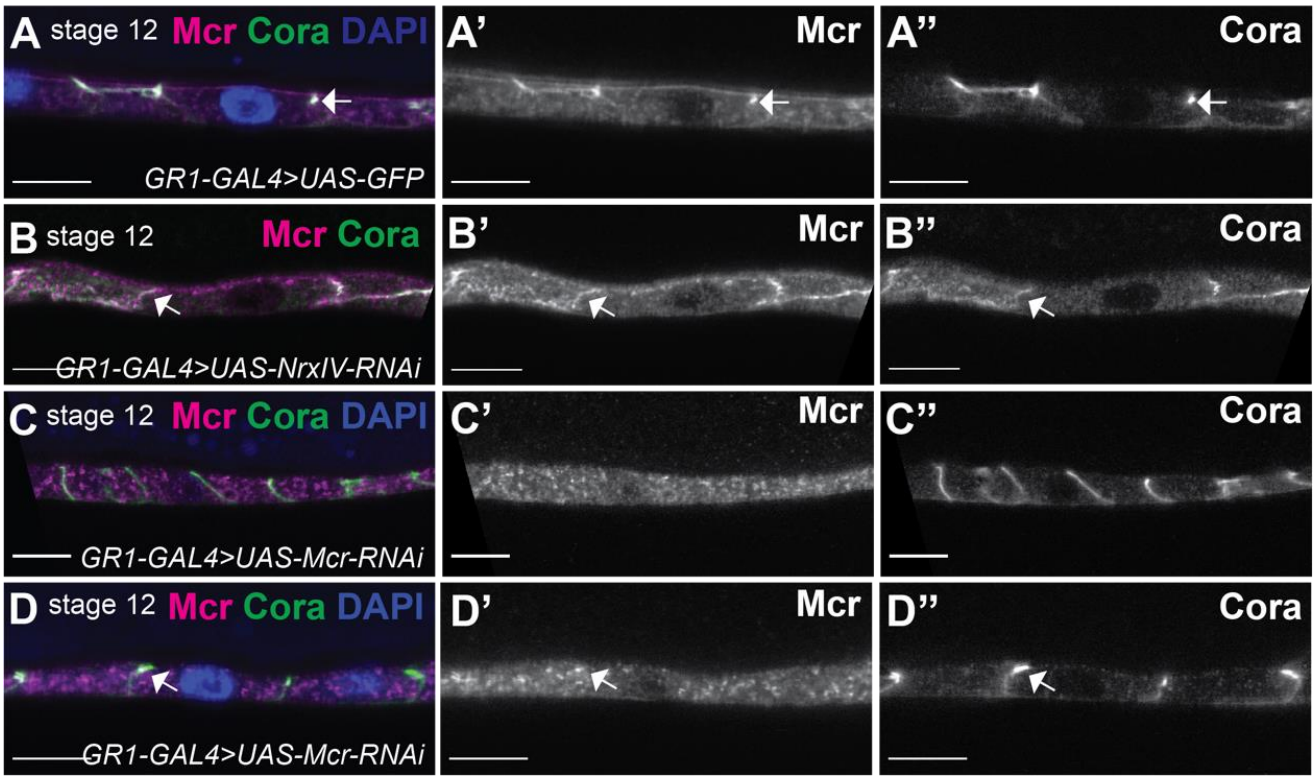

Figure 2. 6 The apical-lateral localization of Cora depends on *Mcr* and *Nrx-IV*.
(A-D) Confocal optical sections of stage 12 FCs stained with antibodies against Mcr (magenta, and in ' panels) and Cora (green, and in " panels) and labeled with DAPI (blue). Mcr and Cora co-localize at the presumptive SJ in control stage 12 egg chambers (A), whereas Mcr and Cora localize along the lateral membrane of *NrxIV-RNAi* expressing FCs (B). In most *Mcr-RNAi*-expressing stage 12 egg chambers, Cora localizes laterally (C), whereas in some egg chambers, Cora is enriched apically (arrow in D''), but is often associated with Mcr puncta (arrow in D'). Scale bar = 10µm.

We next wanted to investigate whether the relocalization of SJ proteins to the presumptive SJ required endocytosis and recycling. In the embryonic hindgut, Cora, Gliotactin (Gli), Sinu, and Melanotransferrin (Mtf) localize with the early endosomal marker, Rab5, and partially localize with the recycling marker, Rab11 during SJ biogenesis (Tiklová et al. 2010). Moreover, blocking Rab5 or Rab11 function prevents Cora, Gli, Sinu, and Mtf apical-lateral localization (Tiklová et al. 2010), and thus SJ formation. To determine if similar processes occur during SJ formation in FCs, we expressed a dominant negative version of Rab5 (*UAS-Rab5^{DN}*) in FCs using *GR1-GAL4* and examined the expression of Mcr and Cora in stage 11 FCs. In wild-type FCs at that stage, Mcr and Cora are enriched at the apical-lateral membrane (completely penetrant in 91 cells from 15 egg chambers; arrows in **Figure 2. 7**A), whereas both Mcr and Cora remain localized along the lateral membrane in the *Rab5^{DN}*-expressing FCs (n=97 cells, 15 egg chambers; **Figure 2. 7**B). Similarly, Cora and Mcr co-localize at the apical-lateral membrane of the FCs of stage 12 egg chambers (n=64 cells, 15 egg chambers; arrows in **Figure 2. 7**C), whereas knocking down the expression of Rab11 in stage 12 FCs results in the mislocalization of Cora and Mcr (n=23 cells, total 70 cells), 16 egg chambers; arrow in **Figure 2. 7**D). Cora is exclusively mislocalized along the lateral membrane in these cells, whereas Mcr is most frequently missing from the plasma membrane, either in punctate cytoplasmic foci or completely gone (in 21 of the 70 *Rab11-RNAi* cells; **Figure 2. 7**D). Interestingly, we noted that the FE in *Rab5^{DN}*- and *Rab11-RNAi*-expressing egg chambers are taller in the apical/basal dimension than similarly staged wild-type egg chambers (compare **Figure 2. 7**A with 2.7B and **Figure 2. 7**C with 2. 7D), although the effect is often observed with *Rab5^{DN}* than with *Rab11-RNAi*. Taken together, these results suggest that similar to embryonic epithelia, the maturation of SJs in the FE requires Rab5-mediated endocytosis and Rab11-mediated recycling.

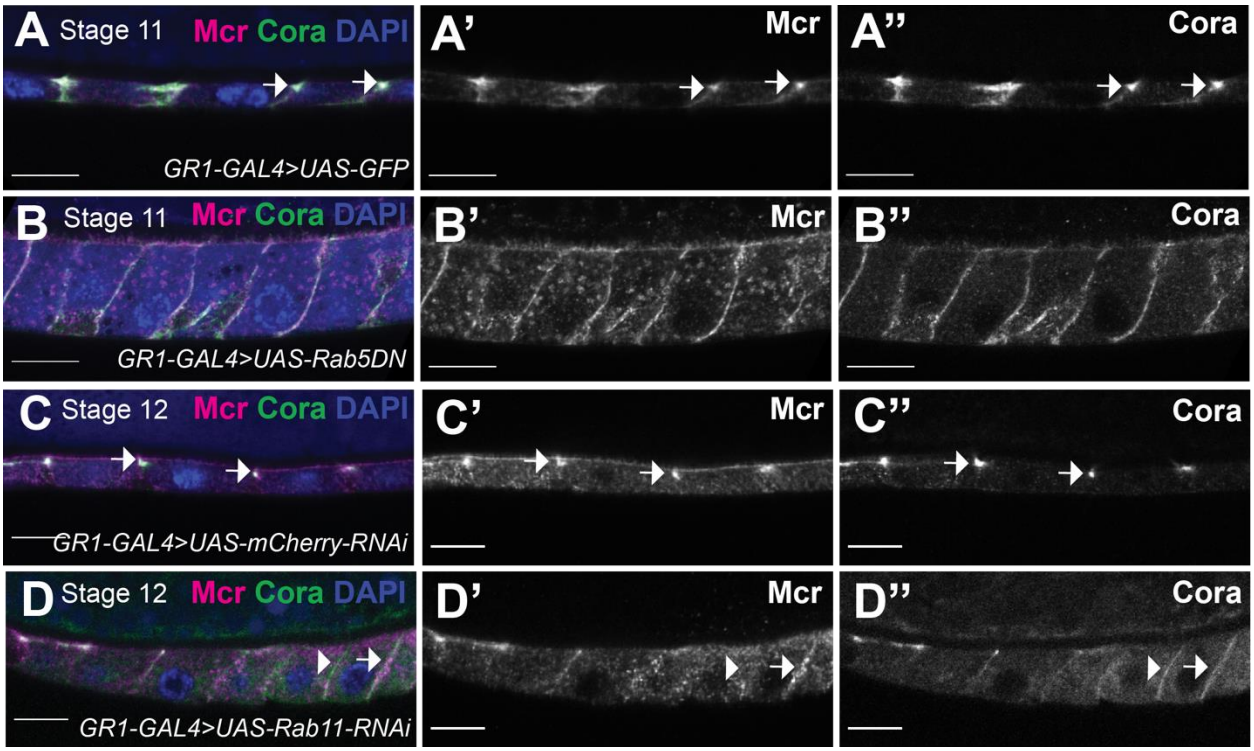

Figure 2. 7 Mcr and Cora require Rab5 and Rab11 for their correct localization at the SJ. (A-D) Confocal optical sections of stage 11 (A and B) or stage 12 (C and D) FCs stained with antibodies against Mcr (magenta, and in ' panels) and Cora (green, and in " panels) and labeled with DAPI (blue). While Mcr and Cora co-localize at the apical-lateral membrane of stage 11 and 12 control FCs (arrows in A and C), both Cora and Mcr fail to localize at the SJ in $Rab5^{DN}$-expressing FCs (B). In *Rab11-RNAi*-expressing FCs (D), Cora localizes along the lateral membrane (arrow in D''), whereas Mcr is either missing (arrowhead in D') or localizes along the lateral membrane (arrow in D'). Anterior is to the left. Scale bars = 10µm.

2.4 Discussion

In this study, we have demonstrated that a subset of SJ proteins is expressed in egg chambers throughout oogenesis and are required for critical morphogenetic processes that shape the egg, including egg chamber elongation, dorsal appendage formation and border cell migration (required to form the micropyle). Interestingly, the subcellular localization of these SJ proteins in the ovarian FCs changes coincident with the establishment of the occluding junction in much the same way that they do during embryogenesis in ectodermal epithelial cells (Tiklová et al. 2010), suggesting that a similar maturation process for the SJ occurs in this tissue.

Biogenesis of the SJ in the FE

The mechanisms of SJ biogenesis in embryonic epithelia has been well-studied and involves several steps in which transmembrane SJ proteins are first localized all along lateral plasma membranes (by stage 12 of embryogenesis), but then must be endocytosed and recycled back to the plasma membrane prior to aggregating in the region of the presumptive SJ (between stages 13 and 16; Tiklová et al. 2010). Prior to this relocalization step, SJ proteins show high mobility in the plane of the membrane by Fluorescence Recovery After Photobleaching (FRAP) analysis, but become strongly immobile during relocalization (Oshima and Fehon 2011). As these steps are occurring (e.g. stage 14 of embryogenesis), electron-dense material begins to accumulate between adjacent cells in the presumptive SJ that takes on the appearance of ladder-like septae by stage 17 of embryogenesis (Tepass and Hartenstein 1994). Functional studies indicate that the occluding function of the junction is established late in embryogenesis, near the end of stage 15 (Paul et al. 2003). Importantly, the process of SJ biogenesis is interdependent on

the function of all core components of the junction and several accessory proteins including Rab 5 and Rab 11 (Ward et al. 1998; Genova and Fehon 2003; Tiklová et al. 2010).

Here, we observe that many of these same steps occur in the maturation of SJs in the FE. We first show that SJ proteins are expressed in the FE beginning early in ovarian development where they localize all along the lateral membrane (**Figure 2. 1**). These proteins appear to become enriched at the presumptive SJ by stage 11 (**Figure 2. 6**). The relocalization of SJ proteins to the SJ requires core SJ proteins including Mcr and Nrx-IV, and accessory proteins including Rab5 and Rab11 (**Figure 2. 6** and **Figure 2. 7**). Prior studies indicate the presence of electron dense material between FE cells as early as stage 6 (Müller 2000), with a ladder-like appearance of extracellular septae by stage 10B (Mahowald 1972). A recent study of the occluding function in the FE show a similar pattern of protein localization for endogenously tagged Neuroglian-YFP and Lachesin-GFP, and demonstrates that an intact occluding junction is formed during stage 11 of oogenesis (Isasti-Sanchez et al. 2020). It is interesting to note the FE is a secondary epithelium initiated by a mesenchymal to epithelial transition (Tepass et al. 2001), and yet SJ biogenesis appears to be very similar to that observed in the primary epithelia found in the embryo.

SJ proteins are required for morphogenetic events during oogenesis

The similarities in the dynamic expression of SJ proteins in the FE and embryonic epithelia, coupled with the observation that SJ proteins are required for numerous embryonic developmental events (Hall et al. 2014) and references therein) motivated us to explore whether SJ proteins have similar roles in morphogenetic processes that shape the egg. Using a targeted RNAi approach, we show that reducing the expression of Mcr, Nrx-IV, Cont, Cora, Sinu, or Lac

throughout oogenesis in the FCs results in stage 14 egg chambers with lower aspect ratio that is statistically significant than the control, with many showing additional defects in dorsal appendages (Figure 2. 3and **Figure S2. 2**). The initiation and maintenance of egg elongation is achieved at various stages throughout oogenesis (Gates 2012; Bilder and Haigo 2012; Cetera and Horne-Badovinac 2015). From stage 3-6, a gradient of JAK-STAT signaling is required at each pole of the egg chamber to promote Myosin II-based apical cell contractions (Alégot et al. 2018). From stage 6-8, the formation of a robust planar polarized molecular corset - consisting of basal actin cytoskeleton and basement membrane protein fibrils - is required for egg elongation, and requires collective FC migration over a static basement membrane (Gutzeit et al. 1991; Frydman and Spradling 2001; Bateman et al. 2001; Viktorinová et al. 2009; Haigo and Bilder 2011; Horne-Badovinac et al. 2012; Cetera et al. 2014; Isabella and Horne-Badovinac 2016; Cerqueira Campos et al. 2020). During the middle stages of oogenesis (stages 9 and 10), basal actin stress fibers undergo actomyosin contractions, which contribute to egg elongation (He et al. 2010; Qin et al. 2017). Finally, later in oogenesis, the maintenance of a planar polarized molecular corset is required to retain an elongated egg chamber shape (Haigo and Bilder 2011; Cha et al. 2017; Cerqueira Campos et al. 2020). Future studies are needed to determine if SJ proteins are required for the establishment and/or maintenance of egg shape. Since many of the events involved in egg elongation occur prior to the formation of a functional (and ultrastructurally intact) occluding junction, it raises the possibility that SJ proteins have a function in morphogenesis that is independent of their role in forming a tight occluding junction, much as they do in the embryo.

Stage 14 egg chambers from many of the *SJ-RNAi* lines possessed aberrant dorsal appendages, often characterized by misshapen, broken or missing appendages (Figure 2. 3and **Figure S2. 2**). The formation of dorsal appendages occurs during stages 10B-14 and requires

cell shape changes and cell rearrangements, coupled with chorion protein secretion (Dorman et al. 2004). Similar morphogenetic processes are required for dorsal closure and head involution during embryogenesis (VanHook and Letsou 2008; Hayes and Solon 2017), defects strongly associated with zygotic loss of SJ expression in the embryo (Hall and Ward 2016). We are interested to determine if the mechanism by which SJ proteins contribute to dorsal appendages formation and dorsal closure and head involution are similar. Potential roles could involve regulating the cytoskeleton to facilitate cell shape changes and rearrangements, but another intriguing possibility is that SJ proteins may also be required for chorion protein secretion or crosslinking. Broken and missing dorsal appendages may result from mechanical disruption due to chorion defects. Notably, embryos with mutations in many different SJ genes show defects in the embryonic cuticle including faint denticle belts and delamination of cuticle layers (Lamb et al. 1998; Hall and Ward 2016).

Our observation that specifically knocking down the expression of several SJ proteins in border cells results in defective border cell migration (**Figure 2. 5**) supports a role for SJ proteins in morphogenesis, independent of their role in forming an occluding junction. The phenotypes we observed include failing to complete migration and partial disassociation of the complex by the end of stage 10, which is prior to the formation of an intact SJ. Although the penetrance of these phenotypes is mild (**Figure 2. 5**I and J), it is possible that these phenotypes underestimate the full requirement of SJ proteins in border cell migration since this process takes a relatively short time (4-6 hours) (Prasad and Montell 2007), while SJ proteins are thought to be very stable in the membrane (Oshima and Fehon 2011). One caveat to the idea that perdurance may account for the mild phenotypes is that *C306-GAL4* does not appear to produce a stronger phenotype than *slbo-GAL4*, even though it is expressed earlier and is presumably knocking down

SJ proteins longer. Perhaps knocking the proteins down more quickly using the DeGradFP system (Caussinus, Kanca, and Affolter 2011) could address this possibility in the future. These phenotypes also indicate a potential role for SJ proteins in cell adhesion and/or cell polarity during migration. Specifically, we note that Mcr appears to be enriched in polar cell membranes that contact border cells at the leading edge of the cluster (those that are oriented closest to the oocyte) in wild-type egg chambers (**Figure 2. 4**). Whether SJ proteins are required for aspects of planar polarity in the border cell cluster is an interesting unanswered question. Perhaps the incomplete migration defect results from a meandering migration through the nurse cells, something that has been observed for knockdown of DE-Cadherin in border cells (Cai et al. 2014). Live imaging studies should be able to distinguish between pathfinding defects and a general reduction in speed or premature stopping. A role for SJ proteins in cell adhesion in the ovary has been reported previously. Reducing the level of Nrg in FCs results in the failure of newly divided FCs to reintegrate into the FE, indicating a role for *Nrg* in lateral cell adhesion (Bergstralh et al. 2015). In addition, expressing a null allele of *Nrg* in FCs enhances the invasive tumor phenotype of a *Discs Large* (*Dlg*) mutation (Wei et al. 2004).

2.5 Materials and Methods

Fly stocks

All *Drosophila* stocks were maintained on media consisting of corn meal, sugar, yeast, and agar on shelves at room temperature or in incubators maintained at a constant temperature of 25°C. GAL4 lines used in this study are as follows: *GR1-GAL4* (Bloomington Drosophila Stock Center (BDSC) #36287), *Slbo-GAL4, UAS-mCD8-GFP* (BDSC#76363), and *C306-GAL4; GAL80^{ts}/Cyo* (a gift from Jocelyn McDonald, Kansas State University, Manhattan, Kansas). RNAi stocks used for these studies are as follows: *UAS-Mcr-RNAi* (BDSC#65896 and Vienna Drosophila Resources Center (VDRC)#100197), *UAS-Cora-RNAi* (BDSC#28933 and VDRC#9787), *UAS-Nrx-IV-RNAi* (BDSC#32424 and VDRC#9039), *UAS-Cont-RNAi* (BDSC#28923), *UAS-mCherry-RNAi* (BDSC#35787), *UAS-Lac-RNAi* (BDSC#28940), and *UAS-Sinu-RNAi* (VDRC#44929). *UAS-Rab5^{DN}* (BDSC#9771) was used to inhibit normal Rab5 function and *UAS-Rab11-RNAi* (BDSC#27730) was used to knock down Rab11 in the follicle cells. *UAS-GAL80^{ts}* (BDSC#7108) was used to conditionally inhibit *GR1-GAL4* activity in the *UAS-Rab11-RNAi* experiment. *UAS-GFP* (BDSC#1521) was crossed to *GR1-GAL4* as a control for the egg shape experiments. *Slbo-GAL4, UAS-mCD8-GFP* was crossed to *UAS-mCherry-RNAi* as a control for one set of border cell migration studies, whereas *C306-GAL4; GAL80^{ts}/Cyo* was crossed to *UAS-Dcr* (BDSC#24646) as a control for the other set of border cell migration studies. *w^{1118}* (BDSC# 5905) was used as the wild-type stock for determining the expression of Mcr, Cont, Nrx-IV and Cora in the follicle cells.

Fly staging

w^{1118} 1-2-day-old females and males were collected and reared at 25ºC on fresh food sprinkled with yeast for five to six days before the females were dissection for antibody staining. For egg elongation analyses, crosses were maintained at 25ºC, and 1-2-day-old females (control and *UAS-RNAi*-expressing) were mated with sibling males and maintained at 29-30ºC for 3 days before dissection. For border cell migration analyses, *Slbo-GAL4* crosses were kept at 25ºC, whereas *C306-GAL4/UAS-Dcr; GAL80*^{ts}*/SJ-RNAi* crosses were kept at 18ºC to prevent GAL4 activation. 1-2-day-old flies with the appropriate genotype (*Slbo-GAL4, UAS-mCD8-GFP/UAS-RNAi* or *C306-GAL4 /UAS-Dcr;UAS-RNAi;GAL80*^{ts}) were shifted to 29-30ºC for 48 hours before dissection. It should be noted that by crossing *UAS-GFP* to *C306-GAL4*, we observed the expression of GFP in polar cells in stage 10, but not stage 9 egg chambers (data not shown). For *Rab11-RNAi* experiment, crosses were maintained at 18ºC and 2-3-day-old males and females with the appropriate genotype (*GR1-GAL4>UAS-mCherry-RNAi, UAS-GAL80ts or GR1-GAL4>UAS-Rab11-RNAi, UAS-GAL80ts*) were collected and reared at 29ºC-30ºC overnight before dissection. For the *Rab5*^{DN} experiment, crosses were maintained at 25ºC, and 1-2-day-old females were mated to sibling males and maintained at 29-30ºC for 3 days before dissection.

Egg aspect ratio measurements

Stage 14 egg chambers were selected for analysis based on the overall morphology of the egg and the absence of nurse cells nuclei by DAPI staining. Stage 14 egg chambers that have irregular edges or touch other egg chambers were excluded from the analysis to prevent inaccurate measurements. Egg length (anterior-posterior) and width (dorsal-ventral) were measured using the ImageJ/Fiji (http://fiji.sc) (Schindelin et al. 2012) straight-line tool, and aspect ratio was calculated as length divided by width using Excel Microsoft.

Border cell migration quantification

Stage 10 egg chambers were identified based on the morphology of the egg (oocyte occupies half the egg chamber, whereas the other half is occupied by the nurse cells and centripetal cells). We used the GFP signal in *Slbo-GAL4* crosses and DAPI and/or Fas3 staining in *c306-GAL4* crosses to identify the location of the border cell cluster in stage 10 egg chambers. The location of the border cell cluster was quantified and grouped into four categories - complete, incomplete, failed migration, and disassociated cluster based on the location of the cluster relative to the oocyte in a stage 10 egg chamber (**Figure 2. 5**). In some cases, border cell clusters display two phenotypes such as complete and dissociated. In this case, we quantified both phenotypes in one egg chamber.

Immunostaining and image acquisition

Ovaries were dissected in 1X Phosphate-buffered saline (PBS), fixed in 4% Paraformaldehyde for 20 minutes, washed three times in 1X PBS, and then permeabilized in a block solution (1X PBS + 0.1% Triton + 1% Normal Donkey Serum) for 30 minutes before incubation with primary antibodies either overnight at 4ºC or 2-4 hours at room temperature (~23-25ºC). The following antibodies were used at the given dilutions: guinea pig (gp) anti-Cont 1:2000 (Faivre-Sarrailh et al. 2004) and rabbit (rab) anti-Nrx-IV 1:500 (Baumgartner *et al*. 1996) obtained from Manzoor Bhat, University of Texas Health Science Center, San Antonio, TX, gp anti-Mcr 1:1000 (Hall *et al*. 2014), mouse (m) anti-Cora (C566.9 and C615.16 mixed 1:1, obtained from the Developmental Studies Hybridoma Bank (DSHB) at the University of Iowa, Iowa City, IA; Fehon *et al.* 1994) 1:50, rat anti-*D*E-cad (DCAD2, DSHB) 1:27, and m anti-Fas3 (7G10, DSHB)

1:260. DAPI (1mg/ml) was used at a dilution of 1:1000. Secondary antibodies were obtained from Jackson ImmunoResearch Laboratories (West Grove, Pennsylvania, USA) and were used at 1:500.

Images were acquired using an Olympus FV1000 confocal microscope equipped with Fluoview software (version 4.0.3.4). Objectives used included an UPLSAPO 20X Oil (NA:0.85), a PLAPON 60X Oil (NA: 1.42), and an UPLSAPO 100X Oil (NA:1.40). Stage 14 egg chambers were imaged using Nikon Eclipse 80*i* compound microscope with Nikon Plan Apo 10X Air (NA:0.45). Raw images were rotated and cropped in ImageJ/Fiji. Micrographs were adjusted for brightness using Adobe Photoshop 21.1.1 (San Jose, CA) or Image/Fiji. Adobe Illustrator 24.1 was used to compile the figures.

Statistical Analysis

An unpaired *t*-test was used to calculate the P values in egg chamber aspect ratio between control and SJ mutant stage 14 egg chambers using GraphPad Prism 8 (https://www.graphpad.com) (version 8.4.2).

Acknowledgements

We thank Jocelyn McDonald, the Bloomington *Drosophila* Stock Center, and the Vienna *Drosophila* RNAi Center for fly stocks. We thank Manzoor Bhat and the Developmental Studies Hybridoma Bank (created by the NICHD of the NIH and maintained at The University of Iowa, Department of Biology, Iowa City, IA 52242) for antibodies used in this study. We thank Brian Ackley for the use of his Olympus FV1000 confocal microscope. We thank Lindsay Ussher for preliminary studies on border cell migration and thoughtful discussions on the project. We also

thank Sally Horne-Badovinac, Jocelyn McDonald, Yujun Chen, and members of the Ward lab for helpful discussion about the project and manuscript.

Figure S2.1

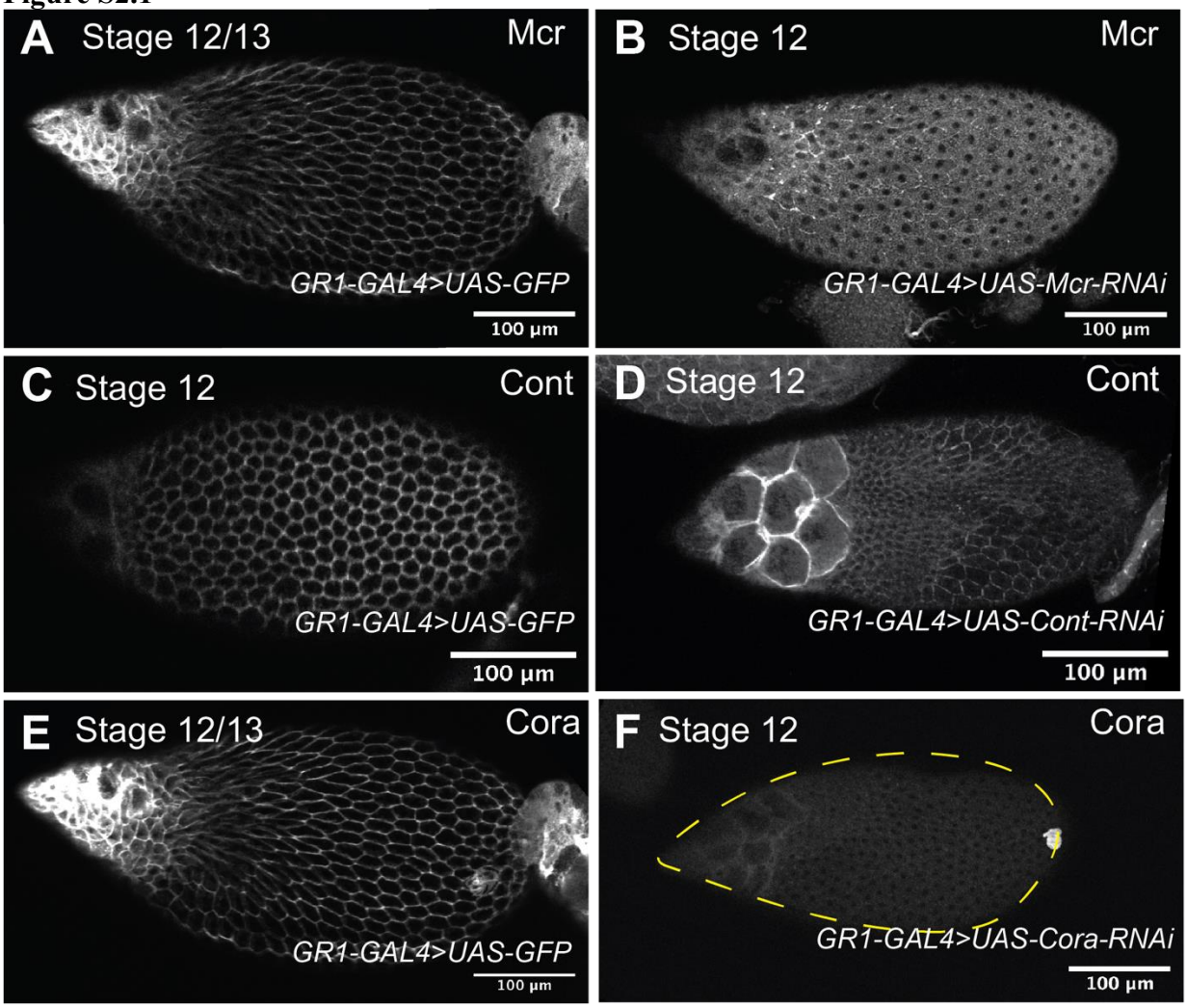

Figure S2. 1 Mcr, Cont, and Cora are knocked down in the FE.
(A, C, and E) Confocal sections of stage 12/13 (A and E) and stage 12 (C) stained with Mcr (A), Cont (C), or Cora (E). (B, D, and F) Confocal sections of stage 12 egg chambers expressing *Mcr-RNAi* (B), *Cont-RNAi* (D), or *cora-RNAi* (F) in the FE. Note that level of the proteins is significantly knocked down in the *RNAi*-expressing egg chambers. A and E are images from the same egg chamber co-stained for Mcr (A) and Cora (E). Anterior is to the left and posterior is to the right. Scale bar = 100µm.

Figure S2.2

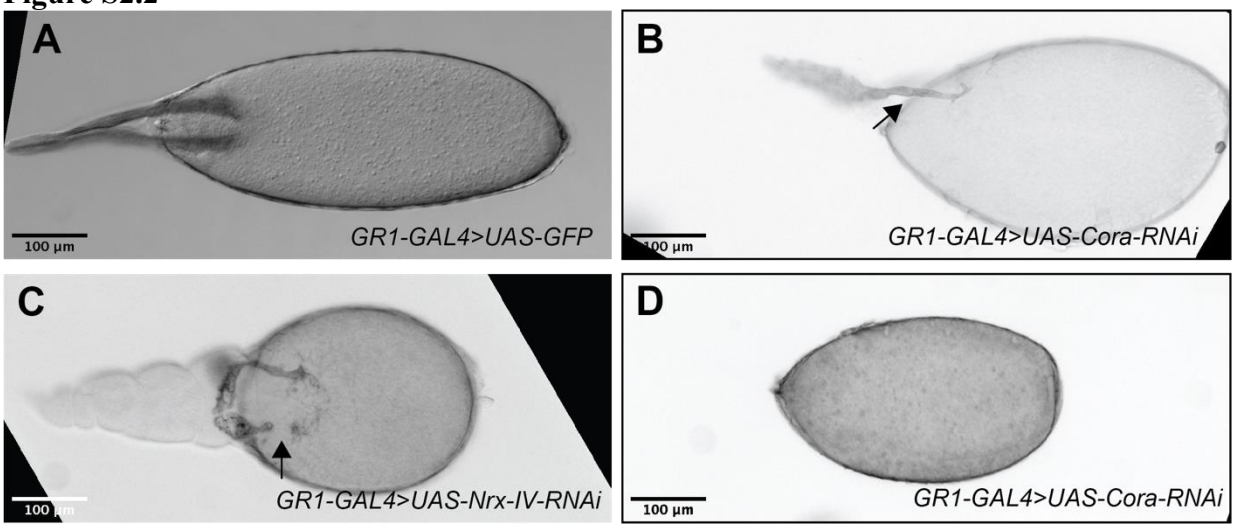

Figure S2. 2 Examples of dorsal appendages defects in *SJ-RNAi* stage 14 egg chambers. (A–D) Brightfield micrographs of stage 14 egg chambers of control (A) and *cora-RNAi* (B and D) and *Nrx-IV-RNAi* (C). While dorsal appendages are formed in control egg chambers with consistent thickness along the stalk of the appendage (A), the stalk of intact dorsal appendages in *SJ-RNAi* egg chambers are usually thinner near the oocyte with a wider and flatten paddle (black arrow in B). (C) An example of the broken dorsal appendages (black arrow in C) and missing dorsal appendages (D) phenotypes in *SJ-RNAi* expressing egg chambers. Anterior is to the left and posterior is to the right. Scale bar = 100µm.

Figure S2. 3

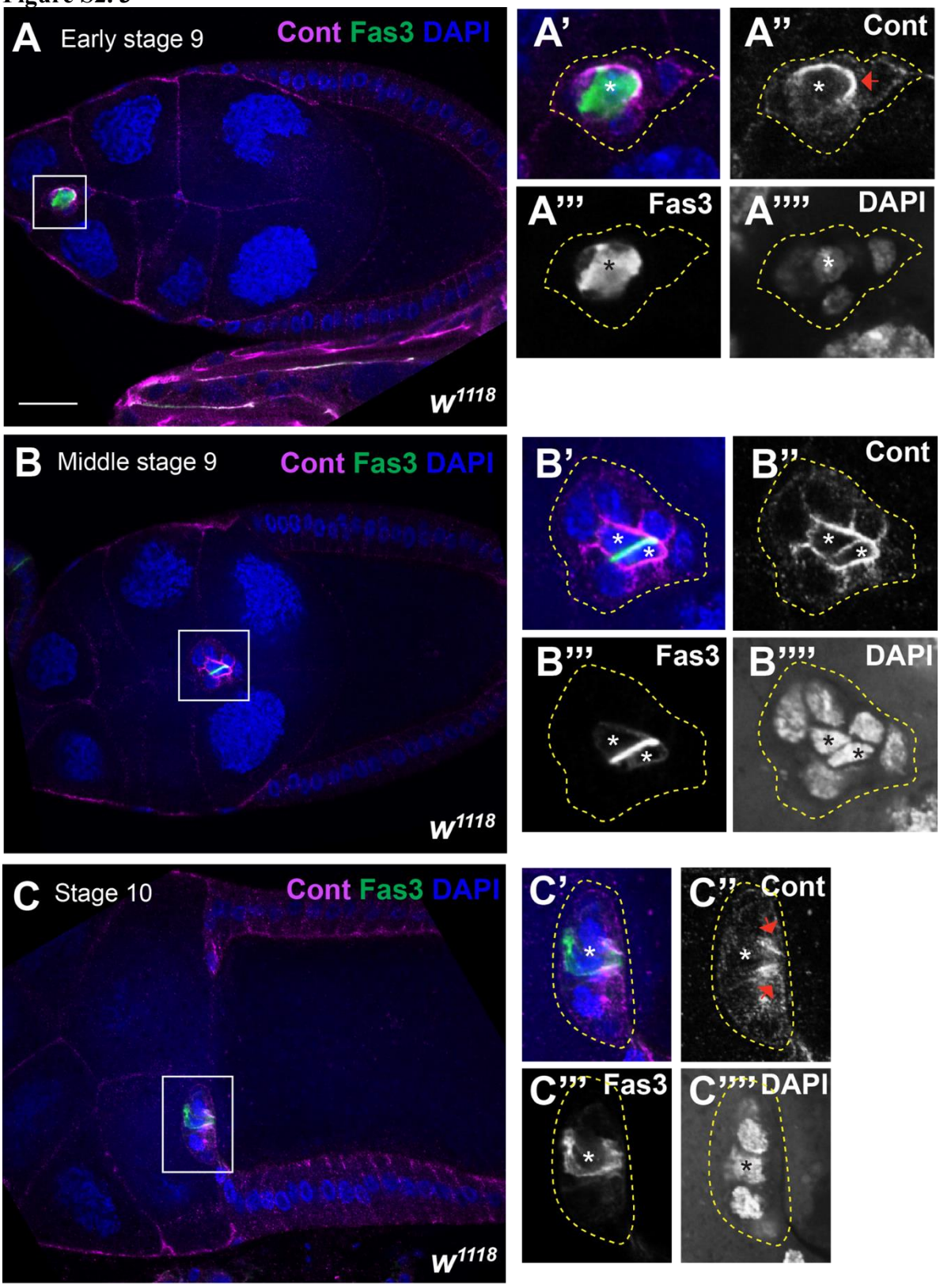

Figure S2. 3 Cont expression in the border cluster throughout border cell migration.

(A–C) Confocal sections of wild-type early stage 9 (A), middle stage 9 (B), and stage 10 (C) stained with Cont (magenta), Fas3 to mark the polar cells (green) and labeled with DAPI (blue). (A'–A'''', B'–B'''', and C'–C'''') are zoomed in images of the border cell cluster in A-C. Cont is expressed in the border cell cluster with the strongest expression in the polar cells (A'', B'', C'', and D''). Cont also shows a symmetric localization at the leading edge of the cluster (red arrows in A'' and C''). Anterior is to the left. Scale bar = 25μm.

Figure S2.4

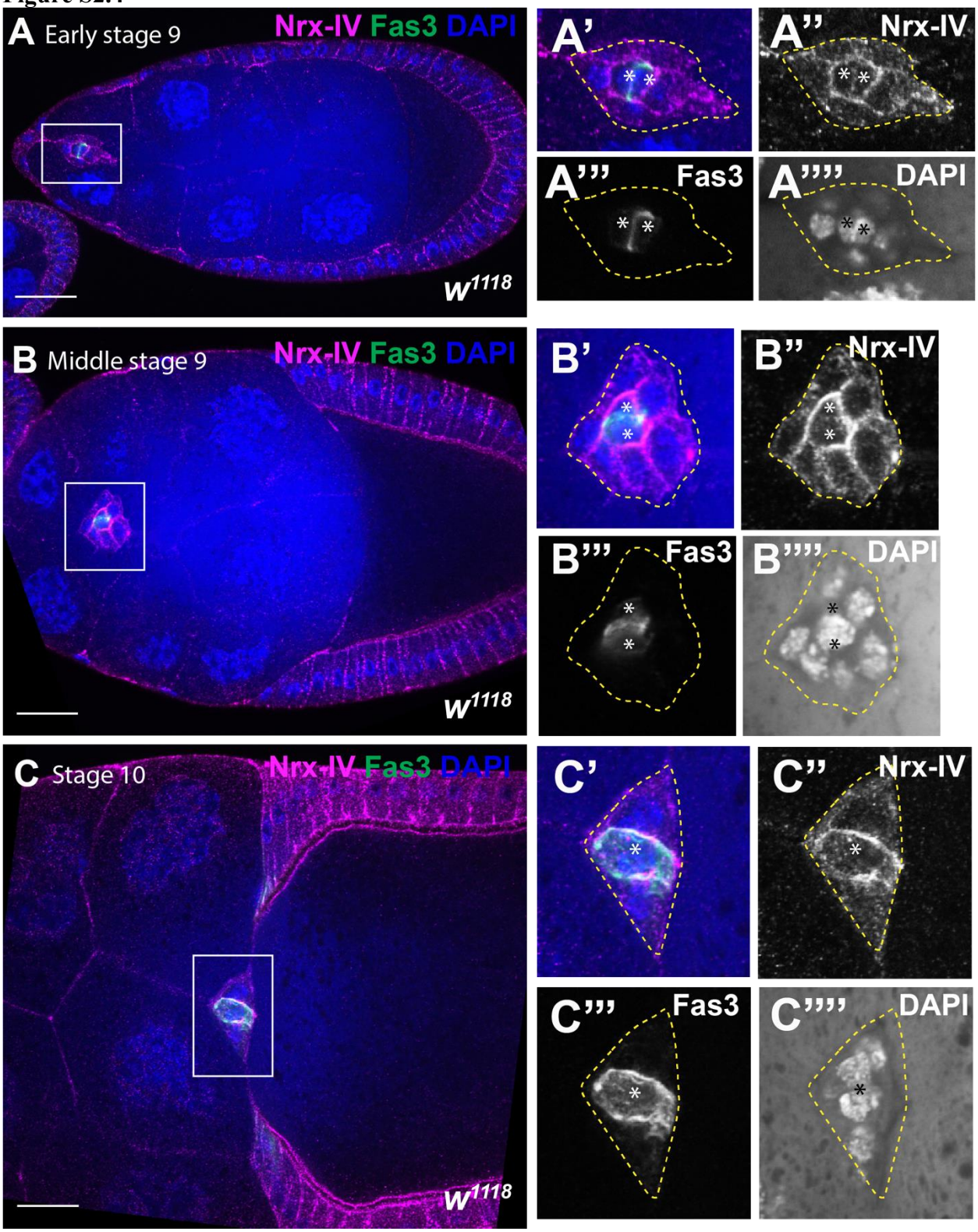

Figure S2. 4 Nrx-IV expression in the border cell cluster during border cell migration. (A–C) Confocal sections of early stage 9 (A), middle stage 9 (B), and stage 10 wild-type egg chambers stained with Nrx-IV (magenta), Fas3 to mark the polar cells (green) and labeled with

DAPI (blue). (A'–A''''), (B'-–B''''), and (C–C'''') are zoomed in images of A, B, and C. Note the localization of Nrx-IV in the border cell cluster throughout border cell migration with enrichment at the polar cells-border cells contacts (A'', B'', and C''). Anterior is to the left. Scale bar = 25μm.

Figure S2. 5

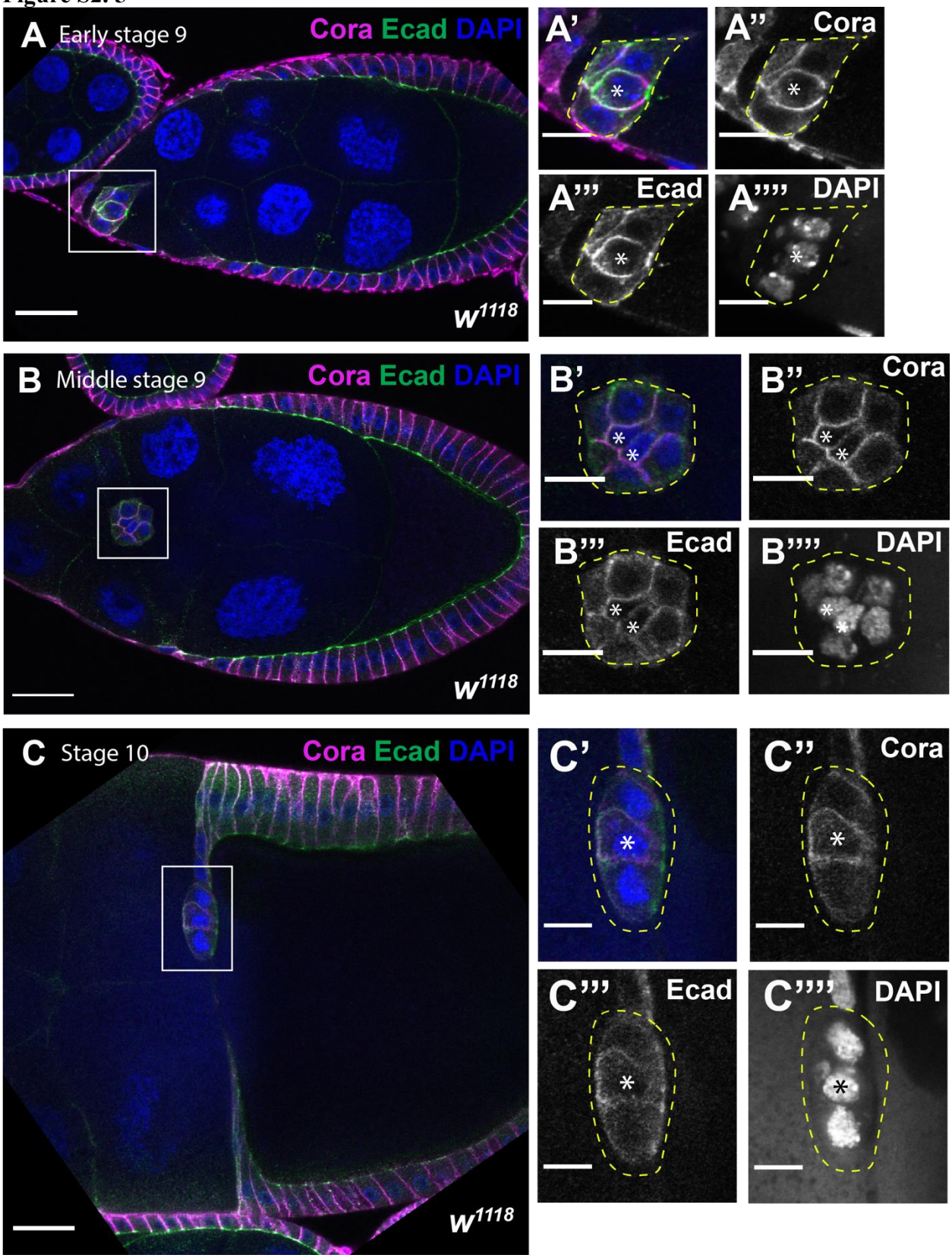

Figure S2. 5 Cora expression in the border cell cluster during border cell migration.

(A–C) Confocal sections of wild-type egg chambers at early stage 9 (A), middle stage 9 (B), and stage 10 (C) stained with Cora (magenta), Ecad (green), and labeled with DAPI (blue). (A'–A''''), (B'–B''''), and (C'–C'''') are zoomed in images of A, B, and C. Cora is expressed in the polar cells and border cells throughout border cell migration with high level at the polar cells-border cells interface (A'', B'', and C''). Anterior is to the left. Scale bar = 25μm.

Chapter III: The septate junction protein Macroglobulin complement-related is required for maintenance of monolayered epithelium and eggshell formation during *Drosophila* egg morphogenesis

The data and text in Chapter III is a manuscript in preparation for submission with a tentative title as:

Alhadyian, H. and Ward R. “The septate junction protein Macroglobulin complement-related is required for maintenance of monolayered epithelium and eggshell formation during *Drosophila* egg morphogenesis.”

3.1 Abstract

The formation of specialized epithelial tissues requires dynamic and precise coordination of cell shape changes, cellular rearrangements, and cell migration, a process known as morphogenesis. Morphogenesis is regulated via the cell cytoskeleton, polarized protein trafficking, and propagation of mechanical forces within cells and across tissues. The proper integration of these cellular events is essential for morphogenesis to occur normally. The *Drosophila* egg chamber serves as a model system to study morphogenesis. Each egg consists of germline cells that are encapsulated by a monolayered somatic cells known as follicle cells (FCs), which are the major driving force of egg morphogenesis. We have shown that components of the invertebrate occluding junctions, known as the septate junction (SJ), are expressed in the FCs throughout oogenesis and are required for egg morphogenesis, including egg elongation. Egg elongation is a process by which a sphere-shaped egg elongates across the anterior-posterior axis. This process requires the formation and maintenance of the molecular corset, which consists of planar polarized actin cytoskeleton and extracellular matrix fibrils. To further examine the mechanism by which SJ proteins are required for egg elongation, we focused our study on the core SJ component, Macroglobulin complement-related (Mcr). We find that Mcr is dispensable for establishing the formation of the molecular corset early in oogenesis as both actin and the basement membrane Collagen IV fibrils are formed. Instead, Mcr is required late in oogenesis to maintain a monolayered epithelium, basal actin stress fibers, and integrin enrichment at the focal adhesion sites. By using scanning and transmission electron microscopy, we find that the eggshell of Mcr-depleted late-stage egg chambers is compromised. In particular, stage 12 Mcr-depleted egg chambers lack the wax layer, whereas stage 14 Mcr-depleted egg chambers appear to lack the FCs imprints and have broken dorsal appendages. Given that Mcr is required for the

maintenance of the molecular corset and for the formation of the eggshell late in oogenesis, which is after SJ maturation, we propose that Mcr requirement in egg elongation is likely to be SJ-dependent. Further studies are needed to determine the mechanisms by which Mcr is required for egg elongation late in oogenesis.

3.2 Introduction

Morphogenesis describes a myriad of conserved cellular processes that contribute to the developmental shaping of tissues and organs in multicellular organisms. Many of the cellular processes involved in morphogenesis require cell shape changes, cellular rearrangements, and cell movement.

In *Drosophila*, components of the invertebrate occluding junction, known as the septate junction (SJ), are essential for morphogenetic events throughout fly development (Hall and Ward 2016; Fehon, Dawson, and Artavanis-Tsakonas 1994; Venema, Zeev-Ben-Mordehai, and Auld 2004; Banerjee et al. 2008; Lamb et al. 1998; Moyer and Jacobs 2008). In ectodermally-derived epithelia, SJ resides in the apical-lateral domain, just basal to the adherens junction (Noirot-timothée et al. 1978; Izumi and Furuse 2014). We recently showed that SJ proteins are similarly required for morphogenetic developmental events during oogenesis, including egg elongation, border cell migration, and dorsal appendages formation (Chapter II). While these studies demonstrate the importance of SJ proteins in epithelial morphogenesis, the role SJ proteins play in these morphogenetic events remains elusive.

The most well-studied role for SJ proteins is in establishing the occluding junction as a transepithelial barrier (e.g., Hall et al. 2014; Behr, Riedel, and Schuh 2003). Interestingly, many of the embryonic and egg chamber morphogenetic events that require SJ proteins occur prior to the formation of the occluding junction, suggesting an essential non-occluding function for SJ proteins in morphogenesis (Hall and Ward 2016; Chapter II). To further explore the role of SJ proteins in morphogenesis, we analyzed the role of the core SJ protein Macroglobulin complemented-related (Mcr) during oogenesis, specifically in the morphogenetic event known as egg elongation.

Mcr is a transmembrane protein that belongs to the thioester-containing protein family involved in innate immunity in the fly (Stroschein-Stevenson et al. 2006). Loss-of-function mutations in *Mcr* result in embryonic lethality with specific defects in dorsal closure, head involution, and salivary gland and tracheal morphogenesis (Hall et al. 2014; Hall and Ward 2016). We have recently shown that Mcr is expressed in the *Drosophila* follicular epithelium (FE) throughout oogenesis (Chapter II). Mcr localizes in puncta at the plasma membrane of follicle cells (FCs) during the early stages of oogenesis. By stage 10B/11, Mcr becomes enriched at the apical-lateral membrane, coincident with the formation of ultrastructural SJs in the FE (Mahowald, 1972; Müller, 2000). Knocking down Mcr in the FE interferes with egg elongation and produces eggs with deformed dorsal appendages (Chapter II). The mechanism by which Mcr is required for egg elongation is unknown.

A *Drosophila* egg consists of two cell populations – a 16-cell germline cyst that is surrounded by a layer of somatic cells known as follicle cells (FCs) (Horne-Badovinac and Bilder 2005). FCs contribute to the majority of the morphogenetic processes during oogenesis, including egg elongation, border cell migration, dorsal appendage morphogenesis, and eggshell formation (Horne-Badovinac and Bilder 2005). Egg elongation is a process by which the egg chamber changes its shape from round - as in stage 1 - to elongated - as in stage 14 (**Figure 3. 1**A) (Gates 2012; Horne-Badovinac 2014). Four known mechanisms contribute to egg elongation. The first mechanism occurs from stages 3–6 and it involves apical actomyosin contraction mediated via a gradient of the JAK-STAT signaling at each pole of the egg chamber (Alégot et al. 2018). The second mechanism occurs during stages 6–8, where FCs migrate on a static basement membrane to promote the planar polarization of the basal actin cytoskeleton (Gutzeit, Eberhardt, and Gratwohl 1991; Cetera et al. 2014). FC migration also results in the

basal deposition of extracellular matrix (ECM) fibrils via Rab10-mediated exocytosis (Lerner et al. 2013; Isabella and Horne-Badovinac 2016). During stages 9–10, actomyosin contractions at the basal domain further contribute to egg elongation (He et al. 2010; Qin et al. 2017). Together, planar-polarized actin stress fibers and ECM fibrils form a *molecular corset*, which constrains egg chamber growth to promote elongation along the anterior-posterior axis (Gutzeit, Eberhardt, and Gratwohl 1991). The mechanism that is required for maintaining the elongated-shaped egg occurs stages 11–14, where actin stress fibers change their orientation to align perpendicular to the anterior-posterior axis. The maintenance of a planar-polarized molecular corset throughout oogenesis is important for retaining the elongated-shaped egg later in oogenesis (Haigo and Bilder 2011; Cerqueira Campos et al. 2020).

In addition to controlling egg shape, FCs synthesize and secrete eggshell components in a multistep process that is temporally and spatially regulated. During stages 8–10, FCs secrete the vitelline membrane proteins in the extracellular space between the oocyte and the FCs (Spradling 1993). During stages 10B–12, FCs secrete the wax layer (Papassideri 1993). The wax layer seals the oocyte, rendering it impermeable to the outside environment. From stages 11–14 of oogenesis, the chorion proteins are secreted to form a three-layer chorion, including inner-chorion, endo-chorion, and exo-chorion (Margaritis, Kafatos, and Petri 1980). Eggshell secretion results in a mature egg with FC imprints and specialized eggshell structures, including the micropyle (a hole for sperm entry), the operculum (a soft area for larval hatching), and two appendages located at the dorsal anterior region of the egg (Cavaliere et al. 2008).

In this study, we examined the role of Mcr in egg elongation and eggshell formation. We find that Mcr function is dispensable for early events in egg chamber elongation, including FC migration and the formation of a molecular corset. However, late in oogenesis, Mcr is essential

for the maintenance of actin cytoskeleton stress fibers and FE monolayer. In addition, Mcr is required for the secretion of the wax layer and chorion layers. Together, these results suggest that Mcr is required late in oogenesis and raises the possibility that its function may be related to the formation of the occluding junction.

3.3 Results

Mcr is required for egg elongation late in oogenesis

We have recently shown that a number of SJ genes (*Cont*, *cora*, *sinu*, *Nrx-IV*, and *Mcr*) are required for egg elongation (Chapter II). To further examine the role of SJ proteins in egg elongation, we focused our analysis on Mcr. *Mcr* loss-of-function mutations are embryonic lethal (Hall et al. 2014; Hall and Ward 2016), and so we used the *GAL4-UAS-RNAi* system to knock down the level of Mcr in the ovaries, specifically in the FCs (Brand and Perrimon 1993). *GR1-GAL4* was used to drive the expression of *UAS-Mcr-RNAi* in the FCs of stages 4–14 egg chambers (Gupta and Schüpbach 2003; Wittes and Schüpbach 2018). By measuring the length (anterior-posterior) and width (dorsal-ventral) of stage 14 egg chambers, we find that Mcr-depleted egg chambers are shorter but not wider than the control (**Figure 3. 1**B-E). Moreover, the aspect ratio of length to width of stage 14 egg chambers expressing *Mcr-RNAi* (average ratio= 1.8) is significantly smaller than the control (average ratio=2.1; unpaired *t*-test $P<0.0001$) (**Figure 3. 1**F). To determine at which stage of oogenesis Mcr is required for egg elongation, we measured the length and width of stages 5–14 and calculated the aspect ratio as described above. The aspect ratio of stages 8 and 9 *Mcr-RNAi*-expressing egg chambers is significantly smaller than the control (**Figure 3. 1**H; unpaired *t*-test $P<0.01$). However, at stages 10–11, the aspect ratio recovers to control levels, but falls again at stages 13–14 (**Figure 3. 1**H; unpaired *t*-test $P<0.0001$).

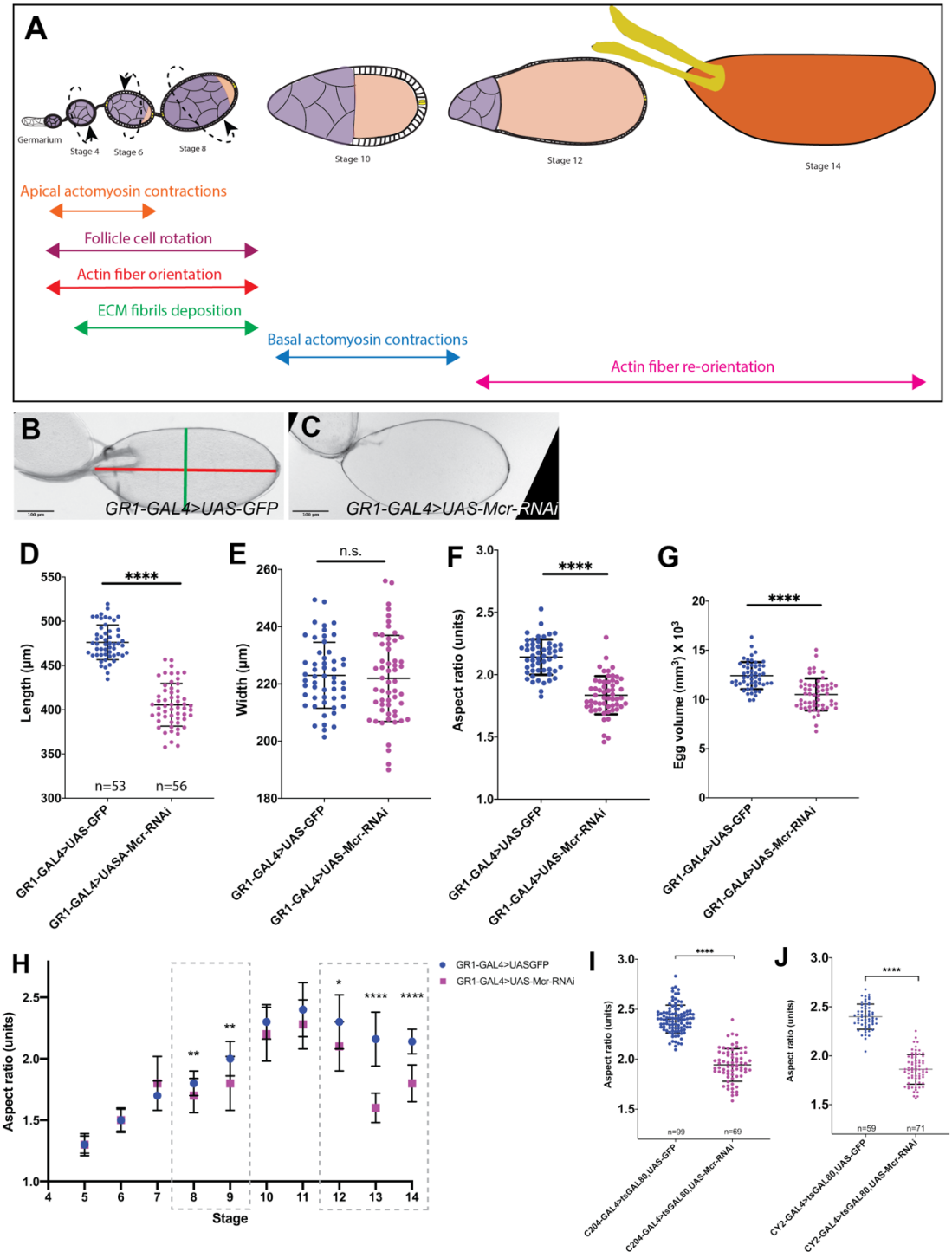

Figure 3. 1 Mcr is required for egg elongation late in oogenesis.
(A) Diagram of a single ovariole showing different stages of egg development. The *Drosophila* egg chamber undergoes 14 stages through which the egg elongates across the anterior-posterior axis. Four mechanisms contribute to egg elongation. During stages 3–6, apical actomyosin contractions promote elongation at the anterior-posterior poles. During stages 6–8, follicle cell (FCs) migration aligns basal actin filaments as they deposit ECM fibrils perpendicular to the anterior-posterior axis. Together, planar-polarized actin filaments and ECM fibrils form the

molecular corset, which constrains the width of the egg and promotes egg growth across the anterior-posterior axis. During stages 9–10B, basal actomyosin contraction contributes to egg elongation by relaxing and constricting the basal surface area. During stages 11–12, actin stress fibers depolymerize, and re-orient perpendicular to the anterior-posterior axis using the planar polarized ECM fibrils as a polarity cue. (B-C) Brightfield images of control (A) and *Mcr-RNAi*-expressing egg chambers (C). Measurements of length (D), width (E), aspect ratio (length/width) (F), and volume (G) of control and *Mcr-RNAi*-expressing stage 14 egg chambers. Aspect ratio measurement of control and *Mcr-RNAi* from stage 5 to stage 14 egg chambers. Note that the aspect ratio of *Mcr-RNAi*-expressing egg chambers deviates from the control at stages 8 and 9. At stages 10 and 11, the aspect ratio recovers, but falls again at stage 12 of oogenesis relative to control egg chambers. Knocking down the level of Mcr in the FCs by stage 8 (I) or stage 9 (J) is sufficient to block egg elongation. Unpaired *t*-test, *P* *<0.05, **<0.01, ****<0.0001. Error bars in all panels represent standard deviation. *n* = number of samples. In panel H, egg samples are 11>*n*<21 for control and 8>*n*<24 for *Mcr-RNAi* experiments. Scale bar = 100µm. Anterior to the left and posterior to the right. The diagram in modified from Alhadyian, Shoaib, and Ward 2021; *G3* Journal (see chapter II for details).

Mcr is not required for the establishment phase of egg elongation

Finding that the aspect ratio of stages 8–9 egg chambers is significantly different from control egg chambers promoted us to investigate a possible requirement for Mcr in the establishment phase of egg elongation. During stages 1–8 of oogenesis, FCs migrate perpendicular to the anterior-posterior axis (Haigo and Bilder 2011; Cetera et al. 2014). As the FCs migrate, basal actin filaments begin to align in the same direction of migration (Cetera et al. 2014). FCs migration also promotes the deposition of planar polarized ECM fibrils via Rab10-mediated exocytosis (Lerner et al. 2013; Isabella and Horne-Badovinac 2016). Together, planar-polarized actin filaments and ECM fibrils form the "molecular corset", which is essential for the establishment phase of egg elongation (Gutzeit, Eberhardt, and Gratwohl 1991; Viktorinová et al. 2009). To determine if Mcr is required for the formation of the molecular corset, we first measured the rate of FCs migration in *Mcr-RNAi*-expressing and control FCs. The migration rate in *Mcr-RNAi* FCs is not significantly different from those in control egg chambers (**Figure 3. 2**A-C) (n=9 control and n=6 *Mcr-RNAi*). Consistent with this observation, phalloidin staining

indicated that *Mcr-RNAi*-expressing FCs have planar-polarized actin filaments that are perpendicular to the anterior-posterior axis and are indistinguishable from those produced in control egg chambers (control n=13 and *Mcr-RNAi* n=10) (**Figure 3. 2**D-E). Additionally, we examined the planar polarization of Collagen IV fibrils, which is a major component of the ECM (Isabella and Horne-Badovinac 2015). To do so, we used Viking (Vkg)-GFP (a GFP-protein trap of the alpha subunit of collagen IV; (Buszczak et al. 2007). Not surprisingly, Collagen IV fibrils align perpendicular to the anterior-posterior axis in *Mcr-RNAi*-expressing stage 8 egg chambers similar to the control (control=20, *Mcr-RNAi*=10) (**Figure 3. 2**F-G). Together, these results suggest that Mcr is not required for FC migration and the planar polarization of actin stress fibers and Collagen IV fibrils, and suggest a later requirement for Mcr in egg elongation. Consistent with this idea, knocking down Mcr by late stage 8 using *C204-GAL4* results in lower aspect ratio that is statistically significant than the control (average ratio of control= 2.4 and Mcr-depleted stage 14 egg chambers =1.9, unpaired *t*-test $P<0.0001$) as does knocking Mcr down by stage 9 using *CY2-GAL4* (average ratio of control= 2.3 and Mcr-depleted stage 14 egg chambers =1.8, unpaired *t*-test $P<0.0001$) (**Figure 3. 1**I and J).

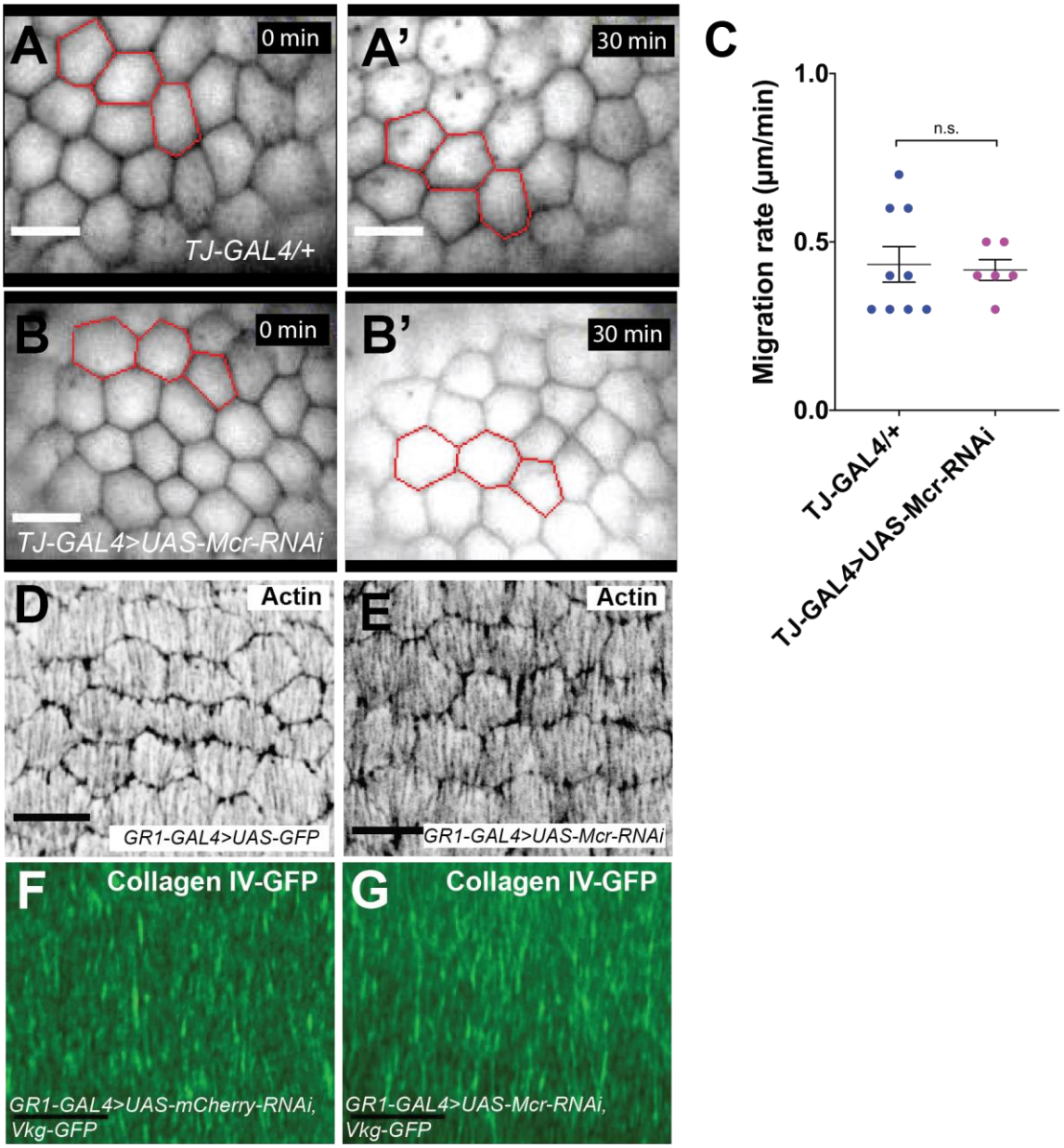

Figure 3. 2 Mcr is not required for follicle cell migration or the planar polarization of the molecular corset components during the establishment phase of egg elongation.
(A and B) Still images of time-lapse movies acquired at the basal surface of control (A) and *Mcr-RNAi*-expressing follicle cells (FCs) (B). (C) Travel distance of FC migration of control and *Mcr-RNAi*-expressing egg chambers (n= 9 control and n=6 Mcr-depleted egg chambers). (D and E) Confocal micrographs of the basal membrane of control (D) and *Mcr-RNAi*-expressing (E) stage 8 FCs labeled with phalloidin to visualize basal actin cytoskeleton. (F and G) Confocal micrographs of the basement membrane of control (F) and *Mcr-RNAi*-expressing stage 8 egg chambers visualized with Collagen IV-GFP. Note that Collagen IV-GFP fibrils are deposited by the FCs in *Mcr-RNAi* egg chambers. Unpaired *t*-test, error bars represent standard deviation. Anterior is to the left and posterior to the right. Scale bar = 10µm.

Mcr is essential for basal actin stress fibers organization late in oogenesis

The observation that Mcr is not required for the establishment phase of egg elongation, and that knocking down Mcr as late as stage 9 results in stage 14 eggs with an aspect ratio that is significantly different than the control, suggest a late requirement for Mcr in egg elongation. Therefore, we focused our analysis on events occurring in late-stage egg chambers. At stage 11, actin stress fibers disassemble and form new planar-polarized fibers perpendicular to the anterior-posterior axis (Delon and Brown 2009). The correct orientation of actin stress fibers depends on planar polarized ECM fibrils, which act as a polarity cue for actin re-orientation (Cerqueira Campos et al. 2020). Together, planar-polarized ECM fibrils and actin stress fibers maintain the elongated-shape egg from stages 12–14 (Viktorinová et al. 2009; Haigo and Bilder 2011). In *Mcr-RNAi*-expressing stage 12 egg chambers, planar polarized Collagen IV fibrils are indistinguishable from those found in wild-type egg chambers (control n= 12 and *Mcr-RNAi* n=10 egg chambers) (**Figure 3. 3**A and B), whereas basal actin stress fibers appear disrupted (**Figure 3. 3**C and D). Specifically, while basal actin stress fibers are oriented perpendicular across the anterior-posterior axis in wild-type egg chambers (**Figure 3. 3**C) (n=19 stage 12 egg chambers), actin stress fibers in *Mcr-RNAi*-expressing FCs are either disorganized (red arrow in Figure 3. 3D), displaced at the cell periphery (compare green arrow in C to D in **Figure 3. 3**), or are severely reduced or missing (yellow asterisk in **Figure 3. 3**D) (n=26 stage 12 egg chambers).

The displaced and disorganized actin stress fiber phenotypes seen in *Mcr-RNAi*-expressing FCs is similar to that reported for egg chambers mutant for the integrin beta subunit Myospheriod (Bateman et al. 2001; Delon and Brown 2009) We therefore examined the localization of integrin in the FCs of stage 12 egg chambers. In wild-type FCs, integrin is enriched at the focal adhesion sites of stage 12 egg chambers (n=14, 17 stage 12 egg chambers)

(Figure 3. 3E). In contrast, *Mcr-RNAi*-expressing FCs either showed reduced enrichment of integrin staining or completely lacked integrin at the focal adhesions (n=7 stage 12 egg chambers) (**Figure 3. 3**F). Consistent with these results, knocking down Mcr late in oogenesis (using *CY2-GAL4>UAS-Mcr-RNAi*) resulted in similar disorganized actin stress fibers and reduced enrichment of integrin in stage 12 egg chambers (data not shown).

To confirm that these cellular defects were due to the loss or reduction of Mcr, we induced mitotic clones of the null allele Mcr^{D13} and examined actin stress fiber formation and integrin expression in stage 12 egg chambers. Consistent with the RNAi phenotypes, FCs within the Mcr^{D13} clone show reduced levels of actin stress fibers or lose them altogether (n=11 stage 12 egg chambers) (**Figure 3. 3**G). Interestingly, we occasionally observed heterozygous FCs adjacent to *Mcr* mutant clones with disorganized and/or missing actin stress fibers (n=6 out of 7 stage 12 egg chambers) (red arrow in **Figure 3. 3**G'). Integrin expression was similarly disrupted in the Mcr^{D13} mutant clones. Whereas the surrounding heterozygous FE showed robust integrin staining, FCs in Mcr^{D13} mutant clones either have less enrichment of integrin at the focal adhesions or completely lack integrin (n=5, 6 stage 12 egg chambers) (**Figure 3. 3**H). We also observed a few clones where integrin was abolished from the focal adhesions at the interface between mutant and heterozygous cells (n=3, 6 stage 12 egg chambers) (red and green arrows in **Figure 3. 3**H). Together, these experiments demonstrate that Mcr is required for the expression of integrins and the organization of actin stress fibers in late-stage egg chambers, suggesting that Mcr may be required non-cell autonomously for the formation or maintenance of these

structures.

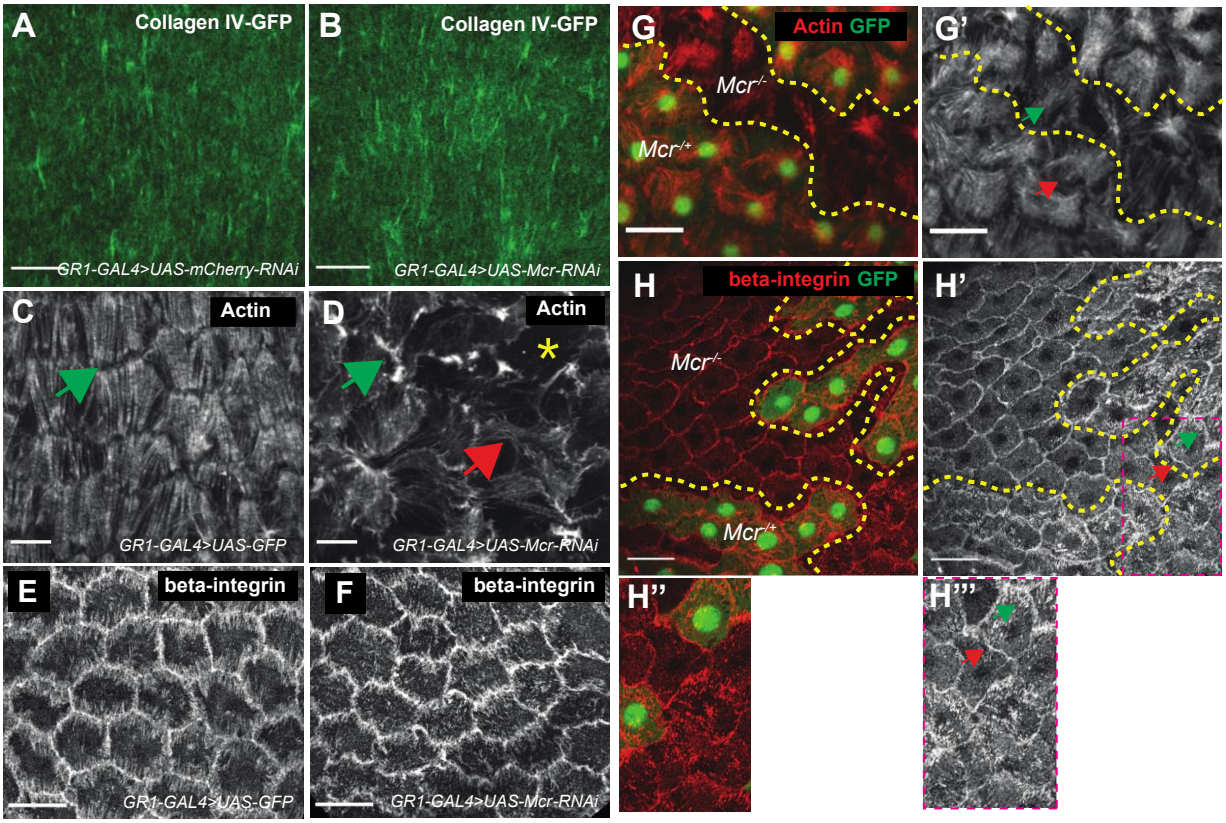

Figure 3. 3 Mcr is required for actin stress fibers organization and integrin expression and localization late in oogenesis.
(A-F) Confocal micrographs of stage 12 basement membrane of wild-type (A, C, and E) and *Mcr-RNAi*-expressing egg chambers (B, D, and F) expressing Collagen IV-GFP to visualize the fibrils. (C-F) Confocal micrographs of the basal surface of wild-type (C and E) and *Mcr-RNAi*-expressing (D and F) follicle cells (FCs) labeled with phalloidin to visualize basal actin stress fibers (C and D) or immunostained with an antibody against beta-Integrin (E-F). Note that Collagen IV fibrils are maintained in Mcr-depleted FCs when compared to the control (compare B to A). Actin stress fibers, on the other hand, are disorganized in some *Mcr-RNAi*-expressing FCs (compare D to C). In these cells, actin stress fibers are either abolished (yellow asterisk in D) or weakly formed (red arrow in D) (compare D to C). Moreover, beta-Integrin is enriched at the focal adhesion sites of wild-type FCs but shows less enrichment in *Mcr-RNAi*-expressing FCs (compare F to E). (G and H) Confocal micrographs of the basal membrane of stage 12 FCs mosaic for the null Mcr allele Mcr^{D13} (heterozygous cells; GFP^{+}, Mcr null cells; GFP^{-}) labeled with phalloidin to mark actin (G) or stained with an antibody against beta-Integrin (H). Note that actin stress fibers are disorganized within Mcr null clones (green arrow in G') as well as in adjacent wild-type FCs (red arrow in G'). Beta-Integrin is also less enriched at the focal adhesion sites in Mcr null clones (red arrow in H') and in wild-type cells adjacent to the clones (green arrow in H'-H'''). Anterior is to the left and posterior is to the right. Scale bar=10µm in A-D and 20µm in E-H.

Mcr is required to maintain a monolayered FE late in oogenesis

While examining stage 12 *Mcr-RNAi* egg chambers, we noticed that many of them did not show the regular hexagonal arrangement of FCs that is typical in wild-type egg chambers (**Figure 3. 4**A). Instead, when we image through the focal plane containing the adherens junction in the FE of *Mcr-RNAi* egg chambers, we find cells that either lack hexagonal shape (red and green arrows in in **Figure 3. 4**B) or show gaps in E-cadherin (E-cad) staining (the middle cells within the dashed outline area in **Figure 3. 4**C). In some cases, we observe cells coming together in a rosette structure. Examining a Z-series through the egg chambers in region containing a rosette (white arrow in **Figure 3. 4**D) revealed the presence of one or more cells that were above (apical) to the FE (white arrow in **Figure 3. 4**D') (n=8 out of 22 stage 12 egg chambers). We never observed this cell delamination phenotype in the FE of control egg chambers (n=15 stage 12 egg chambers).

Given that some Mcr-depleted FCs appear to delaminate from the FE, we wondered if the lack of actin stress fibers we observed in **Figure 3. 3** is a reflection of cells undergoing delamination. Therefore, we re-examined actin stress fiber organization in *Mcr-RNAi* stage 12 egg chambers through a Z-series (n=7, stage 12 egg chambers). Because phalloidin staining requires a different protocol than the one we used for antibodies staining, we relied on cortical actin and stress fibers as a read out of the cell membrane and basal actin stress fibers, respectively. By analyzing a Z-series through the epithelium of stage 12 egg chambers, we found that the areas in the FE where actin signal is bright (yellow arrow in **Figure 3. 4**G) are cells that appear to be delaminated (yellow arrow in **Figure 3. 4**G'). Interestingly, in many cases the cells surrounding the extruded cell maintain basal stress fibers.

From stages 10–13, FCs undergo flattening to accommodate the increase size of the oocyte due to rapid nurse cell dumping (Spradling 1993) (**Figure 3. 5**A). We wondered if *Mcr-RNAi* cells are defective in their ability to change shape, and whether that may contribute to localized differences in tension leading the epithelium to expel one or a small number of cells. We therefore stained FCs with the lateral membrane marker, alpha-spectrin, and the apical marker, atypical protein kinase C (aPKC) and measured the length (apical-basal) and the width (space between two lateral membranes) of FCs in *Mcr-RNAi* and control stage 12 egg chambers (**Figure 3. 5**A). No significant difference was observed for the height or width of FCs between control and Mcr-depleted stage egg chambers (**Figure 3. 5**B and C), indicating that *Mcr-RNAi* FCs are competent to undergo cell flattening. Interestingly, we noticed that whereas aPKC is correctly localized to the apical domain of the FCs expressing *Mcr-RNAi* (n= 12 control and n=16 *Mcr-RNAi* stage 12 egg chambers) (**Figure 3. 5**D' and E'), alpha-spectrin localization was altered. In Mcr-depleted FCs, alpha-spectrin appears all along the apical domain in addition to its normal localization along the lateral domain (n=15 out of 16 stage 12 egg chambers) (white arrow in **Figure 3. 5**D'' and E''). This result suggests that knocking down the level of Mcr in the FCs induces a mild defect in apical-basal polarity, which is consistent with the finding of a multilayered epithelium.

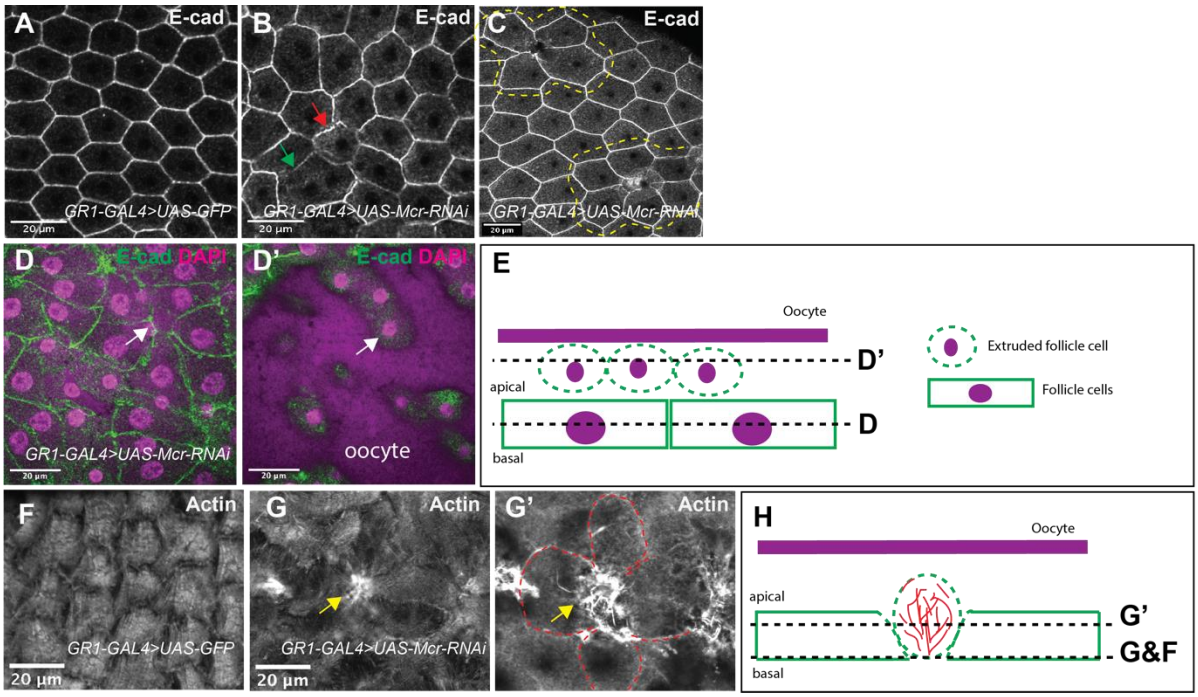

Figure 3. 4 Mcr is required for maintaining a monolayered epithelium.
Confocal micrographs of control (A) and *Mcr-RNAi*-expressing stage 12 egg chambers (B and C) stained with the adherens junction marker E-cadherin (E-cad). (A) In the control egg chamber, the follicle cells (FCs) are hexagonal in shape, whereas the epithelium of *Mcr-RNAi* egg chambers have inconsistent morphology (B and C). (B) Mcr-depleted FCs have smaller cell area (red arrow in B) or appear to be on a different focal plane from the rest of the epithelium (green arrow in B). (C) An example of a rosette formation in Mcr-depleted FCs (top and bottom dashed yellow outlines), where the middle cell appears to be excluded from the epithelium by the surrounding 6 cells. (D and D') Confocal micrographs from a Z-series taken through the follicular epithelium of stage 12 Mcr-depleted egg chamber. Slices from the Z-series of the middle (D) and apical planes (D') of Mcr-depleted stage 12 egg chamber stained with E-cad (green) to outline the FCs and DAPI (magenta) to label the nuclei. (D) Note that at the middle view, 6 cells are joined together in the middle (white arrow in D) above 3 cells that are present in the apical view (white arrow in D'). (E) A hypothetical diagram of how extruded cells look in a cross-sectional view. (F and G) Confocal micrographs of the basal surface of control (F) and Mcr-depleted (G) stage 12 egg chambers labeled with phalloidin to mark actin. Note the bright actin staining (yellow arrow in G), which corresponds to collapsed actin filaments (yellow arrow in G'). (H) A hypothetical diagram of how the actin cytoskeleton in extruded cells look in a cross-sectional view. Note that the images in this figure are taken from the ventral side of the egg chamber in A, B, and E and the dorsal side of the egg chamber in C, D, and F. Anterior is to the left and posterior is to the right. Scale bar= 20µm.

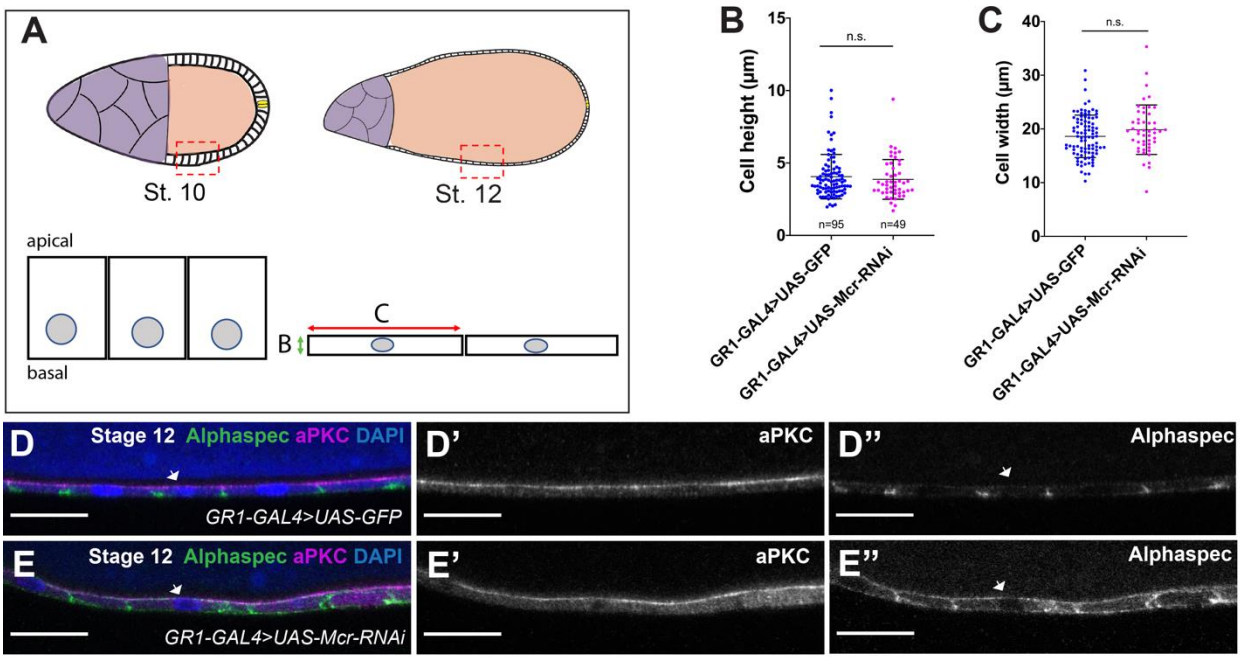

Figure 3. 5 *Mcr-RNAi*-expressing follicle cells undergo cell flattening but have a mild defect in apical-basal polarity.

(A**)** Diagram of stage 10 (St. 10) and stage 12 (St. 12) egg chambers showing the cell shape change that occurs during these stages of oogenesis. From stages 10–12, the nurse cells (purple) dump their content into the oocyte (orange), which results in a substantial increase in the volume of the oocyte. As a result, columnar follicle cells (FCs) of stage 10 flatten to accommodate the increase in the egg surface area. (B and C) Length and width measurements of stage 12 FCs. The width was measured as the space between two lateral membrane (red double arrow in stage 12 FCs in A), whereas the height was measured of one lateral membrane per cell (green double arrow in stage 12 FCs in A). (D and E) Confocal micrographs of control (D) and *Mcr-RNAi*-expressing follicular epithelium (E) stained with the apical membrane marker aPKC (magenta), the lateral membrane marker alpha-spectrin (green) and labeled with DAPI (blue). Note that aPKC is correctly localized at the apical membrane of Mcr-depleted FCs (compare D' to E'), whereas the lateral membrane marker alpha-spectrin appears at the apical as well as the lateral membrane in Mcr-depleted FCs (compare white arrow in D'' to E''). Anterior is to the left and posterior to the right. Scale bar=20µm.

Eggshell formation is compromised in *Mcr-RNAi* egg chambers

During the course of these investigations, it became obvious that females whose egg chambers express *Mcr-RNAi* failed to lay eggs. Instead, stage 14 egg chambers accumulate in these females' ovaries. Whereas control females lay on average 207 eggs, females expressing *Mcr-RNAi* in the FCs lay 0 eggs (see Materials and Methods). This appears to be due to the lack of Mcr as we observed the exact same phenotype when we drove *Mcr-RNAi* using a different ubiquitous FC GAL4 line (Traffic jam-GAL4; data not shown). This egg laying defect in *Mcr-RNAi* females is not due to an increase in egg width nor volume (**Figure 3. 1**E and G), and we rarely observe eggs occluding the oviduct. Moreover, *Mcr-RNAi* eggs do ovulate as we observe late stage 14 egg chambers that lack the FE surrounding the oocyte.

Many *Mcr-RNAi* stage 14 egg chambers are fragile, yellowish in color, and have abnormal dorsal appendages. These phenotypes are similar to egg chambers with defective eggshell formation, which motivated us to examine the eggshell morphology in *Mcr-RNAi* egg chambers (Velentzas et al., 2018a and Velentzas et al., 2018b). At stages 11–14, FCs secrete the chorion eggshell layers, which consists of inner-chorion, endochorion, and exochorion. These layers, mainly the endochorion, contribute to the formation of the eggshell structures. Eggshell structures include two anterior dorsal appendages (DA in **Figure 3. 6**A), the micropyle (Mp in **Figure 3. 6**A), and the operculum (Op in **Figure 3.6**A) (King and Koch 1963). In addition, the secretion of the endochorion results in FC imprints consisting of elevated ridges (R in **Figure 3. 6**A') and pillars (P in **Figure 3. 6**A') (Margaritis, Kafatos, and Petri 1980). To determine if Mcr is required for the formation of the chorion layers, we analyzed the morphology of stage 14 egg chambers using scanning electron microscopy (SEM). Because *Mcr-RNAi*-expressing egg chambers are never laid by the females, we retrieved control and *Mcr-RNAi*-expressing stage 14

egg chambers directly from the ovaries, but after they had ovulated as shown by the lack of the FE. In control stage 14 egg chambers, complete eggshell structures are formed, including the dorsal appendages, the micropyle, and the operculum (n=9, stage 14 egg chambers) (**Figure 3. 6**A). *Mcr-RNAi*-expressing egg chambers, on the other hand, have either broken or missing dorsal appendages, consistent with our recent observation (Chapter II) (n=12, 14 egg chambers) (**Figure 3. 6**B). Moreover, FC imprints in these eggs are unevenly formed, with large sections showing no obvious imprints at all (n=14 egg chambers) (compare **Figure 3. 6**A' to B' right side). Note that when imprints are visible in the mutant, the hexagonal-shaped cell morphology observed in the control egg chamber is aberrant (compare **Figure 3. 6**A' to B' left side).

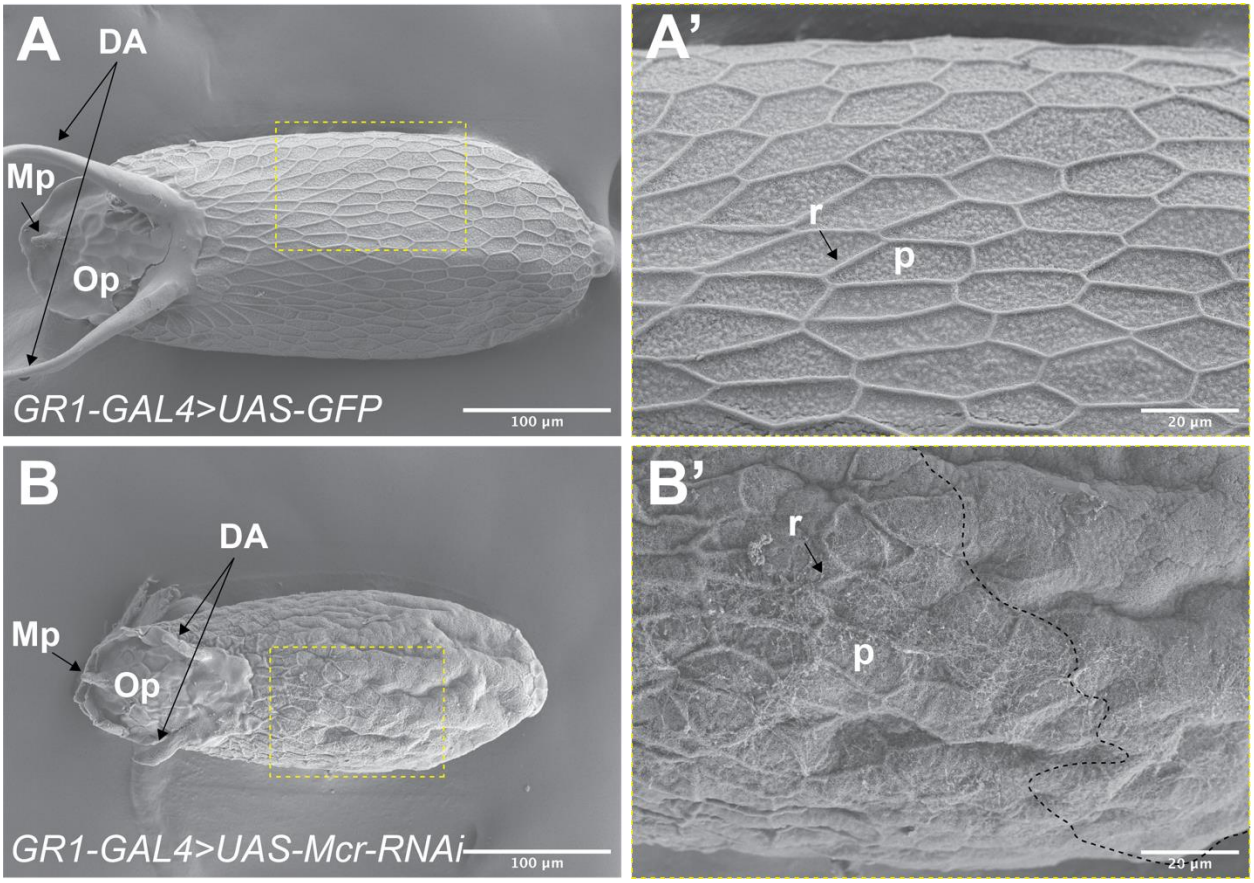

Figure 3. 6 Mcr is required for eggshell formation by stage 14 of oogenesis.
(A-B) Scanning electron micrographs acquired from the dorsal side of control (A) and *Mcr-RNAi*-expressing stage 14 egg chambers (B). The eggshell of a wild-type stage 14 egg chamber consists of anterior dorsal appendages (DA), the micropyle (Mp), and the Op (operculum). (A') Higher magnification image of the boxed region in A showing the FCs imprints, which consists

of ridges (r) and pillars (p). (B) Whereas the micropyle and operculum in the eggshell of *Mcr-RNAi*-expressing egg chamber are formed, the dorsal appendages appear short or broken. (B') Higher magnification image of the boxed region in B showing an inconsistent ridge morphology (B', left side) and smooth eggshell (B', right side). DA (dorsal appendages), Mp (micropyle), Op (operculum), ridges (r) and pillars (p). Anterior is to the left and posterior to the right. Scale bars= 100µm in A and B and 20µm in A' and B'.

Prior to the secretion of the chorion proteins, FCs secrete two additional eggshell layers, the vitelline membrane and wax layer. At stages 8–10, FCs secrete the vitelline proteins – known as vitelline bodies – in the extracellular space between the FCs and oocyte, which coalesce to form a vitelline membrane encasing the oocyte (Cavaliere et al. 2008). At stages 10B–12, wax vesicles are secreted apically by the FCs (Papassideri 1993). The vesicles are then compressed into longitudinal layers as a result of oocyte growth (Papassideri 1993). To determine if these layers are formed in *Mcr-RNAi*-expressing egg chambers, we incubated stage 14 control and *Mcr-RNAi* egg chambers in trypan blue and determined the percentage of the egg chambers that prevented the penetration of the dye into the oocyte. While 96% (n=83) of stage 14 control egg chambers exclude the dye, only 10% (n=723) of *Mcr-RNAi*-expressing stage 14 egg chambers exclude the dye, suggesting a defect in the formation or integrity of the vitelline membrane and/or wax layer (**Figure 3. 7**A and B). In order to distinguish between the two possibilities, we examined the ultrastructure of stage 12 egg chambers using transmission electron microscopy (TEM). We conducted this analysis in stage 12 egg chambers because the formation of the vitelline membrane and wax layer is complete by this stage of oogenesis (Papassideri 1993; Margaritis, Kafatos, and Petri 1980). Notably, *Mcr-RNAi*-expressing egg chambers form a vitelline membrane, although the thickness was inconsistent in 3 of the 4 stage 12 egg chambers we imaged (**Figure 3. 7**C'and D'). Interestingly, Mcr-depleted egg chambers lack the compressed wax plaques located between the vitelline membrane and the apical surface of the FCs (n=4 *Mcr-*

RNAi and 6 control stage 12 egg chambers) (red arrow in **Figure 3. 7**C' and D'). Moreover, in 2 of the 4 *Mcr-RNAi* egg chambers we imaged a substantial number of cytoplasmic vesicles could be observed (red asterisks in **Figure 3. 7**D), whereas we did not observe this phenotype in control egg chambers (n=6 egg chambers). Finally, it appeared that the apical membrane of Mcr-depleted FCs dissociates from the interface between the FC membrane and the oocyte (n=3 out of 4 *Mcr-RNAi* and 6 control egg chambers) (red arrows in **Figure 3. 7**C and D). Together, these data indicate a requirement for Mcr in the formation of the eggshell layers.

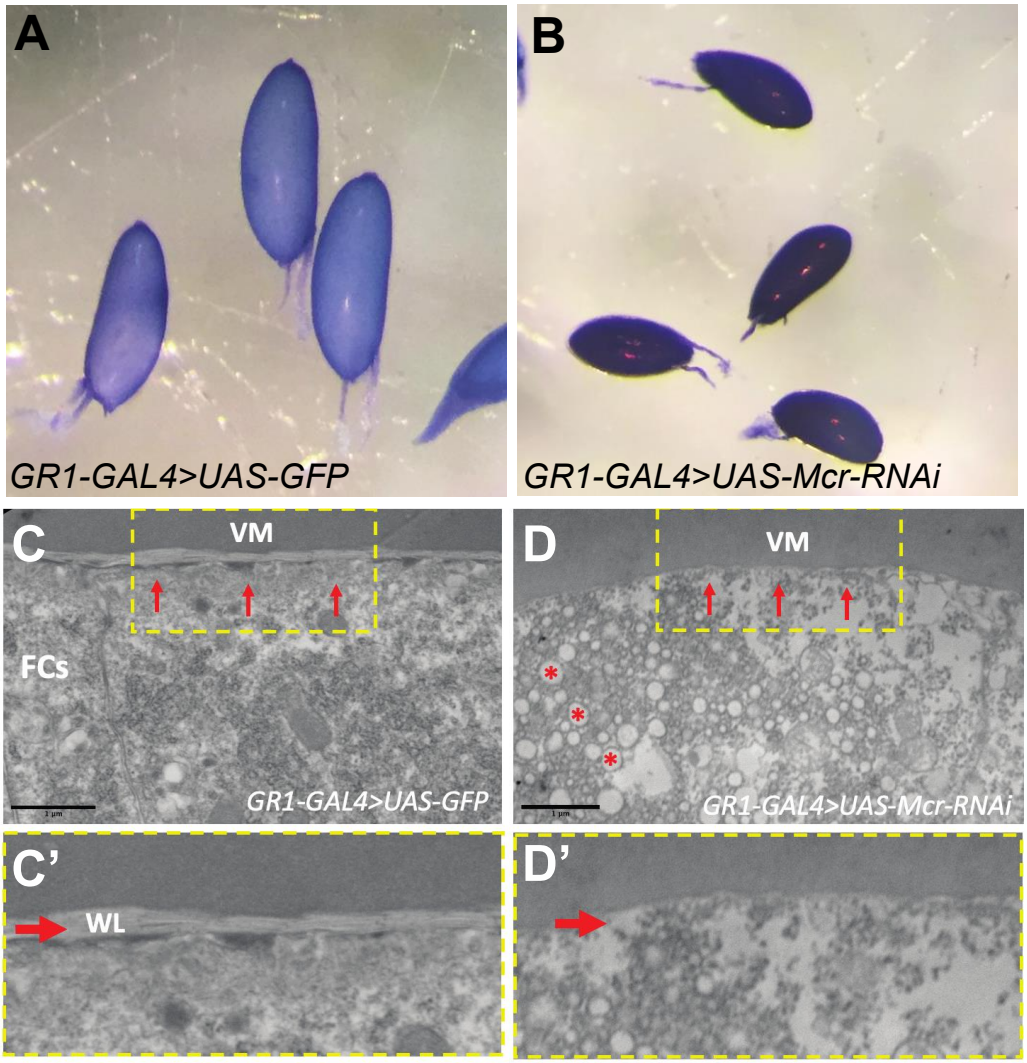

Figure 3. 7 The integrity of the eggshell is compromised in stage 14 *Mcr-RNAi* egg chambers.

(A-B) Photographs of control (A) and *Mcr-RNAi*-expressing stage 14 egg chambers (B) after 1 hour of incubation in trypan blue. The dye accumulates in the oocytes of Mcr-depleted eggs (dark blue) (B), whereas the dye in control egg chambers does not penetrate the oocytes (light blue) (A). Note the photographs of A and B are not captured with the same magnification. (C and D) Transmission electron micrographs of control (C) and *Mcr-RNAi*-expressing (D) stage 12 follicle cells (FCs). Note the apical separation (red arrows in D) and the accumulation of cytoplasmic vesicles (red asterisks in D) in Mcr-depleted FCs. (C' and D') Zoomed in images of the boxed region in C and D showing the lack of the wax layer in *Mcr-RNAi*-expressing FCs (compare red arrow in C' to D'). VM (vitelline membrane), FCs (follicle cells) and WL (wax layer). Scale bar= 1µm in C and D.

3.4 Discussion

In our previous study (Chapter II), we demonstrated that Mcr and other SJ proteins are required for morphogenetic processes during oogenesis, including egg elongation and dorsal appendage formation. Here we examined mechanisms that are known to play a role in establishing and maintaining elongated eggs during early and late stages of oogenesis, respectively. We find that Mcr is not required for establishing the egg shape. Instead, Mcr is required late in oogenesis of for maintaining monolayered epithelium, actin and integrin localization, and the secretion of the eggshell layers, which may contribute to the egg elongation defects in these eggs.

Mcr is required for maintaining an elongated-shaped egg

Early in oogenesis, egg elongation requires setting up a planar polarized molecular corset, consisting of actin stress fibers and ECM fibrils (Gates 2012; Horne-Badovinac 2014). The maintenance of this corset throughout oogenesis is essential to retain the elongated-shaped egg (Gates 2012; Horne-Badovinac 2014). Here, we find that Mcr is not required for establishing the molecular corset as Mcr-depleted FCs undergo FC migration and form planar polarized actin and collagen fibrils (**Figure 3. 2**). Instead, Mcr is required late in oogenesis (stages 12–14) to maintain the egg shape. By examining stage 12 egg chambers, we found that Mcr is required for basal actin stress fibers organization and integrin localization. Interestingly, the loss of basal organization seems stochastic where only a few cells seem to have misorganized actin or lose actin altogether (**Figure 3. 3**). At the other end of the epithelium, immunostaining of the adherens junction marker E-cadherin (E-cad) revealed a range of morphological abnormalities in *Mcr-RNAi*-expressing egg chambers (**Figure 3. 4**). We observed *Mcr-RNAi*-expressing FE that fails to maintain hexagonal shape, as well as a number of instances in which the FCs form rosette

structures. Interestingly, we see areas around the rosette structures where E-cad seems to be missing, so we wondered if the loss of E-cad in these areas is due to missing cells or cells that are being extruded. By taking a Z-series through the egg chamber, we find that in areas lacking E-cad, cells are being extruded to the apical side of the epithelium. This raised a question whether cells lose their basal contacts and then get pushed out of the epithelium or if they lose junctional E-cad and become migratory. Future studies using live imaging with markers for the adherens junction and focal adhesions will elucidate the mechanism of cell extrusion.

FC division ceases by stage 6 of oogenesis (Spradling 1993), which suggests against the possibility that extruded cells are proliferating cells, although we have not tested this experimentally. Thus, it would be important to examine cell proliferation by staining against phospho-histone 3 to confirm the lack of cell division in stage 12 egg chambers. If Mcr-depleted FCs are delaminating in the absence of cell proliferation, then a smaller number of remaining cells has to accommodate the same surface area covering the oocyte. Therefore, it is possible that cell delamination leads to unequal distribution of mechanical forces across the epithelium, which subsequently results in more cells losing their cell-ECM contacts. The overall loss of cell-ECM contacts may lead to the round egg phenotype in a similar way as disrupting ECM integrity late in oogenesis via collagenase (Haigo and Bilder 2011).

Mcr is required for eggshell formation

Eggshell formation occurs in three steps (Cavaliere et al. 2008). First, at stages 8-10, FCs secrete the vitelline membrane proteins in the space between the FCs and the oocyte (Cavaliere et al. 2008). During nurse cell dumping (stages 10-12), the wax layer is secreted over the vitelline membrane, whereas the chorion layers are secreted from stages 11–14 (Cavaliere et al. 2008).

Based on the TEM data, the vitelline membrane in Mcr-depleted egg chambers seems to be secreted and form normally (**Figure 3. 7**). In contrast, *Mcr-RNAi*-expressing egg chambers lack the wax layer and chorion layers. Moreover, the eggshell of stage 14 mutant egg chambers is clearly disrupted as shown through SEM analyses (**Figure 3. 6**). It is possible that the round eggs phenotype in *Mcr-RNAi*-egg chambers is a result of the lack of a wax layer or rigid eggshell. Consistent with this idea, knocking down the level of *s38*, a gene that encodes a major chorion protein, produces defective eggshell and results in shorter egg chambers (Velentzas et al. 2018). Finally, we propose that the cause of the round egg phenotype in *Mcr-RNAi* egg chambers is a combination of defective eggshell and defective FE-ECM interactions.

The role of SJs in egg morphogenesis

Many of the morphogenetic defects in Mcr-depleted egg chambers occur after the SJ forms. This raises the question of whether the defects we observe in Mcr-depleted egg chambers are due to a specific role for Mcr (and potentially other SJ proteins) that is independent of the SJ or if it is due to the lack of a functional SJ. There is a number of evidence for SJ proteins to function independent of their role in the occluding junction (Wells et al. 2013; Hall and Ward 2016; Lim et al. 2019). However, there are reasons to believe that these defects could arise from specific defects in assembling a SJ. For example, the lipids and chorion proteins could be secreted, but then leak between FCs to the point that intact layers do not form. Alternatively, it is possible that the SJ, once formed, serves as a lateral membrane landmark aiding in the direction of secretion. Under this circumstance, wax layer components and chorion proteins could be mis-sorted basally or remain in intracellular vesicles unable to be delivered to the apical surface. The observation of large numbers of vesicles in *Mcr-RNAi* stage 12 FCs (**Figure 3. 6**) supports such an idea. Similar

defects in the secretion of cuticle proteins have been reported in zygotic loss of function mutations of SJ proteins during embryogenesis (Hall and Ward 2016), although how these defects arise is still unknown.

Another possibility for SJ proteins requirement in secretion is through maintaining apical-basal polarity. During mid-embryogenesis, SJ proteins are required in collaboration with Yurt to maintain apical-basal polarity (Laprise et al. 2009). Although it is unclear if SJ proteins also play a role in maintaining apical-basal polarity in the FE, the apical localization of the lateral membrane protein alpha-spectrin in Mcr-depleted FCs suggests a mild defect in apical-basal polarity. As such, delaminated FCs lose E-cad that could be due to degradation that is not replaced by new synthesis, or by recycling defects. Additional work will be needed to address these issues.

3.5 Materials and Methods

Fly stocks

All stocks were maintained at 25ºC. GAL4 lines used in this study are as follow: *GR1-GAL4* (Bloomington Drosophila Stock Center (BDSC) #36287), *C204-GAL4* (BDSC# 3751), *CY2-GAL4* (gift from Julie Merkle, University of Evansville, Indiana), and *Traffic Jam-GAL4* (gift from Sally Horne-Badovinac, University of Chicago, Illinois). The RNAi line used in this study is *UAS-Mcr-RNAi* (Vienna Drosophila Resources Center (VDRC)#100197). *UAS-tsGAL80* (BDSC#7018) is on third chromosome and was used for the *CY2-GAL4* experiment, whereas *UAS-tsGAL80* (BSDC#7108) is on the second chromosome and was used for the *C204-GAL4* experiment. *Collagen IV-GFP* protein trap line is a gift from Julie Merkle, University of Evansville, Indiana. *FRT40AMcr^{D13}/Cyo-Dfd-GMR-nv-YFP* is a gift from Stefan Lusching, University of Münster, Germany. *hsFLP;FRT40GFP* line was used to generate Mcr null clones in the FCs. *w^{1118}* (BDSC#5905) was used for the egg laying analysis. Crosses were maintained at 25ºC, except flies bearing *UAS-tsGAL80*. These crosses were maintained at 18ºC to deactivate GAL4 activity. For experimental crosses, 1-2-day-old females were mated with sibling males and reared at 29ºC-30ºC for three days and dissected on the fourth day, except for the egg laying experiment. In this experiment, *GR1-GAL4>UAS-GFP* or *GR1-GAL4>UAS-Mcr-RNAi* females were mated with *w^{1118}* males and reared at 29ºC-30ºC for four days.

Generation of Mcr null clones

For generating Mcr null clones, 1-2-day-old females and males with this genotype (*hsFLP/+ or hsFLP/Y;FRT40AGFP/FRT40AMcr^{D13}*) were collected and reared on fresh food sprinkled with yeast at 25ºC overnight. For generating Mcr null clones, flies were heat shocked for 3 days (1

hour/day) in a 37ºC incubator. After the last round of heat shock, flies were transferred to a new vial with fresh food and yeast and reared for five days and dissected on the 6th.

Immunostaining and image acquisition

For antibody staining, ovaries were dissected in 1X Phosphate-buffered Saline (PBS), fixed in 4% Paraformaldehyde (PFA) for 20 minutes (pH=7.5), washed three times in 1X PBS, and then blocked in a blocking solution (1X PBS + 0.1% Triton + 1% Normal Donkey Serum) for 30 minutes followed by primary antibody staining at 4ºC overnight or at room temperature for 2 hours. For labeling the actin cytoskeleton, ovaries were dissected in Schneider's Drosophila Medium [Gibco, Paisley, Scotland, UK, Cat. No. 21720-024] + 20% fetal bovine serum (FBS) [Gibco, Cat No. 16140-0063] at room temperature, pH=7.0-7.4. Next, eggs were fixed in 8% PFA made in 1X PBS (pH=7.5) plus Alexa Flour 647 or 568 Phalloidin [Thermofisher Scientific, Reference# A22287 and # A12380, respectively] at (1:500) for 15 minutes while rocking at room temperature. Then, eggs were washed three times in 1X PBS and then incubated with 1X PBS + 0.2% Triton with Phalloidin at (1:500) at room temperature for 2 hours or overnight at 4ºC while rocking. Eggs were then washed one time with 1X PBS before mounting in homemade mounting media.

Antibodies used in this work are as follow: rat anti-Ecad (DCAD2, Developmental Studies Hybridoma Bank (DSHB)) at 1:27, mouse (m) anti-Mys (CF. 6G11-s, DSHB) at 1:25, m anti-alpha-spectrin (3A9, DSHB) at 1:10. Rabbit anti-aPKC (sc-216, Santa Cruz Biotechnology) at 1:500. Secondary antibodies were obtained from Jackson ImmunoResearch Laboratories (West Grove, Pennsylvania, USA) and were used at 1:500. DAPI (1mg/ml) was used at a dilution of 1:1000.

Images were acquired on an Olympus FV1000 confocal microscope equipped with Fluoview software (version 4.0.3.4). Objectives used in this study are as follow an UPLSAPO 20X Oil (NA:0.85), a PLAPON 60X Oil (NA:1.42), and an UPLSAPO 100X Oil (NA:1.40). For stages 14 eggs chambers in Figure 1 and live imaging experiments in Figure 2, we used Nikon Eclipse 80*i* compound microscope with Nikon Plan Apo 10X Air (NA:0.45) and Nikon Plan Apo 20X (NA:0.75) Air objectives, respectively. Raw images were rotated and cropped in ImageJ/Fiji (Schindelin et al. 2012), adjusted for brightness in ImageJ/Fiji or in Adobe Photoshop 21.1.1 (San Jose, CA). To compile the figures, Adobe Illustrator 24.1 was used.

Live imaging and travel distance analysis

Ovaries were dissected in live imaging media that consists of Schneider's Drosophila Medium [Gibco, Paisley, Scotland, UK, Cat. No. 21720-024] + 20% FBS [Gibco, Cat. No. 16140-0063] + 0.6X Antibiotic Antimycotic Solution [Corning, Cat. No. 30-004-CI] (pH=7.0-7.4) at room temperature. Eggs were transferred to a live imaging medium supplemented with 10% insulin (human recombinant) [Sigma Aldrich, Insulin, Cat. No. 91077C-250MG] containing CellMask [ThermoFisher Scientific, Cat. No. C10045] at 1:500. Eggs were imaged using a Nikon Eclipse 80*i* compound microscope for 30 minutes with 2 minutes intervals. To determine the travel distance, the Manual Tracking plugin in Fiji was used. The leading edge of one follicle cell membrane was either marked at the start and end of the movie or marked at each time frame. Next, the travel distance value was divided by the total number of minutes to calculate the travel distance in μm. Only one egg/female was imaged at a time.

Egg aspect ratio and volume measurements

The aspect ratio of egg chambers was determined by dividing the length (anterior-posterior) by the width (dorsal-ventral). The length (L) and width (W) measurements were determined using the straight-line tool in ImageJ/Fiji (Schindelin et al. 2012). Dorsal appendages of stage 14 egg chambers were excluded from the analysis. The volume of stage 14 egg chambers was calculated using this equation $(1/6)\ \pi\ W^2L$ (Markow, Beall, and Matzkin 2009). Microsoft Excel was used to calculate the aspect ratio and volume measurements.

Egg preparation for SEM analysis

Drosophila eggs were dissected in Schneider's *Drosophila* Medium [Gibco, Paisley, Scotland, UK, Cat. No. 21720-024] at room temperature, and fixed with 4% Paraformaldehyde (PFA; from a stock solution of 16% PFA in aqueous solution [Sigma Aldrich, St. Louis, MO, Cat. No. P6148, Lot. No. MKCD5277], pH 7.4) diluted in Schneider's Drosophila Medium [Gibco, Paisley, Scotland, UK, Cat. No. 21720-024] overnight at 4 °C. On the next day, eggs were rinsed with 0.2M Cacodylate buffer (Sodium Cacodylate Trihydrate, Electron Microscopy Sciences, Ft. Washington, PA, Cat. No. 12300, Lot. No. 124-65-2; pH 7.4) two times (5 min each) and stained with 0.5% Osmium tetroxide diluted in 0.2M Cacodylate buffer for 1h at room temperature inside a fume hood. Then, the eggs were rinsed with Cacodylate buffer two times (5 min each) and transferred to a porous beaker immersed in methanol and placed into a pressure chamber for critical point drying. Eggs were dehydrated using a K850 Critical Point Drier (Quorum Technologies Ltd, UK) using the procedure suggested by the company.

SEM imaging

Each egg was mounted on an aluminum stub with carbon tape for image acquisition. Images were acquired on a Cold Field Emission Scanning Electron Microscope (Hitachi High Technologies, SU8230 series) with an yttrium aluminum garnet (YAG) *backscattered electron* detector at 5.0 kV accelerating voltage, aperture 2 (80 µm diameter), high probe, condenser lens at 5, and a working distance between 8.0 to 10.0 mm. Images were captured at 2560 x 1920 pixels with 32 to 64s scan speed.

Egg laying assay

1-2-day old virgin females (*GR1-GAL4>UAS-GFP* or *GR1-GAL4>UAS-Mcr-RNAi*) were mated with w^{1118} males and reared at 29ºC-30ºC on blue food (0.05% bromophenol blue [LOT#10285478, ACROS Organic] prepared in standard fly food) sprinkled with yeast for 3 days. On the third day, flies were transferred to a new vial and laid eggs were counted 23 hours after the transfer. The number of flies in each vial was fixed with 6 females and 6 males/vial.

Blue dye intake

1-2-day old females and males with the appropriate genotypes (*GR1-GAL4>UAS-GFP* or *GR1-GAL4>UAS-Mcr-RNAi*) were reared at 29ºC-30ºC on standard fly food sprinkled with yeast for 3 days and dissected on the fourth. Each vial contained 6 females and 2 males. Ovaries were dissected in 1X PBS. Stage 14 egg chambers with no follicular epithelium were then incubated in 0.4% Trypan Blue [Gibco, LOT#2101513, REF#15250-061] for 1 hour. Next, the eggs were washed with 1X PBS until the PBS was clear. Eggs with dark blue dye color were counted as permeable, whereas eggs with light blue color were counted as impermeable.

Preparation of *Drosophila* stage 12 eggs for TEM analysis

Stage 12 egg chambers were dissected in Schneider's *Drosophila* Medium [Gibco, Paisley, Scotland, UK, Cat. No. 21720-024] supplemented with 20% FBS [Gibco, Cat. No. 16140-0063], and fixed with 4% Paraformaldehyde (PFA; from a stock solution of 16% PFA in aqueous solution [Sigma Aldrich, St. Louis, MO, Cat. No. P6148/ Lot. No. MKCD5277], pH 7.4) diluted in Schneider's *Drosophila* Medium [Gibco, Paisley, Scotland, UK, Cat. No. 21720-024] for 1 hr. The egg chambers were then pos-fixed in Karnovsky's fixative (2.5% glutaraldehyde/ 2% PFA) diluted in 0.2 M Cacodylate buffer (Sodium Cacodylate Trihydrate, Electron Microscopy Sciences [EMS], Ft. Washington, PA, Cat. No. 12300/ Lot. No. 124-65-2; pH 7.4) overnight at 4 °C. On the next day, eggs were rinsed with 0.2M Cacodylate buffer twice (5 min each) and stained with 0.5% Osmium tetroxide diluted in 0.2M Cacodylate buffer for 1hr at room temperature (RT) inside a fume hood. Then, the egg chambers were rinsed with Cacodylate buffer twice (5 min each), rinsed with 50% ethanol (5 min), stained with 1% *p*-phenylenediamine (Sigma Aldrich, Cat. No. P6001/ Lot. No. WXBB8077V) diluted in 70% ethanol (5 min), and continuing dehydration in 95% ethanol (3 min), 100% ethanol twice (3 min each) and 1:1 ethanol: 100% acetone (3 min), followed by slow resin infiltration steps (1:1 100% acetone: Embed 812 resin [5 min], 1:3 100% acetone: Embed 812 resin [5 min], 100% Embed 812 resin [1 hr] {Embed 812 resin consists of: (1) Embed 812 - EMS, Cat. No. 14900/ Lot. No. 921120; (2) Dodecenyl Succinic Anhydride – EMS, Cat. No. 13700/ Lot. No. 970325; Nadic Methyl Anhydride – EMS, Cat. No. 19000/ Lot. No. 970325}). Egg samples stayed immersed in Embed 812 resin overnight at RT inside the fume hood. On the next day, egg chambers were moved individually to a flat mold filled with embedding resin (Embed 812 resin + DMP-30 [EMS, Cat. No. 13600/ Lot. No. 90-72-2]) and placed inside an oven at 60 °C for 48 hours.

Tissue sectioning and Imaging

Egg chambers were sectioned between 80-100 nm thickness by using a Sorvall MT2 ultramicrotome and an ultra 45° angle diamond knife (Diatome, PA, model No. MF2407). Before ultra-thin sectioning, thick sections (200-300 nm) were collected, stained with Toluidine blue and observed under a Leica DM750 Brightfield microscope to confirm the region of interest within the tissue sample. Ultra-thin sections were mounted on copper grids (100 mesh) and imaged on a Cold Field Emission Scanning Electron Microscope (Hitachi High Technologies, SU8230 series) with a Dark Field-Scanning Transmission Electron Microscope (DF-STEM) detector (position height at 3). Imaging with the electron beam was done at 5.0-15.0 keV, 10 pA, 6.0 to 8.0 mm working distance, 2560x1920 pixel frame size with 32s scan speed or higher.

Statistical analysis

An unpaired *t*-test was used to calculate the *P* values in all experimental data between control and Mcr-depleted egg chambers using GraphPad Prism 8 (https://www.graphpad.com).

Acknowledgments

We thank Sally Horne-Badovinac, Julie Merkle, Stefan Lusching, the Bloomington *Drosophila* Stock Center, and the Vienna *Drosophila* RNAi Center for fly stocks. We thank Jocelyn McDonald and her lab members including Yujun Chen for the training on live imaging. We thank Brian Ackley for the use of his Olympus FV1000 confocal microscope. We thank Eduardo Rosa-Molinar and Noraida Martinez-Rivera from the Microscopy and Analytical Imaging Facility at the University of Kansas for conducting the SEM and TEM experiments. We also

thank Tina Tootle, Sally Horne-Badovinac and her lab members, and members of the Ward lab for helpful discussion about the project and manuscript.

Chapter IV: Concluding remarks and future directions

Concluding remarks and Future Directions

Morphogenesis is crucial for many developmental events, and involves precise temporal and spatial regulation of cell shape changes, cellular rearrangement, and cell migration. In *Drosophila melanogaster*, several studies revealed a requirement for core SJ proteins in epithelial morphogenesis during embryogenesis (e.g., Fehon, Dawson, and Artavanis-Tsakonas 1994; Wu and Beitel 2004; Hall and Ward 2016). It is intriguing that many of the developmental events that require SJ proteins occur before the maturation of the SJ. These observations raised the question that SJ protein function in morphogenesis may not be simply through maintaining a tight seal in the epithelium. Instead, SJ proteins may facilitate cellular processes, including polarized protein secretion, cell-cell adhesion, and regulating tissue mechanics.

Due to their early requirement in animal survival and development (Hall and Ward 2016), few studies have explored SJ proteins requirements in tissue morphogenesis at post-embryonic stages (Venema, Zeev-Ben-Mordehai, and Auld 2004; Moyer and Jacobs, 2008). Here we used the adult *Drosophila* egg chamber as a model system to investigate SJ biogenesis and the role of SJ proteins in egg morphogenesis. Although previous studies showed the expression of a few SJ proteins in the ovary (e.g., Schneider et al. 2006; Maimon, Popliker, and Gilboa, 2014; Ng et al. 2016), this work is the first to determine the subcellular localization of these proteins in the follicular epithelium (FE) throughout oogenesis. In the second chapter of my dissertation, I described my findings that SJ biogenesis in the FE is similar to that in the embryonic epithelia (Tiklová et al. 2010). In both tissues, SJ proteins localize along the lateral membrane during the early-middle stages of development but become gradually enriched at the apical-lateral membrane later in development. This re-localization event requires Rab5-mediated endocytosis and Rab11-mediated recycling. SJ biogenesis also requires the correct localization of other core

SJ proteins at the junction. Using tissue-specific RNAi-mediated knock-down against at least four distinct SJ proteins, we determined that SJ proteins are required for egg morphogenetic events, including egg elongation, border cell migration, and dorsal appendages formation. Interestingly, the morphogenetic defects associated with knocking down different SJ proteins in the FCs are similar, suggesting that these proteins may function together. Since many of the morphogenetic events that require SJ proteins function occur throughout oogenesis, it suggested a non-junctional requirement for SJ proteins in egg morphogenesis. Altogether, Chapter II lays the foundation for the SJ field to explore SJ protein requirements in morphogenesis using the *Drosophila* egg as a model system.

In the third chapter, we used a combination of RNAi-mediated knock-down and mitotic clones to investigate the role of Mcr in egg morphogenesis. We find that Mcr is required late in oogenesis for actin stress fibers organization, integrin localization, and maintaining FE morphology. Mcr is also required for eggshell formation, which is secreted by the FCs late in oogenesis. Interestingly, a similar requirement for Mcr in protein secretion was shown during embryogenesis. *Mcr* mutant embryos (and other SJ mutant embryos) have a thin and underdeveloped cuticle, suggestive of defects in cuticle protein secretion (Hall and Ward 2016). The secretion of the embryonic cuticle and the chorion layers in the egg occurs after the SJ is physiologically tight (stage 16 of embryogenesis and stages 11-14 of oogenesis), suggesting an SJ-dependent requirement for SJ proteins in the secretion of these proteins (Hillman and Lesnik 1970; Mahowald 1972; Cavaliere et al. 2008; Hall and Ward 2016; Isasti-Sanchez, Munz-Zeise, and Luschnig 2020).

An area for further exploration is to determine the mechanism by which SJ proteins are involved in protein secretion. SJ formation during the late stages of ovarian development could

be necessary to provide the epithelia with a gate function that retains secreted proteins at the apical domain for further protein processing and crosslinking. The gate function hypothesis is supported by the fact that imprints the wild-type eggshells reflect the outline of the FCs underneath it (Dobens and Raftery 2000). Since Mcr-depleted eggshells lack the imprints, the gate function is likely compromised (Chapter III). Western blot analysis of chorion proteins of the adult female hemolymph can be used to test this hypothesis. Because adult *Drosophila* has an open circulatory system, proteins can circulate through the hemolymph throughout the fly body. Therefore, if chorion proteins are secreted but pass between the FCs, the hemolymph of Mcr-depleted flies should contain chorion proteins, whereas the hemolymph of control flies should not. An alternative approach to test if the eggshell proteins are being secreted but leak between the cells is via examining Green Fluorescence Protein (GFP)-tagged chorion proteins. Using this approach combined with live imaging will be useful to visualize chorion protein localization as the FCs secrete them in live egg chambers.

Another possibility for SJs involvement in protein secretion is via segregating the plasma membrane into apical and basolateral domains. This "cellular fence" model has been extensively investigated in the tight junction (Zahraoui, Louvard, and Galli 2000). Further, several studies revealed the association of the small GTPases of the Rabs family to the tight junction (Zahraoui, Louvard, and Galli 2000). A similar mechanism is likely to be present in invertebrate epithelia and may involve the SJ, which was suggested by Lamb et al. 1998. The formation of the SJ may also organize polarized microtubules, which in turn direct cargos to the secretion sites. A study by Louvard in vertebrate epithelia indicates that apically secreted cargos are targeted to the cell-cell contact before they reach their final destination at the apical membrane (Louvard 1980). Interestingly, ultrastructural studies point that microtubule structures near the SJ in the FCs of

stage 12 egg chambers (Mahowald 1972). These observations suggest that occluding junctions may be essential for targeted protein secretion. The data in Chapter III further support this hypothesis as FE expressing *Mcr-RNAi* accumulates cytoplasmic vesicles and lacks the wax layer and eggshell imprints. The use of GFP-tagged chorion proteins would determine if the proteins are being directed to the apical membrane and subsequently secreted or are accumulated in the cytoplasm due to mispolarized protein trafficking. Therefore, examining microtubule polarization and its association with the SJ would determine if microtubules organization is aberrant in Mcr-depleted FCs.

A promising area of study is to examine the role of SJ proteins in tissue mechanics and cell-cell adhesion during oogenesis. Chapter III shows that *Mcr-RNAi*-expressing FCs delaminate from the FE of stage 12 egg chambers, which is after SJ is formed. Late in oogenesis (stages 11–12/13) and within 3.5 hours, the egg grows rapidly due to yolk uptake and the cytoplasmic transport of nurse cell content into the oocyte (Spradling 1993). Because the FCs number is fixed early in oogenesis (Spradling1993), the only way for the FCs to accommodate the increase in egg volume is via dramatic cell shape changes. As such, columnar FCs flatten over the oocyte, which generates mechanical strain in the FE (Fletcher et al. 2018). Coincident with cell flattening, SJ proteins become enriched at the apical-lateral region of the FCs, forming an SJ (Mahowald 1972; Müller 2000; Isasti-Sanchez, Munz-Zeise, and Luschnig 2020). At the same time, integrin complexes become enriched at the focal adhesion sites where basal actin stress fibers terminate (Delon and Brown 2009). Modulating cell–extracellular matrix adhesion has a direct effect on egg elongation (He et al. 2010). Moreover, *integrin* mutant FCs have reduced basal cell surface and experience high membrane tension (Santa-Cruz Mateos et al. 2020). The reduced basal surface could be a result of cell delamination as FCs mutant clones for

integrin have collapsed actin stress fibers and appear at a different focal plane similar to what we observed in Mcr-depleted FCs (Delon and Brown 2009). Therefore, maintaining the correct level of cell-ECM adhesions could be necessary for propagating the mechanical forces across the epithelium, thus, promoting actin stress fibers and integrin assembly at the basal surface of the FCs.

Given that many SJ proteins contain adhesive domains (e.g., Cont, Mcr, Lac, Nrx-IV) and the fact that SJ is fixed at the membrane once it is formed (Oshima and Fehon 2011), the formation of the SJ could provide another layer of support to cell–cell adhesions during cell flattening. The formation of the SJ may also regulate the trafficking of other adhesion molecules to the plasma membrane. A potential candidate to be affected in Mcr-depleted FCs is E-cadherin since it is absent in the membrane of extruded cells. Whether the mechanism through which SJ affects cell-cell adhesion is via directly strengthening cell-cell adhesion or regulating trafficking of E-cadherin is unknown. In either scenario, cell-cell adhesion dynamic is likely to be compromised, which subsequently affects membrane tension and cell-ECM adhesion. Therefore, examining membrane tension via laser ablation experiment of cell-cell contacts is needed. If Mcr-depleted FCs experience increased membrane tension, a faster rate of recoil would be expected. Finally, it would also be interesting to test if the cell delamination phenotype seen in Mcr-depleted FCs can be recapitulated in tissues experiencing high level of cell shape changes and mechanical stress, such as the leg imaginal discs of the *Drosophila* larvae.

The findings in this dissertation demonstrated a requirement for SJ proteins in egg morphogenetic events, with Mcr being required late in oogenesis for egg elongation and eggshell formation. While reviewing the literature in oogenesis, it became clear to me that there is a gap in our understanding of the cellular processes of late-stage egg chambers. Therefore, it would be

essential to analyze egg morphogenesis of wild-type late-stage egg chambers by using a combination of live imaging, morphometric analysis, and mathematical modeling. The results from these studies would greatly further our understanding of the cellular behaviors that contribute to egg morphogenesis late in oogenesis, which will help us understand the defects seen in mutant egg chambers at this stage of oogenesis.

We are at the beginning of understanding the mechanisms by which SJ proteins regulate morphogenesis. The non-occluding junctional requirement of the SJ in tissue morphogenesis was first appreciated from the discovery of *coracle* in 1994 (Fehon, Dawson, and Artavanis-Tsakonas 1994). Subsequent studies revealed a shared requirement for SJ proteins during embryonic epithelial morphogenesis (Hall and Ward 2016; Wu and Beitel 2004), while other studies on the larval imaginal discs showed a requirement for these proteins in planar cell polarity (Venema, Zeev-Ben-Mordehai, and Auld 2004; Moyer and Jacobs, 2008). The work presented here further demonstrates that the role of SJ proteins in morphogenesis is conserved across development. The discovery that core SJ proteins are required for morphogenetic events during oogenesis provides the field with a new system to explore the molecular and cellular mechanisms by which SJ proteins are involved in morphogenesis.

References

Alégot, H., P. Pouchin, O. Bardot, and V. Mirouse. 2018. “Jak-Stat Pathway Induces Drosophila Follicle Elongation by a Gradient of Apical Contractility.” *ELife* 7:e32943.

Bachmann, André, Margarete Draga, Ferdi Grawe, and Elisabeth Knust. 2008. “On the Role of the MAGUK Proteins Encoded by Drosophila Varicose during Embryonic and Postembryonic Development.” *BMC Developmental Biology* 8: 55.

Banerjee, S, R. J. Bainton, N. Mayer, R Beckstead, and M. A. Bhat. 2008. “Septate Junctions Are Required for Ommatidial Integrity and Blood-Eye Barrier Function in Drosophila.” *Developmental Biology* 317: 585–99.

Bateman, J., R. S. Reddy, H. Saito, and D. Van Vactor. 2001. “The Receptor Tyrosine Phosphatase Dlar and Integrins Organize Actin Filaments in the Drosophila Follicular Epithelium.” *Current Biology* 11: 1317–27.

Bätz, T., D. Förster, and S. Luschnig. 2014. “The Transmembrane Protein Macroglobulin Complement-Related Is Essential for Septate Junction Formation and Epithelial Barrier Function in Drosophila.” *Development* 141: 899–908.

Baumgartner, S., J. T. Littleton, K. Broadie, M. A. Bhat, R. Harbecke, J. A. Lengyel, R. Chiquet-Ehrismann, A. Prokop, and H. J. Bellen. 1996. “A Drosophila Neurexin Is Required for Septate Junction and Blood-Nerve Barrier Formation and Function.” *Cell* 87: 1059–1068.

Behr, M., D. Riedel, and R. Schuh. 2003. “The Claudin-like Megatrachea Is Essential in Septate Junctions for the Epithelial Barrier Function in Drosophila.” *Developmental Cell* 5: 611–620.

Ben-Zvi, D. S., and T. Volk. 2019. “Escort Cell Encapsulation of Drosophila Germline Cells Is Maintained by Irre Cell Recognition Module Proteins.” *Biology Open* 8:bio039842.

Bergstralh DT, Lovegrove HE, St Johnston D. 2015. "Lateral Adhesion Drives Reintegration of Misplaced Cells into Epithelial Monolayers." *Nature Cell Biology* 17: 1497-1503

Bieber, A. J., P. M. Snow, M. Hortsch, N. H. Patel, J. R. Jacobs, Z. R. Traquina, J. Schilling, and C. S. Goodman. 1989. “Drosophila Neuroglian: A Member of the Immunoglobulin Superfamily with Extensive Homology to the Vertebrate Neural Adhesion Molecule L1.” *Cell* 59 : 447–60.

Bilder, D. 2004. “Epithelial polarity and proliferation control: links from the Drosophila neoplastic tumore suppressors.” *Genes and Development* 18: 1909-1925.

Bilder, D., and N. Perrimon. 2000. “Localization of apical epithelial determinants by the basolateral PDZ protein Scribble.” *Nature* 403: 676-680.

Bilder, D., and S. L. Haigo. 2012. “Expanding the Morphogenetic Repertoire: Perspectives from the Drosophila Egg.” *Developmental Cell* 22 : 12–23.

Brand, A. H., and N. Perrimon. 1993. “Targeted Gene Expression as a Means of Altering Cell Fates and Generating Dominant Phenotypes.” *Development* 118: 401–415.

Buszczak, M. S. Paterno, D. Lighthouse, J. Bachman, J. Planck, S. Owen, A. D. Skora, T. G., Nystul, B. Ohlstein, A. Allen, J. E. Wilhelm, T. D. Muphy, R. W. Levis, E. Matunis, N. Srivali, R. A. Hoskins and A. C. Spradling. 2007. “The carnegie protein trap library: a versatile tool for Drosophila developmental studies.” *Genetics* 175: 1505-1531.

Cai, D., S. C. Chen, M. Prasad, L. He, X. Wang, V. Choesmel-Cadamuro, J. K. Sawyer, G. Danuser, and D. J. Montell. 2014. “Mechanical Feedback through E-Cadherin Promotes Direction Sensing during Collective Cell Migration.” *Cell* 157: 1146–59.

Cerqueira Campos, F. C., C. Dennis, H. Alégot, C. Fritsch, A. Isabella, P. Pouchin, O. Bardot, S. Horne-Badovinac, and V. Mirouse. 2020. “Oriented Basement Membrane Fibrils Provide a Memory for F-Actin Planar Polarization via the Dystrophin-Dystroglycan Complex during Tissue Elongation.” *Development* 147:dev186957.

Caussinus, E., O. Kanca, and M. Affolter. 2011. “Fluorescent Fusion Protein Knockout Mediated by Anti-GFP Nanobody.” *Nature Structural and Molecular Biology* 19: 117–121.

Cavaliere, V., F. Bernardi, P. Romani, S. Duchi, and G. Gargiulo. 2008. “Building up the Drosophila Eggshell: First of All the Eggshell Genes Must Be Transcribed.” *Developmental Dynamics* 237: 2061–272.

Cetera, M., and S. Horne-Badovinac. 2015. “Round and Round Gets You Somewhere: Collective Cell Migration and Planar Polarity in Elongating Drosophila Egg Chambers.” *Current Opinon Genetic Development* 32: 10–15.

Cetera, M., G. R. Ramirez-San Juan, P. W. Oakes, L. Lewellyn, M. J. Fairchild, G. Tanentzapf, M. L. Gardel, and S. Horne-Badovinac. 2014. “Epithelial Rotation Promotes the Global Alignment of Contractile Actin Bundles during Drosophila Egg Chamber Elongation.” *Nature Communications* 5: 5511.

Cha, I. J., J. H. Lee, K. S. Cho, and S. B. Lee. 2017. “Drosophila Tensin Plays an Essential Role in Cell Migration and Planar Polarity Formation during Oogenesis by Mediating Integrin-Dependent Extracellular Signals to Actin Organization.” *Biochemical Biophysical Research Communications* 484: 702–709.

Rice, C., O. De, H. Alhadyian, S. Hall, R. Ward. 2021. “Expanding the junction:new insight into non-occluding roles for septate junction proteins during development. ” *Jouranl of Developmental Biology* 9: 11.

Conder, R., H. Yu, B. Zahedi, and N. Harden. 2007. “The Serine/Threonine Kinase DPak Is Required for Polarized Assembly of F-Actin Bundles and Apical-Basal Polarity in the Drosophila Follicular Epithelium.” *Developmental Biology* 305: 470–782.

Crest, J., A. Diz-Mun˜oz, D.Y. Chen, D.A. Fletcher, and D. Bilder. 2017. “Organ Sculpting by Patterned Extracellular Matrix Stiffness.” *ELife* 6: e24958.

Deligiannaki, M., A. L. Casper, C. Jung, and Gaul U. 2015. “Pasiflora Proteins Are Novel Core Components of the Septate Junction.” *Development* 142: 3046–3057.

Delon, I, and N. H. Brown. 2009. “The Integrin Adhesion Complex Changes Its Composition and Function during Morphogenesis of an Epithelium.” *Journal of Cell Science* 122: 4363–4374.

Dobens, L. L., and L. A. Raftery. 2000. “Integration of Epithelial Patterning and Morphogenesis In Drosophila Ovarian Follicle Cells.” *Developmental Dynamics* 93: 80–93.

Dorman, J. B., K. E. James, S. E. Fraser, D. P. Kiehart, and C. A. Berg. 2004. “Bullwinkle Is Required for Epithelial Morphogenesis during Drosophila Oogenesis.” *Developmental Biology* 267: 320–341.

Duhart, J. C., T. T. Parsons, and L. A. Raftery. 2017. “The Repertoire of Epithelial Morphogenesis on Display: Progressive Elaboration of Drosophila Egg Structure.” *Mechanism Development* 148: 18-39.

Faivre-Sarrailh, C., S. Banerjee, J. Li, M. Hortsch, L. Monique, and M. A. Bhat. 2004. “Drosophila Contactin, a Homolog of Vertebrate Contactin, Is Required for Septate Junction Organization and Paracellular Barrier Function.” *Development* 131: 4931–4942.

Falk, G. J., and R. C. King. 1964. “Studies on the Developmnetal Genetics of the Mutant Tiny of Drosophila Melanogaster.” *Growth* 28: 291–324.

Fehon, R. G., I. A. Dawson, and S. Artavanis-Tsakonas. 1994. “A Drosophila Homologue of Membrane-Skeleton Protein 4.1 Is Associated with Septate Junctions and Is Encoded by the Coracle Gene.” *Development* 120: 545–557.

Felix, M., M. Chayengia, R. Ghosh, A. Sharma, and M. Prasad. 2015. “Pak3 Regulates Apical-Basal Polarity in Migrating Border Cells during Drosophila Oogenesis.” *Development* 142: 3692–3703.

Fletcher, G. C., M. D. Carmen Diaz-de-la-Loza, N. Borreguero-Muñoz, M. Holder, M. Aguilar-Aragon, and B. J. Thompson. 2018. “Mechanical Strain Regulates the Hippo Pathway in Drosophila.” *Development* 145:dev159467.

Frydman, H. M., and A. C. Spradling. 2001. “The Receptor-like Tyrosine Phosphatase Lar Is Required for Epithelial Planar Polarity and for Axis Determination within Drosophila

Ovarian Follicles." *Development* 128: 3209–20.

Gates, J. 2012. "Drosophila Egg Chamber Elongation: Insights into How Tissues and Organs Are Shaped." *Fly* 6: 213–227.

Genova, J. L., and R. G. Fehon. 2003. "Neuroglian, Gliotactin, and the Na+/K+ ATPase Are Essential for Septate Junction Function in Drosophila." *Journal Cell Biology* 161: 979–989.

Green, C. R., and P. R. Bergquist. 1982. "Phylogenetic Relationships within the Invertebrata in Relation to the Structure of Septate Junctions and the Development of 'occluding' Junctional Types." *Journal of Cell Science* 53: 279–305.

Gupta, T., and T. Schüpbach. 2003. "Cct1, a Phosphatidylcholine Biosynthesis Enzyme, Is Required for Drosophila Oogenesis and Ovarian Morphogenesis." *Development* 130: 6075–6087.

Gutzeit, H. O., W. Eberhardt, and E. Gratwohl. 1991. "Laminin and Basement Membrane-Associated Microfilaments in Wild-Type and Mutant Drosophila Ovarian Follicles." *Journal Cell Science* 100: 781–788.

Haigo, S. L., and D. Bilder. 2011. "Global Tissue Revolutions in a Morphogenetic Movement Controlling Elongation." *Science* 331: 1071–1074.

Hall, S., C. Bone, K. Oshima, L. Zhang, M. McGraw, B. Lucas, R. G. Fehon, and R. E. Ward. 2014. "Macroglobulin Complement-Related Encodes a Protein Required for Septate Junction Organization and Paracellular Barrier Function in Drosophila." *Development* 141: 889–898.

Hall, S., and R. E. Ward. 2016. "Septate Junction Proteins Play Essential Roles in Morphogenesis Throughout Embryonic Development in Drosophila." *G3* 6: 2375–2384.

Hayashi, S., and T. Kondo. 2018. "Development and Function of the Drosophila Tracheal System." *Genetics* 209: 367–380.

Hayes, P., and J. Solon. 2017. "Drosophila Dorsal Closure: An Orchestra of Forces to Zip Shut the Embryo." *Mechanism Development* 144: 2–10.

He, L., X. Wang, H. L. Tang, and D. J. Montell. 2010. "Tissue Elongation Requires Oscillating Contractions of a Basal Actomyosin Network." *Nature Cell Biology* 12: 1133–1142.

Hijazi, A., M. Haenlin, L. Waltzer, and F. Roch. 2011. "The Ly6 Protein Coiled Is Required for Septate Junction and Blood Brain Barrier Organisation in Drosophila." *PLoS ONE* 6:e17763.

Hijazi, A., W. Masson, B. Augé, L. Waltzer, M. Haenlin, and F. Roch. 2009. "Boudin Is Required for Septate Junction Organisation in Drosophila and Codes for a Diffusible

Protein of the Ly6 Superfamily." *Development* 136: 2199–2209.

Hildebrandt, A., R. Pflanz, M. Behr, T. Tarp, D. Riedel, and R. Schuh. 2015. "Bark Beetle Controls Epithelial Morphogenesis by Septate Junction Maturation in Drosophila." *Developmental Biology* 400: 237–247.

Hillman, R., and L. H. Lesnik. 1970. "Cuticle Formation in the Embryo of Drosophila Melanogaster." *Journal Morphology* 131: 383–395.

Horne-Badovinac, S. 2014. "The Drosophila Egg Chamber-a New Spin on How Tissues Elongate." *Integrative Comparative Biology* 54: 667–676.

Horne-Badovinac, S., 2020. "The Drosophila Micropyle as a System to Study How Epithelia Build Complex Extracellular Structures." *Philosopical Transactions Royal Society B Biological Sciences* 375:20190561.

Horne-Badovinac, S., and D. Bilder. 2005. "Mass Transit: Epithelial Morphogenesis in the Drosophila Egg Chamber." *Developmental Dynamic* 232: 559–574.

Horne-Badovinac, S., J. Hill, G. Gerlach, W. Menegas, and D. Bilder. 2012. "A Screen for Round Egg Mutants in Drosophila Identifies Tricornered, Furry, and Misshapen as Regulators of Egg Chamber Elongation." *G3* 2: 371–378.

Ile, K. E., R. Tripathy, V. Goldfinger, and A. D. Renault. 2012. "Wunen, a Drosophila Lipid Phosphate Phosphatase, Is Required for Septate Junction-Mediated Barrier Function." *Development* 139: 2535–2546.

Isabella, A. J., and S. Horne-Badovinac. 2015a. "Building from the Ground up: Basement Membranes in Drosophila Development." *Current Topics in Membranes* 76: 305–336.

Isabella, A., and Horne-Badovinac, S. 2015b. "Dynamic Regulation of Basement Membrane Protein Levels Promotes Egg Chamber Elongation in Drosophila." *Developmental Biology* 406: 212–221.

Isabella, A., and Horne-Badovinac, S. 2016. "Rab10-Mediated Secretion Synergizes with Tissue Movement to Build a Polarized Basement Membrane Architecture for Organ Morphogenesis." *Developmental Biology* 38: 47–60.

Isasti-Sanchez, J., F. Munz-Zeise, and S. Luschnig. 2020. "Transient Opening of Tricellular Vertices Controls Paracellular Transport through the Follicle Epithelium during Drosophila Oogenesis." *Developmental Biology 56: 1083-1099.*

Izumi, Y., and M. Furuse. 2014. "Molecular Organization and Function of Invertebrate Occluding Junctions." *Seminar Cell Developmental Biology* 36: 186–193.

Jonusaite, S., A. Donini, and S. P. Kelly. 2016. "Occluding Junctions of Invertebrate Epithelia."

Journal of Comparative Physiology 186: 17–43.

Khammari, A., F. Agnès, P. Gandille, and A. M. Pret. 2011. "Physiological Apoptosis of Polar Cells during Drosophila Oogenesis Is Mediated by Hid-Dependent Regulation of Diap1." *Cell Death and Differentiation* 18: 793–805.

King, By R C, and Elizabeth a Koch. 1963. "Studies on the Ovarian Follicle Cells of Drosophila." *Quarterly Journal Microscopical Science* 104: 297–320.

Königsmann, T., I. Parfentev, H. Urlaub, D. Riedel, and R. Schuh. 2020. "The Bicistronic Gene Würmchen Encodes Two Essential Components for Epithelial Development in Drosophila." *Developmental Biology* 463: 53–62.

Koride, S., L. He, L.-P. Xiong, G. Lan, D. J. Montell, and S. X. Sun. 2014. "Mechanochemical Regulation of Oscillatory Follicle Cell Dynamics in the Developing Drosophila Egg Chamber." *Molecular Biology Cell* 25: 3709–3716.

Lamb, R. S., R. E. Ward, L. Schweizer, and R. G. Fehon. 1998. "Drosophila Coracle, a Member of the Protein 4.1 Superfamily, Has Essential Structural Functions in the Septate Junctions and Developmental Functions in Embryonic and Adult Epithelial Cells." *Molecular Biology Cell* 9: 3505–1359.

Laprise, P., K. M. Lau, K. P. Harris, N. F. Silva-Gagliardi, S. M. Paul, S. Beronja, G. J. Beitel, C. J. McGlade, and U. Tepass. 2009. "Yurt, Coracle, Neurexin IV and the Na+, K+-ATPase Form a Novel Group of Epithelial Polarity Proteins." *Nature* 459: 1141–1145.

Lebovitz, R. M., K. Takeyasu, and D. M. Fambrough. 1989. "Molecular Characterization and Expression of the (Na+ + K+)-ATPase Alpha-Subunit in Drosophila Melanogaster." *The EMBO Journal* 8: 193–202.

Lerner, W. D., D. McCoy, A. J. Isabella, A. P. Mahowald, G. F. Gerlach, T. A. Chaudhry, and S. Horne-Badovinac. 2013. "A Rab10-Dependent Mechanism for Polarized Basement Membrane Secretion during Organ Morphogenesis." *Developmental Cell* 24: 159–168.

Lewellyn, L., M. Cetera, and S. Horne-Badovinac. 2013. "Misshapen Decreases Integrin Levels to Promote Epithelial Motility and Planar Polarity in Drosophila." *Journal of Cell Biology* 200: 721–729.

Llimargas, M., M. Strigini, M. Katidou, D. Karagogeos, and J. Casanova. 2004. "Lachesin Is a Component of a Septate Junction-Based Mechanism That Controls Tube Size and Epithelial Integrity in the Drosophila Tracheal System." *Development* 131: 181–190.

Louvard, D. 1980. "Apical Membrane Aminopeptidase Appears at Site of Cell-Cell Contact in Cultured Kidney Epithelial Cells." *Proceedings of the National Academy of Sciences of the United States of America* 77: 4132–4136.

Luschnig S., T. Bätz, K. Armbruster, and Krasnow, M. A. 2006. " Serpentine and vermiform encode proteins with chitin binding and deacetylation domains that limit treacheal tube length in Drosophila. " *Current Biology* 16: 186-194.

Mahowald, A. P. 1972. "Ultrastructural Observations on Oogenesis in Drosophila." *Journal of Morphology* 137: 29–48.

Maimon, I., M. Popliker, and L. Gilboa. 2014. "Without Children Is Required for Stat-Mediated Zfh1 Transcription and for Germline Stem Cell Differentiation." *Development* 141: 2602–2610.

Margaritis, L. H., F. C. Kafatos, and W. H. Petri. 1980. "The Eggshell of Drosophila Melanogaster. Fine Structure of the Layers and Regions of the Wild-Type Eggshell." *Journal Cell Science* 43:1–35.

Markow, T. A., S. Beall, and L. M. Matzkin. 2009. "Egg Size, Embryonic Development Time and Ovoviviparity in Drosophila Species." *Journal of Evolutionary Biology* 22: 430–434.

Montell, D. J. 2003. "Border-Cell Migration: The Race Is On." *Nature Review Molecular Cell Biology* 4:13–24.

Moyer, K. E., and J. R. Jacobs. 2008. "Varicose: A MAGUK Required for the Maturation and Function of Drosophila Septate Junctions." *Developmental Dynamic* 8: 52–67.

Müller, H. A. 2000. "Genetic Control of Epithelial Cell Polarity: Lessons from Drosophila." *Developmental Dynamics* 218: 52–67.

Murphy, A. M., and D. J. Montell. 1996. "Cell Type-Specific Roles for Cdc42, Rac, and Rhol in Drosophila Oogenesis." *Journal Cell Biology* 133: 617–630.

Nelson, K. S., M. Furuse, and G.J. Beitel. 2010. "The Drosophila Claudin Kune-Kune Is Required for Septate Junction Organization and Tracheal Tube Size Control." *Genetics* 185: 831–39.

Ng, B. F., G. K. Selvaraj, C. S. C. Mateos, I. Grosheva, I. Alvarez-Garcia, M. D. Martin-Bermudo, and I. M. Paracios. 2016. "α-spectrin and integrins act together to regulate actomyosin and columnarization, and to maintain a monolayered follicular epithelium." *Development* 143: 1388-1399.

Nilton, Anna, Kenzi Oshima, Fariba Zare, Sunitha Byri, Ulf Nannmark, Kevin G. Nyberg, Richard G. Fehon, and Anne E. Uv. 2010. "Crooked, Coiled and Crimpled Are Three Ly6-like Proteins Required for Proper Localization of Septate Junction Components." *Development* 137: 2427–2437.

Noirot-timothée, C., D. S. Smith, M. L. Cayer, and C. Noirot. 1978. "Septate Junctions in Insects: Comparison between Intercellular and Intramembranous Structures." *Tissue Cell* 10

:125–136.

Ogienko, A. A., L. A. Yarinich, E. V. Fedorova, M. O. Lebedev, E. N. Andreyeva, A. V. Pindyurin, and E. M. Baricheva. 2018. “New Slbo-Gal4 Driver Lines for the Analysis of Border Cell Migration during Drosophila Oogenesis.” *Chromosoma* 127: 475–487.

Oshima, K., and R.G. Fehon. 2011. “Analysis of Protein Dynamics within the Septate Junction Reveals a Highly Stable Core Protein Complex That Does Not Include the Basolateral Polarity Protein Discs Large.” *Journal Cell Science* 124: 2861–2871.

Osterfield, M., C. A. Berg, and S. Y. Shvartsman. 2017. “Epithelial Patterning, Morphogenesis, and Evolution: Drosophila Eggshell as a Model.” *Developmental Cell* 41: 337:348.

Papassideri, Issidora S. 1993. “The Eggshell of Drosophila Melanogaster. VIII. Morphogenesis of the Wax Layer during Oogenesis.” *Tissue Cell* 25: 29–936.

Pascucci, T., J. Perrino, A. P. Mahowald, and G. L. Waring. 1996. “Eggshell Assembly in Drosophila: Processing and Localization of Vitelline Membrane and Chorion Proteins.” *Developmental Biology* 177: 590–598.

Paul, S. M., M. Ternet, P. M. Salvaterra, and G. J. Beitel. 2003. “The Na+/K+ ATPase Is Required for Septate Junction Function and Epithelial Tube-Size Control in the Drosophila Tracheal System.” *Development* 130: 4963–4974.

Petri, J., M. H. Syed, S. Rey, and C. Klämbt. 2019. “Non-Cell-Autonomous Function of the GPI-Anchored Protein Undicht during Septate Junction Assembly.” *Cell Reports* 26: 1641-1653.

Poordy, C. A., and H. A. Schneiderman. 1970. “The Ultrastructure of the Developing Leg of Drosophila Melanogaster.” *Roux Archiv* 166:1–44.

Popkova, A., O. J. Stone, L. Chen, X. Qin, C. Liu, J. Liu, K. Belguise, D. J. Montell, K. M. Hahn, M. Rauzi, X. Wang. 2020. “A Cdc42-Mediated Supracellular Network Drives Polarized Forces and Drosophila Egg Chamber Extension.” *Nature Communications* 11:1921.

Prasad, M., and D. J. Montell. 2007. “Cellular and Molecular Mechanisms of Border Cell Migration Analyzed Using Time-Lapse Live-Cell Imaging.” *Developmental Cell* 12: 997–1005.

Qin, X., B. O. Park, J. Liu, B. Chen, V. Choesmel-Cadamuro, K. Belguise, W. D. Heo, and X. Wang. 2017. “Cell-Matrix Adhesion and Cell-Cell Adhesion Differentially Control Basal Myosin Oscillation and Drosophila Egg Chamber Elongation.” *Nature Communication* 8:14708.

Santa-Cruz Mateos, C., A. Valencia-Expo´sito, I. M. Palacios, and M. D. Martı´n-Bermudo. 2020. “Integrins Regulate Epithelial Cell Shape by Controlling the Architecture and

Mechanical Properties of Basal Actomyosin Networks." *PLoS Genetics* 16:e1008717.

Schindelin, J., I. Arganda-Carreras, E. Frise, V. Kaynig, M. Longair, T. Pietzsch, S. Preibisch, C. Rueden, S. Saalfed, B. Schmid, J. Y. Tinevez, D. J. White, V. Hartenstein, K. Eliceiri, P. Tomancak, and A. Cardona. 2012. "Fiji: An Open-Source Platform for Biological-Image Analysis." *Nature Methods* 9: 676–682.

Schneider, M., A. A. Khalil, J. Poulton, C. Castillejo-Lopez, D. Egger-Adam, A. Wodarz, W. Deng, and S. Baumgartner. 2006. "Perlecan and Dystroglycan Act at the Basal Side of the Drosophila Follicular Epithelium to Maintain Epithelial Organization." *Development* 133: 3805–3815.

Schulte, J., U. Tepass, and V. J. Auld. 2003. "Gliotactin, a Novel Marker of Tricellular Junctions, Is Necessary for Septate Junction Development in Drosophila." *Journal Cell Biology* 161: 991–1000.

Shindo A. 2018. "Models of Convergent Extension during Morphogenesis. " *Wiley Interdisciplinary Reviews: Developmental Biology* 7: e293.

Snow, P. M., A. J. Bieber, and C. S. Goodman. 1989. "Fasciclin III: A Novel Homophilic Adhesion Molecule in Drosophila." *Cell* 59: 313–23.

Solnica-Krezel, L., and D. S. Sepich. 2012. "Gastrulation: Making and Shaping Germ Layers." *The Annual Review of Cell and Developmental Biology* 28: 687:717.

Spradling, A.C. 1993. "Development genetics of oogenesis: In the Development of Drosophila melanogaster." (ed: M. Bate and A. Martiwz-Arias) *Cold Spring Harbor, NY: Cold Spring Harbor Press* 1: 1-70.

Spradling, A. C., M. De Cuevas, D. Drummond-Barbosa, L. Keyes, M. Lilly, M. Pepling, and T. Xie. 1997. "The Drosophila Germarium: Stem Cells, Germ Line Cysts, and Oocytes." *Cold Spring Harbor Symposia Quantitative Biology* 62: 25–34.

Stroschein-Stevenson, S. L., E. Foley, P. H. O'Farrell, and A. D. Johnson. 2006. "Identification of Drosophila Gene Products Required for Phagocytosis of Candida Albicans." *PLoS Biology* 4: 0087–0099.

Tepass, U., and V. Hartenstein. 1994. "The Development of Cellular Junctions in the Drosophila Embryo." *Developmental Biology* 161: 563-596.

Tepass, U., G. Tanentzapf, R. Ward, and R. Fehon. 2001. "Epithelial Cell Polarity and Cell Junctions in Drosophila." *Annual Reviews Genetics* 35: 747–784.

Tiklová, K., K. A. Senti, S. Wang, A. GräCurrency Signslund, and C. Samakovlis. 2010. "Epithelial Septate Junction Assembly Relies on Melanotransferrin Iron Binding and Endocytosis in Drosophila." *Nature Cell Biology* 12: 1071–1077.

VanHook, A., and A. Letsou. 2008. “Head Involution in Drosophila: Genetic and Morphogenetic Connections to Dorsal Closure.” *Developmental Dynamics* 237: 28–38.

Velentzas, A. D., P. D. Velentzas, S. A. Katarachia, A. K. Anagnostopoulos, N. E. Sagioglou, E. V. Thanou, M. M. Tsioka, V. E. Mpakou, Z. Kollia, V.E. Gavriil, I. S. Papassideri, G. T. Tsangaris, A. C. Cefalas, E. Sarantopoulou, D. J. Stravopodis. 2018. “The Indispensable Contribution of S38 Protein to Ovarian-Eggshell Morphogenesis in Drosophila Melanogaster” *Scientific Reports* 8: 1–17.

Venema, D. R., T. Zeev-Ben-Mordehai, and V. J. Auld. 2004. “Transient Apical Polarization of Gliotactin and Coracle Is Required for Parallel Alignment of Wing Hairs in Drosophila.” *Developmental Biology* 275: 301–314.

Viktorinová, I., T. König, K. Schlichting, and C. Dahmann. 2009. “The Cadherin Fat2 Is Required for Planar Cell Polarity in the Drosophila Ovary.” *Development* 136:4123–4132.

Vlachos, S., and N. Harden. 2011. “Genetic Evidence for Antagonism between Pak Protein Kinase and Rho1 Small GTPase Signaling in Regulation of the Actin Cytoskeleton during Drosophila Oogenesis.” *Genetics* 187: 501–512.

Wang, S., S. A. Jayaram, J. Hemphälä, K. A. Senti, V. Tsarouhas, H. Jin, and C. Samakovlis. 2006. “Septate-Junction-Dependent Luminal Deposition of Chitin Deacetylases Restricts Tube Elongation in the Drosophila Trachea.” *Current Biology* 16: 180–185.

Ward, R. E., J. Evans, and C. S. Thummel. 2003. “Genetic Modifier Screens in Drosophila Demonstrate a Role for Rho1 Signaling in Ecdysone-Triggered Imaginal Disc Morphogenesis.” *Genetics* 165: 1397–1415.

Ward, R. E., R. S. Lamb, and R. G. Fehon. 1998. “A Conserved Functional Domain of Drosophila Coracle Is Required for Localization at the Septate Junction and Has Membrane-Organizing Activity.” *Journal Cell Biology* 140: 1463–1473.

Wei, J., M. Hortsch, and S. Goode. 2004. “Neuroglian Stabilizes Epithelial Structure during Drosophila Oogenesis.” *Developmental Dynamics* 230: 800–808.

Wells, R. E., J. D. Barry, S. J. Warrington, S. Cuhlmann, P. Evans, W. Huber, D. Strutt, and M. P. Zeidler. 2013. “Control of Tissue Morphology by Fasciclin III-Mediated Intercellular Adhesion.” *Development* 140: 3858–3868.

Wieschaus, E., C. Audit, and M. Masson. 1981. “A Clonal Analysis of the Roles of Somatic Cells and Germ Line during Oogenesis in Drosophila.” *Developmental Biology* 88: 92–103.

Wittes, J., and T. Schüpbach. 2018. “A Gene Expression Screen in Drosophila Melanogaster Identifies Novel JAK/STAT and EGFR Targets During Oogenesis.” *G3* 9: 47–60.

Wu, V. M., J. Schulte, A. Hirschi, U. Tepass, and G. J. Beitel. 2004. “Sinuous Is a Drosophila

Claudin Required for Septate Junction Organization and Epithelial Tube Size Control." *Journal Cell Biology* 164: 313–323.

Wu, V. M., M. H. Yu, R. Paik, S. Banerjee, Z. Liang, S. M. Paul, M. A. Bhat, and G. J. Beitel. 2007. "Drosophila Varicose, a Member of a New Subgroup of Basolateral MAGUKs, Is Required for Septate Junctions and Tracheal Morphogenesis." *Development* 134: 999–1009.

Woods, D. F. and P. J. Bryant. 1991. "The discs-large tumor suppressor gene of Drosophila encodes a guanylate kinase homolog localized at septate junctions. " *Cell* 66: 451-464.

Xie, T., and A. C. Spradling. 2000. "A Niche Maintaining Germ Line Stem Cells in the Drosophila Ovary." *Science* 290: 328–330.

Yi, P., A. N. Johnson, Z. Han, J. Wu, and E. N. Olson. 2008. "Heterotrimeric G Proteins Regulate a Noncanonical Function of Septate Junction Proteins to Maintain Cardiac Integrity in Drosophila." *Developmental Cell* 15: 704–713.

Zahraoui, A., D. Louvard, and T. Galli. 2000. "Tight Junction, a Platform for Trafficking and Signaling Protein Complexes." *Journal of Cell Biology* 151: 31–36.

Zallen, J. A. and B. Goldstein. 2017. "Cellular Mechanisms of Morphogensis." *Seminars in Cell and Developmental Biology* 67: 101-102.

Zappia, M. P., M. A. Brocco, S. C. Billi, A. C. Frasch, and M. Fernanda Ceriani. 2011. "M6 Membrane Protein Plays an Essential Role in Drosophila Oogenesis." *PLoS ONE* 6:e19715.